JEMS

JOURNAL OF ETA MARITIME SCIENCE

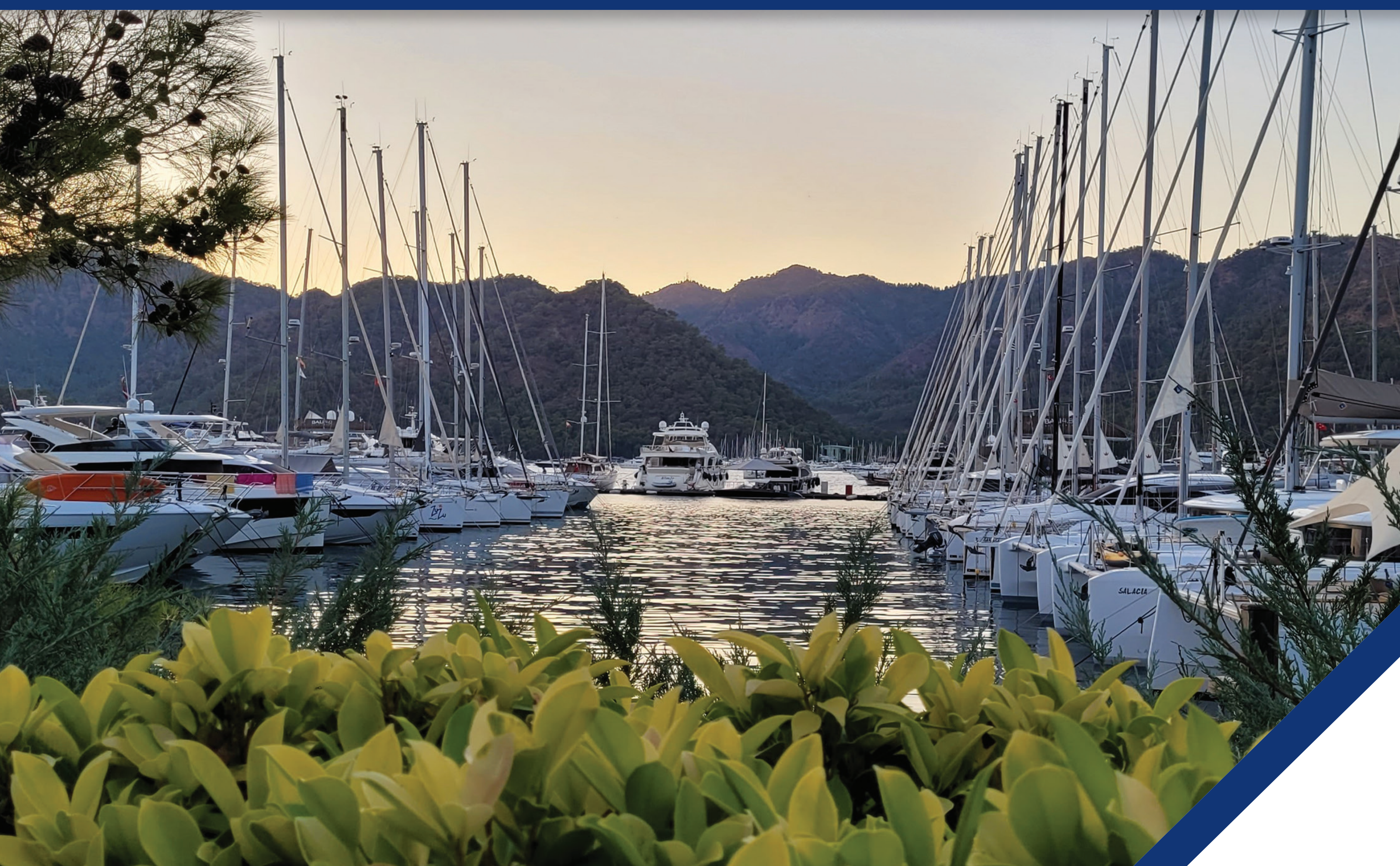

Volume: 9 | Issue: 3

September 2021

ISSN: 2147-2955 ▪ E-ISSN: 2148-9386

UCTEA CHAMBER OF MARINE ENGINEERS 1960

www.jemsjournal.org

JEMS
JOURNAL OF ETA MARITIME SCIENCE
2021 / Volume • 9 - Issue • 3

JEMS
JOURNAL OF ETA MARITIME SCIENCE

2021 / Volume • 9 - Issue • 3

Edioral Board

Journal Info

Owner UCTEA The Chamber of Marine Engineers

Address: Sahrayıcedit Mah. Halk Sk. Golden Plaza No: 29 C Blok K:3 D:6 Kadıköy/İstanbul - Türkiye
Web: gemimo.org **E-mail:** bilgi@gemimo.org **Phone:** +90 216 747 15 51
Fax: +90 216 747 34 35

Publisher Galenos Publishing House
Address: Molla Gürani Mah. Kaçamak Sk. No: 21/1 34093 İstanbul, Turkey
Phone: +90 (212) 621 99 25 **E-mail:** info@galenos.com.tr **Web:** www.galenos.com.tr

ISSN: 2147-2955 / E-ISSN: 2148-9386

Journal website:
www.jemsjournal.org

Online Publication Date:
September 2021

Submit Article:
jag.journalagent.com/jems

Cover Photo:

2021 / Volume 9 / Issue 3
Nas, S. (2021) D-Marin Göcek TURKEY

JEMS
JOURNAL OF ETA MARITIME SCIENCE
2021 / Volume • 9 - Issue • 3

About the JEMS

Since 2020, JEMS has been published in English only

Aim:

Journal of Eta Maritime Science (JEMS) aims to encourage and publish research studies about the challenges and opportunities associated with considerable numbers of understandings in the maritime sector. Besides, JEMS also aims to reach out to relevant audiences by publishing the latest scientific and technological developments. JEMS journal, which is published periodically and regularly in March, June, September, December, may also publish special issues related to the selected topics.

Scope:

Scope of the journal covers national, international and local studies regarding Marine Engineering, Marine Transportation Engineering, Naval Architecture Engineering, Marine Operations, Logistics, Logistics Engineering, Maritime History, Coastal Engineering, Marine Pollution and Environment, Fishing and Fisheries Technology, Shipbuilding and Ocean Engineering.

JEMS is indexed in **Web of Science Emerging Sources Citation Index (ESCI), Tubitak Ulakbim Science Database, Index Copernicus International, Directory of Open Access Journals (DOAJ)**, **EBSCO** and **J-Gate**.

Publisher:

Galenos Publishing House

Publication Charges

There are no submission fees, publication fees or page charges for this journal.

1. **JEMS Article Submission Policy:** Submission of an article implies that the manuscript described has not been published previously in any journals or a conference paper with a DOI number.
2. Submitted articles should be original research papers about any marine related matter.
3. It will not be published elsewhere in English, in Turkish or in any other language, without the written consent of the copyright holder.
4. Articles must be written in proper English.
5. It is essential that the submission file be saved in the valid format of the template of the word processor used.
6. References of information must be indicated.
7. Source files of figures, tables and text graphics should be inserted in the system separately during the application process.
8. To avoid unnecessary errors, you are strongly advised to use the "spell-check" and "grammar-check" functions of your word processor.
9. JEMS operates the article evaluation process with a "double-blind" peer review policy. This means that the reviewers of the paper will not get to know the author's identity (s), and the author(s) will not get to know the reviewer's identity.
10. Editor (s) will decide whether the submissions are eligible for publication in accordance with the reviewers' reports.
11. Authors are obliged to comply with the JEMS Submission Policy.
12. JEMS will be published quarterly.
13. JEMS does not charge any article submission or processing charges.

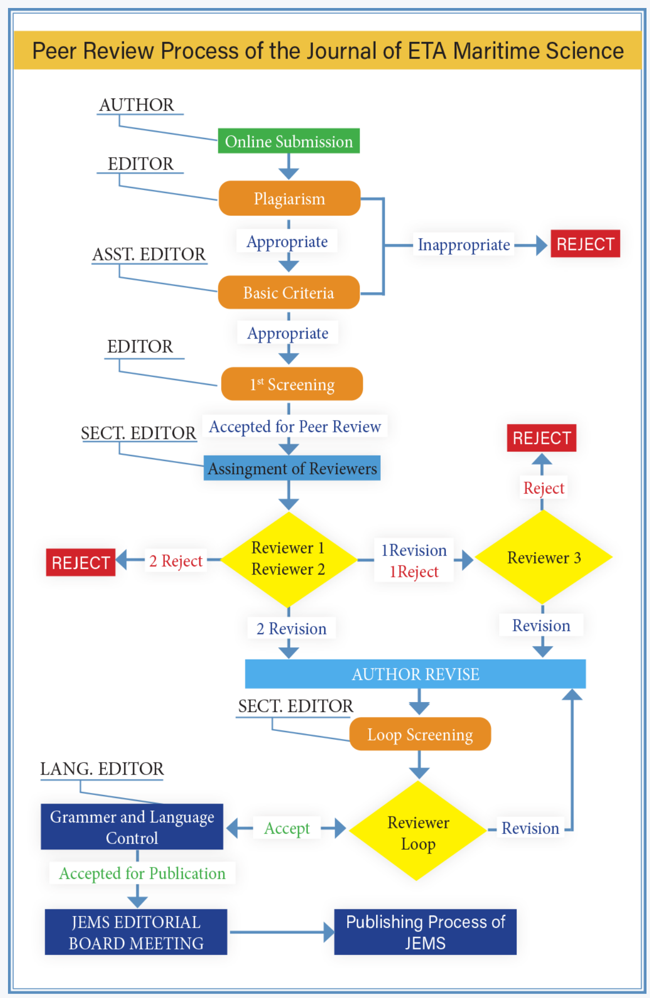

As part of its free access policy, JEMS which is a peer-reviewed journal, provides instant free access by adopting the principle that it will increase the global share of knowledge to introduce scientific research to the public.

Plagiarism Policy

Plagiarism can take place in two forms:

1. Author(s) deliberately copy someone else's work and claim it as their own work.

2. Author(s) copy their own previously published material either in whole or in part without providing appropriate references called "self-plagiarism" or "duplicate publication."

Every manuscript submitted for publication to JEMS is checked for plagiarism after submission and before being sent to the reviewer for evaluation. "iThenticate" is used to detect instances of overlapping and similar text in the submitted manuscript.

Advertisement Policy

1. All advertisements depend on the approval of the Publisher or Editor.

2. Scientific content and decisions made by the editorial board have not been affected by advertising.

3. Advertisements are separate from scientific content.

4. Sales and marketing of the products within the accepted advertising are unfeasible.

5. The editor or publisher of the journal is not responsible for the advertisement and its content. This responsibility entirely belongs to the owner of advertising.

6. Accepted advertisements can be placed on any page approved by the editor or publisher.

7. Advertising is done according to the contract between the advertising company and journal management.

8. Advertising content has not included any distinction of language, religion, race, gender, age, disability, etc.

9. Advertising that is contrary to society and publication ethics must not be published.

10. Advertising produced according to national rules and fulfilling their obligations, such as licenses, are accepted for publishing.

11. Advertisements must be prepared in accordance with competition laws and other relevant regulations.

12. Journal management shall not be liable for pecuniary loss due to errors in the advertising content.

Open Access and CC Licence

JEMS is an open-access journal. The term open access gives the right of readers to read, download, distribute, copy, print, search, or link to the full texts of the articles free of charge. **JEMS** also signed (http://www.budapestopenaccessinitiative.org/list_signatures) Budapest Open Access Initiative (BOAI). According to BOAI (Budapest Open Access Initiative); By "open access" to peer-reviewed research literature, its free availability on the public internet, permitting any users to read, download, copy, distribute, print, search, or link to the full texts of these articles, crawl them for indexing, pass them as data to software, or use them for any other lawful purpose, without financial, legal, or technical barriers other than those inseparable from gaining access to the internet itself. The author(s) and the copyright holder(s) grant(s) to all users free access to articles. Authors retain copyright and grant the journal right of first publication with the work simultaneously licensed under a Creative Commons Attribution License that allows others to share the work to acknowledge the work's authorship and initial publication in this journal. JEMS apply the Creative Commons Attribution-NonCommercial 4.0 International Licence (CC BY-NC 4.0) to all manuscripts to be published.

OPEN ACCESS

Digital Archiving And Preservation Policy

Digital preservation is a set of processes and activities that ensure the retrieval and distribution of information now available in digital formats to guarantee long-term, perpetual access. The preservation policy includes the following measures:

Website archiving

All of the electronic content (website, manuscript, etc.) is stored in three different sources. Content on a server is online and accessible to readers. A copy of the same content is preserved as a backup on two other sources. Should a server fail, other resources can be brought online, and the website is expected to be available in 24-36 hours.

Abstracting/Indexing services

Our journal's Abstracting/Indexing services store essential information about articles. In addition, some of our journals' Abstracting/Indexing services archive metadata about the article and electronic versions of the articles.In this way, copies of articles are presented to the scientific community through these systems as an alternative to journals.

Cessation of publication

If a journal must stop publishing, the articles will remain online and accessible to readers through third parties and archiving processes such as those described above. Content can be accessed through PORTICO when required under certain circumstances, such as when the collection is stopped.

JEMS
JOURNAL OF ETA MARITIME SCIENCE
2021 / Volume • 9 - Issue • 3

Guide for Authors

Abstract

This sample includes the manuscript preparation guideline of Journal of ETA Maritime Science (JEMS). In the abstract section, a brief indicating the novelty and main findings of the study should be written. The text of the abstract should be written fully justified, in italics and 10 pt. The section should be no more than 200 words. The number of keywords should be between 3-5.

Keywords: JEMS, Author, Manuscript, Guide

1. Introduction

Journal of Eta Maritime Science (JEMS) aims to encourage and publish research studies about the challenges and opportunities associated with considerable numbers of understandings in the maritime sector. Besides, JEMS also aims to reach out to relevant audiences by publishing the latest scientific and technological developments. JEMS journal, which is published periodically and regularly, may also publish special issues related to the selected topics. Scope of the journal covers national, international and local studies regarding Marine Engineering, Maritime Transportation Engineering, Naval Architecture Engineering, Marine Operations, Logistics, Logistics Engineering, Maritime History, Coastal Engineering, Marine Pollution and Environment, Fishing and Fisheries Technology, Shipbuilding and Ocean Engineering

2. Page Layout and Format

JEMS publishes studies conducted in **English**. Text is to be prepared with justified alignment, without indentation in the paragraph beginning, in **"Cambria"** format with **10-point** font size and **1,0** line- spacing. There must be **initially 6nk and then 3nk** line spacing between the new launching paragraph and the previous paragraph. Worksheets must be on **A4** paper size, and margins should b**e 4 cm from the top, 4 cm from the bottom, 4 cm from left** and **3.5 cm from right**.

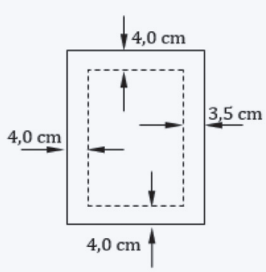

Studies must be submitted online from the journal's web address (http://www.jemsjournal.org). Articles printed or within CD, articles submitted by mail, fax etc., is not acceptable.

The main title of the article must be written in English and should be **set centered** in **12 point-size. Initially, 6nk and after 6nk** space should be left before the main title.

The first letter of the primary headings in the article should be capital letters. All headings and sub-headings should be designed **10 pt, bold** and **located to the left** with **numbering**, and also navy blue color should be used for sub-headings.

The use of tables and figures should be kept to a **minimum**. For readability purposes, the total number of tables and figures should be no more than **10** per article.

1 OrcaFlex Program

1.1 Axis Team

The table heading should be placed above the table. The figure heading should be placed below the figure. **2 nk** spaces should be added **before** the table heading and figure heading, and also **3 nk** spaces should be added next. The "table" and the "figure" should be written in bold and left-aligned. The first letters of the table, figure and equation headings should be written with capital letters. The heading and the content should be written with **"Cambria"** font and **10-point size**. Suppose tables, figures and equations in the study are cited. In that case, their references should be stated. **2 nk spaces** should be added **before** references, and **3 nk spaces** should be added **after**. If tables and figures don't fit into a single column, they should be designed to include two columns. Tables and figures which include two columns should be stated at the top or bottom of the page.

Table 1. Sample Table

Turkish Male Seafarers (n = 131,152)	BMI < 25.0	BMI 25-30	BMI > 30	Number of Participants
16-24 Ages Group	74.1%	22.5%	3.4%	34,421
25-44 Ages Group	44.1%	43.3%	12.6%	68,038
45-66 Ages Group	25.6%	51.1%	23.4%	28,693
All Turkish Male Seafarers	47.9 %	39.6 %	12.5%	131,152
Turkish Male Population	47.3 %	39.0 %	13.7 %	-

In the article, decimal fractions should be separated with dots and numbers should be separated with commas.

Average age: 28.624

Number of participants: 1,044 people

Page numbers, headers and footers should not be added to the study. The journal administration will make these adjustments.

Authors are deemed to have accepted that they have transferred the copyright of their studies to the journal by submitting their studies to our journal. Submitting a study to two different journals simultaneously is not suitable within the frame of academic ethics.

It is required that the studies are original and have not been published elsewhere before. If conference and symposium papers were published in a booklet, in this case, they should be published by JEMS on the condition that the copyright has not been transferred to the first publishing place. The information must be given to the journal editorship about where these kinds of papers were published before.

3. Types of Article

Editorial (ED)

This is an article which the editor prepares for determining journal policies in guiding

research strategies and in making announcements to researchers and authors.

Letter to Editor (LE)

This is a short article grounding upon the objectivity criteria, which the editor addresses to make comments, criticism, and contribution on a previously written and published article. Letter to the editor is used to allow sharing of feedback on the articles published in JEMS. Title, Author, Letter, References (Maximum 6000 words, 15 pages).

Erratum (ER)

This is a notification for announcing corrections, errors and retracts regarding the articles that have been previously published in JEMS.

Original Research (AR)

This is an original research article that contains the findings that reached with the analysis of data obtained using specific methodologies within the context of the research model developed based on a literature review on a specific topic and contains the results which were obtained by the discussion of the findings and the literature (Maximum 6000 words, 15 pages).

Review (RE)

This is an article pertaining to the research compiled by summarizing researches and data which other authors and/or institutions previously carried out. (It cannot be accepted as an original research article) Title, Author, Abstract, Introduction, Literature Review, Conclusion, References (Maximum 6000 words, 15 pages).

Report (RP) Interview (RP)

This is an article pertaining to the short research using structured interview methods with a veteran, recognized with knowledge and expertise in a specific subject, to seek his/her advice in a predetermined topic concerning the maritime industry (Organized by the editor). Title, Author, Abstract, Short biography of the interviewee, Methodology, Questions and Comments, Results, Interview Permit Certificate (Maximum 3000 words).

Case Investigation (RP)

This is an article pertaining to short research prepared to unfold a problem determined during research concerning the maritime industry to offer a solution and develop a method for the solution. Title, Author, Abstract, Case, Problem and Solution Offers, Conclusion, References, Permission Letter (Maximum 2000 words).

Technical Report (RP)

This is an article pertaining to the short research containing the conclusions of analysis on relevant obtained data in matters concerning the maritime industry referenced upon a limited number of literature material. It covers conclusive reports of industrial research, particularly research reports carried out during the period of academic education, etc. Title, Author, Abstract, Introduction, Methodology, Results, References(Maximum 2000 words).

Book Review (BK)

This is an article where an invited reviewer evaluates a newly published book concerning the maritime industry in conformance with a specific methodology. (Maximum 1000 words).

Academic Perspective

This is an article in characteristics of a compilation or a plain text where veteran academicians who are recognized with their academic knowledge and expertise would share their contributions in maritime science, guide young academicians and researchers, and offer solutions for the demands of the maritime industry. (Invited by the editor).

Industrial Perspective

An article in conformance with a specified text format prepared by an expert as an invitee whose knowledge and experience related to their area of expertise is recognized as beneficial by the industry (Invited by the editor). Title, Author, Abstract, Foresight about the subject, Results (Maximum 6000 words, 15 pages).

After the Meeting This article is written to convey the impressions, congress conclusion reports, and information gathered during scientific conventions following a congress, conference, and symposium organized on such matters concerning the maritime industry. (Maximum 500 words).

5. References

The citation style used by our journal is Institute of Electrical and Electronics Engineers (IEEE) Reference Style.

The IEEE Style is used for publications in engineering, electronics, telecommunications, computer science and information technology.

IEEE Style uses a notational method of referencing when referring to a source of information within the text of a document.

You can achieve the IEEE reference style and all reference examples used in our journal at https://jemsjournal.org/guide-for-authors.

JEMS Publication Ethics And Malpractice Statement

ournal of ETA Maritime Science is an independent publication regarding scientific research, and the editor decides its publication policy. The statement signifies the ethical behaviour of the publisher, the editor, the reviewers and the authors. The ethics statement for JEMS is based on ***COPE Code of Conduct and Best Practice Guidelines for Journal Editors and COPE Best Practice Guidelines for Journal Editors*** available at www.publicationethics.org.

A. Duties of Publisher:

Duties of the Publisher

Handling of unethical publishing behaviour

The publisher will take all appropriate measures to modify the article in question, in close cooperation with the editors, in cases of alleged or proven scientific misconduct, fraudulent publication, or plagiarism. This includes the prompt publication of an erratum, disclosure, or retraction of the affected work in the most severe case. Together with the editors, the publisher will take reasonable steps to detect and prevent the publication of articles in which research misconduct occurs and will under no circumstances promote or knowingly allow such abuse to occur.

Editorial Autonomy

JEMS is committed to ensuring the autonomy of editorial decisions without influence from anyone or commercial partners.

Intellectual Property and Copyright

JEMS protects the property and copyright of the articles published in the journal and maintains each article's published version of the record. JEMS provides the integrity and transparency of each published article.

Scientific Misconduct

JEMS's publisher always takes all appropriate measures in respect to fraudulent publication or plagiarism.

B. Duties of Editors:

Decision on Publication and Responsibility

The editor of JEMS keeps under control everything in the journal and strives to meet the needs of readers and authors. The editor is also responsible for deciding which articles submitted to the journal should be published and may be guided by the policies subjected to legal requirements regarding libel, copyright infringement, and plagiarism. The editor might discuss with reviewers while making publication decisions. The editor is responsible for the contents and overall quality of the publication. Editor ought to provide a fair and appropriate peer-review process.

Objectivity

Articles that are submitted to the journal are always evaluated without any prejudice.

Confidentiality

The editor must not disclose any information about a submitted article to anyone other than editorial staff, reviewers, and publisher.

Conflicts of Interest and Disclosure

The Editor of JEMS does not allow any conflicts of interest between the parties such as authors, reviewers and editors. Unpublished materials in a submitted article must not be used by anyone without the express written assent of the author.

Fundamental Errors in Published Works

Authors are obliged to notify the journal's editors or publisher immediately and to cooperate with them to correct or retract the article if significant errors or inaccuracies are detected in the published work. If the editors or publisher learn from a third party that a published work contains a material error or inaccuracy, the authors must promptly correct or retract the article or provide the journal editors with evidence of the accuracy of the article.

C. Duties of Reviewers:

Evaluation

Reviewers evaluate manuscripts without origin, gender, sexual orientation or political philosophy of the authors. Reviewers also ensure a fair blind peer review of the submitted manuscripts for evaluation.

Confidentiality

All the information relative to submitted articles is kept confidential. The reviewers must not be discussed with others except if authorized by the editor.

Disclosure and Conflict of Interest

The reviewers have no conflict of interest regarding parties such as authors, funders, editors, etc.

Contribution to editor

Reviewers help the editor in making decisions and may also assist the author in improving the manuscript.

Objectivity

They always do the objective judgment evaluation. The reviewers express their views clearly with appropriate supporting arguments.

Acknowledgement of Sources

Reviewers ought to identify a relevant published study that the authors have not cited. Reviewers also call to the editor's attention any substantial similarity or overlap between the manuscript and any other published paper of which they have personal knowledge.

D. Duties of Authors:

Reporting Standards

A submitted manuscript should be original, and the authors ensure that the manuscript has never been published previously in any journal. Data of the research ought to be represented literally in the article. A manuscript ought to include adequate detail and references to allow others to replicate the study.

Originality

The authors who want to submit their study to the journal must ensure that their study is entirely original. The words and sentences getting from the literature should be appropriately cited.

Multiple Publications

Authors should not submit the same study for publishing in any other journals. Simultaneous submission of the same study to more than one journal is unacceptable and constitutes unethical behaviour.

Acknowledgement of Sources

Convenient acknowledgement of the study of others has to be given. Authors ought to cite publications that have been efficient in determining the study. All of the sources that used the process of the study should be remarked.

Authorship of a Paper

Authorship of a paper ought to be limited to those who have made a noteworthy contribution to the study. If others have participated process of the research, they should be listed as contributors. Authorship also includes a corresponding author who is in communication with the editor of a journal. The corresponding author should ensure that all appropriate co-authors are included in a paper.

Disclosure and Conflicts of Interest

All sources of financial support should be disclosed. All authors ought to disclose a meaningful conflict of interest in the process of forming their study.

JEMS
JOURNAL OF ETA MARITIME SCIENCE
2021 / Volume • 9 - Issue • 3

Contents

DOI: 10.4274/jems.2021.60134

Journal of ETA Maritime Science 2021;9(3):156

Selçuk Nas

Dokuz Eylül University Maritime Faculty, Department of Maritime Education and Training, İzmir, Turkey

Dear Readers,

We are pleased to introduce JEMS 9 (3) to our valuable followers. There are valuable and intriguing studies in this issue of the journal. We hope that these studies will contribute to the maritime industry. I would like to mention our gratitude toward the authors, who sent their valuable studies for publication in this issue, our reviewers, editorial board, section editors, and the publisher who provided quality publications by following our publication policies diligently.

Yours Sincerely,

Prof. Dr. Selçuk NAS
Editor-in-Chief

Address for Correspondence: Selçuk Nas, Dokuz Eylül University Maritime Faculty, Department of Maritime Education and Training, İzmir, Turkey
E-mail: snas@deu.edu.tr
ORCID ID: orcid.org/0000-0001-5053-4594

ORIGINAL RESEARCH (AR)
DOI: 10.4274/jems.2021.94834

Journal of ETA Maritime Science 2021;9(3):157-167

A Comprehensive Evaluation of Yacht Charter Service Concept: Influence of Voyager-to-Voyager Interaction on Service Satisfaction

Neslihan Paker[1], Osman Gök[2]

[1]İzmir Kavram Vocational School, Department of Logistics Program, İzmir, Turkey
[2]Yaşar University, Department of Business Administration, İzmir, Turkey

Abstract

The study attempts to evaluate yacht charter service attributes considering the service quality, customer satisfaction, and loyalty three-leg framework. Besides visited destinations, the service concept is enlarged with social servicescape dimensions of interaction quality and customer similarity for a holistic approach. A self-administered questionnaire was provided to 359 customers, and the relationships in the research model were tested via structural equation modeling. The results showed that satisfaction depends on the interaction quality, which is strongly related to the similarity between other customers, as well as the quality of the service elements and the attractiveness of the visited destination. This study presents a pioneering research attempt focusing on the influence of customer-to-customer interaction and customer similarity on yacht charter services. Findings of the study provide a theoretical contribution, highlighting the importance of customer-to-customer interaction for service appraisals of customers. Theoretical and practical implications for interaction-dominant services are discussed.

Keywords

Customer-to-customer interaction, Service quality, Customer satisfaction, Services marketing, Marine tourism

1. Introduction

Every service provider must fully understand customer expectations of their service to be competitive in today's markets. In addition, it is difficult to convince customers of the superior value of a service because of its idiosyncratic characteristics. These challenges force academics and practitioners to consider service performance factors in a holistic manner and to examine the relationships between these factors through integrated research models. In services literature, the influences of physical facilities and employees on customer satisfaction have been examined for decades. However, the issue of other customers, an inevitable part of the social dimension of the service environment, needs discussion and should be exemplified [1-3]. With the rise in shared consumption, the issue of other customers' influence on the perceived service performance has attracted more attention, and this subject is considered a major concept in service quality studies.

The yacht charter service is a premium type of marine tourism product [4-6]. Despite significant socio-economic contributions to a national economy [7-9], it is rarely discussed in scientific literature. Chartering companies provide a variety of services from essential to luxury services (e.g., a masseur or sommelier) to be competitive in the market. However, like the pull factors related to the service, the intrinsic motivations of yacht charter customers have played a pivotal role in the service selection and evaluation process. Besides voyaging on the sea, customers also want to socialize with people having similar interests and develop friendships while sailing in untouched nature [10,11]. Therefore, whether acquainted or unacquainted, the other customers represent a major service attribute in

Address for Correspondence: Neslihan Paker, İzmir Kavram Vocational School, Department of Logistics Program, İzmir, Turkey
E-mail: neslihan.paker@kavram.edu.tr
ORCID ID: orcid.org/0000-0001-8087-7758

Received: 01.04.2021
Accepted: 10.06.2021

To cite this article: N. Paker and O. Gök, "A Comprehensive Evaluation of Yacht Charter Service Concept: Influence of Voyager-to-Voyager Interaction on Service Satisfaction." *Journal of ETA Maritime Science*, vol. 9(3), pp. 157-167, 2021.

the yacht chartering context. Thus, recent research proposes a holistic approach for yacht charter service concept, specifically to explore the influences of customer interaction and customer similarity on yacht service satisfaction.

To achieve our research objectives, the blue voyage (BV), which is a crewed type of yacht chartering, is used as a research subject. The BV has been arranged for more than 70 years in Turkey, which is a highly popular yachting destination in the Mediterranean Basin. Some prominent advantages, such as having a zigzag-shaped coastline and several sheltered coves, distinguish the BV from other yacht charters in various destinations. Generally, the voyage duration is one week, and the crew provides at least some services such as transportation, cooking, and housekeeping. The yacht is just large enough to enter bays; the voyagers share limited space. Thus, such a service setting can create an opportunity to observe the influence of customer interaction on satisfaction and makes the BV an ideal research context.

In the following section, we discuss the theoretical background of our study. We then describe the data collection and methodology of the fieldwork and present the findings. In the last section, we discuss the findings and touch upon the theoretical and management implications and potential avenues for future research.

2. Background

2.1. Yacht Charter Services Attributes

The defining attributes of a concept or a product has been widely used in literature for different purposes such as measuring the service quality or customer satisfaction. Considering studies in the hospitality and marine tourism industry, the attributes of yacht charter services can be mainly categorized as physical environment, services, and employees, which are service performance indicators [12-17].

Apart from transporting passengers safely, the essential services given in a yacht include housekeeping and food and beverage that customers expect to be provided at a high-quality level. Since the yacht is far from the shore during the largest part of the tour, the quality of food onboard is highly important for customers. It is possible to see exclusive examples of international cuisine on luxury yachts, as well. In recent years, because of the increase in the healthy eating trend, the customer demand for food with organic ingredients has increased significantly. Cleaning is one of the most important elements in the yacht industry and significantly impacts customer satisfaction. Furthermore, some yachts, like hotels, have many executions such as arranging towels or deck decoration.

Yachts are physical service environments where all relevant services are provided. They provide not only safe transportation but also a comfortable holiday experience. Furthermore, flippers, snorkel, and fishing tackle are available in almost all yachts. In more luxurious yachts, there is a wide range of water toys, such as canoe, sup, inflatable slide, ringo, water bird, and wake surfing. Moreover, some of the tours include yoga activities. The crew is a crucial part of the yacht, expected to be clean, reliable, respectful, willing to serve, and competent at their jobs. The tour can be completed in a pleasant way thanks to the mastery of the staff.

2.2. Pull Factors of Destination as Attributes of Yacht Charter Concept

The destination is a significant determinant element for tourists when choosing a service. Related literature has focused on two interrelated factors [18] as decision-making inputs of a tourist to select a destination: pull and push. Several studies have suggested a significant relationship between the attributes of destination and customer satisfaction [19,20].

Marine tourism products such as cruising, yachting, whale watching, and sunbathing cannot be arranged if the destination, as a part of the service offered, is ignored. The authors of [21] pointed out that the destination is yachters' first decision-making criterion for sailing. Anchoring in safe locations is as important for pleasure yachters as is traveling to attractive places. Based on the findings of [11], safety is one of the most important pull factors of marinas. Similar to marinas, bays can also be considered a type of natural harbor, providing safety on the sea in addition to being naturally attractive.

2.3. Customer-to-customer Interaction and Similarity to Other Customers

The influence of other customers is the most challenging aspect of offering services because it is uncontrollable [22]. Several researchers have claimed that this influence is a tangible clue or a part of physical evidence that facilitates evaluation of the service performance [1,23]. Many studies have revealed that this indicator affects the perceived value, service quality, customer satisfaction, customer retention, and value creation process [2,24,25]. Although it is an integral part of service experience, little academic attention has been paid to the impact of other customers on customers' service evaluations [25,26].

Scholars have discussed customer-to-customer interaction (CCI) from two opposite perspectives. The first is concerned about customers' unsuitable behaviors [25,27], while the other is the social benefit gained from developed friendships with others. Hence, the main aim of CCI is to prevent disturbing situations while providing healthy social interaction opportunities in the service environment. Some scholars have also examined the negative side of CCI that affects satisfaction. For example, in [25], 21 CCI interaction incidents were measured, and six factors (i.e., "protocol and sociable," "violent," and "crude") were obtained, some of which are highly correlated with customer satisfaction. On the other hand, the positive side of CCI is mostly defined by spending enjoyable time with others and developing friendship dimensions [22,28].

The similarity or homogeneity concepts are also addressed along with the CCI concept. The similarity is assumed to affect interaction possibility, willingness to interact with each other, customer satisfaction, and even loyalty toward the service provider [29]. In this context, age, sex, marital status, race, religion, and educational background characteristics are mostly examined as similarity attributes in qualitative studies [24,25]. The authors of [30] pointed out that similarity among customers increases satisfaction in a shopping mall even if there is no connection among customers. The authors of [3] also suggested that customer similarity increases repurchase intentions. The authors of [31] reported that the presence of old customers affects young adults' attitudes negatively with respect to purchase intention and service quality perception in health clubs and restaurants. The authors of [24] and [32] argued that individuals feel better when around others who are similar to them. Moreover, the authors of [33] claimed that cruise passengers feel more comfortable in the service environment if the passengers have similar interests and backgrounds. The authors of [25] claimed that as time spent together increases, homogeneity has more effect on satisfaction. The authors of [34] stated that the intensity and amount of time spent together has a positive effect on interaction in the cruise industry. Furthermore, the authors of [24] and [34] emphasized the crucial importance of compatibility when other customers are expected to share, there is close physical proximity among customers, and a high probability of conversation exists among customers in the service environment.

2.4. Service Quality, Customer Satisfaction, and Loyalty

Service performance has been measured via service quality (SQ) constructs (e.g., SERVQUAL and SERVPERF) in the services industry since the 1980s. Customer satisfaction (CS), which is an emotional evaluation of service experience [35] and a noteworthy determinant of loyalty (LY), has been implied by marketing concepts with SQ across studies. Many studies have suggested that SQ is an antecedent of CS and LY [36,37] and that a strong relationship exists between CS and LY [38,39].

In [40], a pioneering study was reported, examining the relationships between these constructs in the services industry. Their research offers empirical evidence that SQ is positively associated with CS, and CS influences willingness to reuse overnight hospital care services. The authors of [41] tested the links between SQ, CS, and LY for the banking, dry cleaning, fast food, and pest control industries. Their results suggest that SQ is an antecedent of CS, and CS has a more substantial influence on LY than SQ.

Hospitality and marine tourism studies have also reached similar results. For instance, a study on the hotel industry reveals that SQ is positively related to CS [35]. Studies have shown a link between perceived SQ, satisfaction, and repurchase intention of Hong Kong [17] and North American [13] cruise travelers, and Red Sea yacht tourists [42]. Furthermore, [12] a study on cruise tourist behaviors showed that interactional quality and outcome quality affect satisfaction and loyalty. Generally, CS is described as a moderating variable between SQ and LY [40]. Along with this role, several studies have pointed out that CS serves a mediating function between SQ and LY [43].

3. Research Design

3.1. Blue Voyage Case

The most prominent destinations for the yachting industry have traditionally been Caribbean Islands and Spain, Italy, Greece, France, Croatia, and Turkey in the Mediterranean Basin. Turkey has long, zigzag-shaped shorelines, a long season for yachting from April to October, well-safe bays, and suitable seas for swimming, and tourist hot spots, such as the Lycian Way and Cleopatra Beach, which differentiate it from other destinations. The BV is a crewed yacht charter, and it has been offered along the west and south parts of Turkey for more than 70 years. This charter is a one week voyage, and transportation, housekeeping, and cooking are the essential services the crew provides. The gulet-type yacht is preferred, which is wooden and specific to Turkey, and it is sufficiently long to enter bays. The yacht generally has eight cabins with double beds, plus crew quarters, making it big enough for approximately 20 persons, including the crew. The voyage can be either exclusive or a cabin charter. The exclusive yacht charter requires that a group of customers rents all the cabins. The customers can be family members or friends. In the cabin charter, customers are unacquainted people who buy the tour from the yacht company independently. The voyagers experience intense interaction while on the yacht for both types of charters. Sometimes, new friendships are formed and existing ones are developed. In some cases, customers from different nations create cultural exchange opportunities on the yacht.

3.2. Questionnaire Development

A total of 12 semistructured interviews with experienced BV customers were conducted to define the yacht charter concept service-specific attributes that impact service evaluation. The first author directed the interviews, and five hours of data were recorded. The respondents stated the yacht rental services' components under six main categories: crew, yacht, gastronomy, activity, destination, and other customers. Thereafter, the constructs were integrated into the model to evaluate yacht charter services, and a questionnaire was designed as a survey instrument based on interview findings and accumulated literature review. Most of the questionnaire items were adapted from literature i.e., [12,13,28,30,32,34,44-46]. The rest of the items are service-specific items based on interview findings (i.e., "The yacht had enough space in shared areas such as on deck and at the dining table., "Bays of the BV destination were quiet and peaceful," "The other customers and I had a similar lifestyle" The other customers had a similar educational level to mine"). Detailed information on the questionnaire constructs is listed in Table 1. Figure 1 depicts the research model. We hypothesize as follows:

H1: Crew attributes are positively related to overall service quality (OSQ).

H2: Yacht attributes are positively related to OSQ.

H3: Gastronomy attributes are positively related to OSQ.

H4: Activity attributes are positively related to OSQ.

H5: Interaction with other customers is positively related to OSQ.

H6: Similarity with other customers (SOC) is positively related to interaction with other customers (CCI).

H7: CCI is positively related to customer satisfaction (CS).

H8: Destination attributes are positively related to CS.

H 9: OSQ is positively related to CS.

H10: CS is positively related to loyalty (LY).

H11: OSQ is positively related to LY.

H12: CS mediates the relationship between OSQ and LY.

The questionnaire had seven main parts. The first part aimed to collect information on the customers' last BV experience and socio-demographics. Subsequently, the quality of gastronomy, activities, crew, yacht, destination, interaction, OSQ, SOC, satisfaction with cruise experience, and loyalty, respectively, were questioned. All the measurement items of the questionnaire were designed as a seven-point Likert-type scale ranging from 1 (= strongly disagree) to 7 (= strongly agree).

Before conducting the survey, the questionnaire was checked via face validity methods. Four tourism/marketing academics and two experienced industry representatives evaluated the questionnaire considering the research purposes. They concurred that the questionnaire can

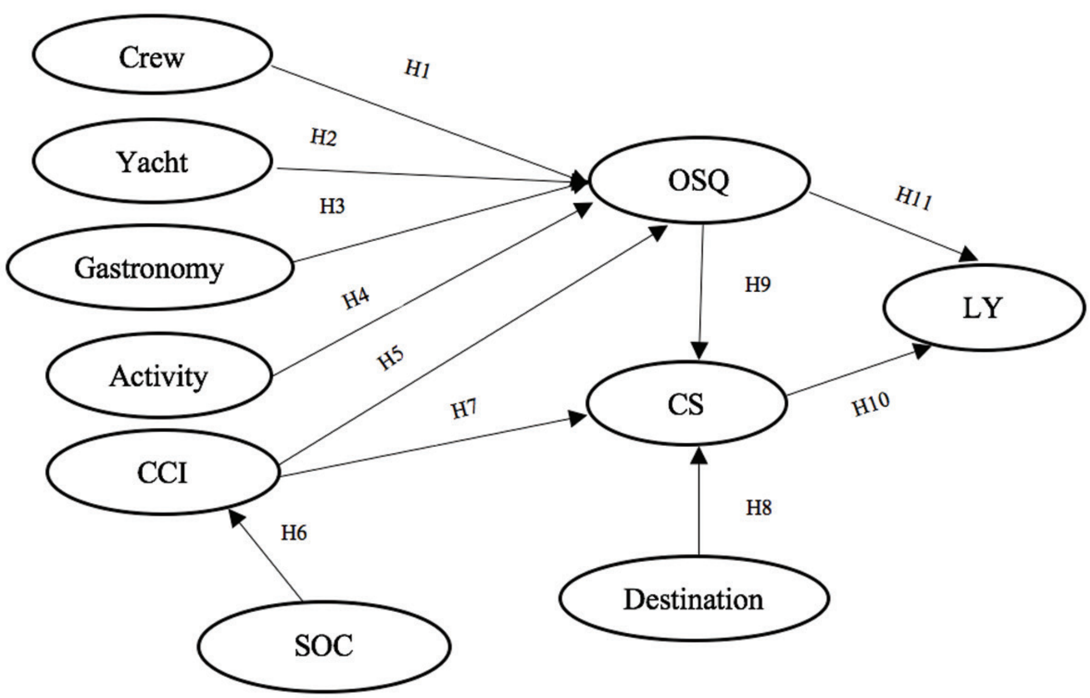

Figure 1. *Research model*

CCI: Customer-to-customer interaction, SOC: Similarity with other customers, LY: Loyalty, OSQ: Overall service quality, CS: Customer satisfaction

Table 1. *Scales*

Constructs	Items
Gastronomy adapted from [12,13]	- Food & beverages were delicious. - Food & beverages' ingredients were natural. - Portion sizes of food & beverages were satisfying.
Activities adapted from [12,13]	- A variety of sports activities was organized (i.e., fishing, diving, cycling, trekking). - A variety of intellectual activities was offered (i.e., historical and gourmet tours, sailing lessons). - A variety of entertainment activities was arranged (i.e., animations, dance parties, night tours).
Yacht adapted from [12,44]	- The yacht had enough space in shared areas such as on deck and at the dining table. - The yachts' cabins were comfortable (i.e., size, air condition, equipment). - The cabins' toilets and showers were convenient. - The yacht had the necessary warnings and information.
Destination adapted from [13,45]	- Bays of the blue voyage destination were safe. - Bays of the blue voyage destination were quiet and peaceful. - Bays of the blue voyage destination had green shorelines. - Sea in the bays had a natural attractiveness.
Crew adapted from [44]	- The crew was neat and clean. - The crew provided service reliably, consistently, and dependably. - The crew was willing and able to provide service in a timely manner. - The crew was competent (i.e., knowledgeable and skillful). - The crew was approachable and easy to contact. - The crew was courteous, polite, and respectful. - The crew listened to me and spoke in a language that I could understand. - The crew made the effort to understand my needs.
CCI adapted from [28,32]	- I developed or enhanced friendships with the other customers. - I enjoyed spending time with the other customers on the yacht. - The other customers made my time there more enjoyable.
OSQ adapted from [44]	- I would say my last blue voyage service was of superior quality. - I believe the last blue voyage service provided was excellent. - I would say my last blue voyage had high standards.
SOC adapted from [30,34]	- The other customers reflected the type of person I am. - The other customers were similar to me. - The other customers and I were of similar ages. - The other customers had a similar educational level to mine. - The other customers and I had a similar life style.
CS adapted from [12]	- Overall, I was satisfied with this blue voyage experience. - Overall, this BV put me in a good mood. - I really enjoyed myself at this blue voyage.
LY adapted from [44]	- I will use this blue voyage company's services again. - If I had to do it over again, I would make the same company choice. - I will recommend this blue voyage company to a friend. - I tell other people positive things about this blue voyage company.

CCI: Customer-to-customer interaction, SOC: Similarity with other customers, LY: Loyalty, OSQ: Overall service quality, CS: Customer satisfaction

measure the related factors, and they also provided constructive recommendations. Moreover, 12 customers with BV experience pre-tested it. Unclear questions were restructured to eliminate ambiguity. Two linguists and two academics, one of whom was competent in marketing, also performed English proofreading of the survey. They also checked English-Turkish and Turkish-English translations for slippage and made necessary corrections.

3.3. Sampling Process and Profile of the Sample

The survey was conducted in the most popular destinations of BV (i.e., Bodrum, Marmaris, and Fethiye) between

June 2018 and August 2018, and 359 fully answered questionnaires were obtained. The convenience sampling method was preferred to reach as many respondents as possible considering accessibility difficulties to the sample.

Blue voyagers generally span several age groups. However, 89.1% of the respondents were older than 30. The respondents' marital status was mostly married/living together (74.4%), and gender was distributed almost equally. Most participants were Turkish (77.4%). Moreover, 87.5% had at least a university/college degree. Almost all the respondents had mid-level or higher incomes based on their country's income scale. Approximately half of the respondents defined their income level as high or above. The respondents enjoyed a working status (75.8%), and 71% of them go on vacations at least thrice or thrice a year. The respondents had largely the same amount of experience (first participation in BV), had taken two to three BV excursions, or have had four or more experiences with BV.

3.4. Measurement Validation

3.4.1. Common Method Variance

Three different techniques were used to check for common method variance (CMV) in the study. First, Harman's one-factor test was used. All constructs of the study were examined via principal component analysis using an unrotated factor solution. Six factors were obtained. The single construct accounted for no more than 50% of the variance. A single factor model was also tested. All the measurement items were forced to load a single factor via confirmatory factor analysis (CFA). The fit indices were considerably worse for the one-dimensional model than for the measurement model. Moreover, the marker variable technique (unrelated marker variable) was tested. Using a theoretically unrelated marker variable, the CMV-adjusted correlations were compared with the unadjusted matrix using partial correlation analysis via SPSS. The unrelated marker variable was taken from Fuchs and Reichel's [46] perceived risk scale: "I worried that participating in BV would change the way my family think of me." A small correlation was observed between the marker variable and substantive constructs (i.e., <0.394). The initially significant correlations remained unchanged after adjusting for CMV. Moreover, small correlation value differences exist between the adjusted and unadjusted matrices (i.e., <0.093). As a result, common method bias is not a likely threat to the results of our study.

3.4.2. Confirmatory Factor Analysis

The research model was tested via CFA using AMOS 24. Items those were cross-loaded or loaded to their factors lower than 0.50 were eliminated from the constructs. Moreover, the correlations between constructs were evaluated for discriminant validity violations. The measurement model provided satisfactory results: average variance extracted (AVE) >0.50, construct reliability (CR) >0.7, AVE > maximum shared variance (MSV), and Cronbach's alpha >0.7 for all constructs. Moreover, the results revealed sufficiently high loadings per item per construct (>0.620), and all factor loadings were statistically significant. Therefore, both the convergent validity and discriminant validity of the constructs were strongly supported and the item reliability of the scales was confirmed. Normality testing showed that the skewness of each variable was below 3.0 and that the kurtosis of each variable was below 10.0; therefore, a normality assumption was supported [12] as well. Moreover, standardized residuals were examined. Only two pairs of variables were slightly above the cutoff value (i.e., 4.3), and the rest were below 4.0. CFA results indicated a sufficient fit to the data ($\varkappa 2$=1342, df=684, $p<0.001$, $\varkappa 2$/df=1.963, NFI=0.927, IFI=0.963, TLI=0.957, CFI=0.963, RMSEA=0.052).

Tables 2 and 3 present detailed information on the constructs, and the reliability and validity results of the measurement model.

4. Analysis and Findings

The structural equation modeling analysis was employed to test the proposed model and hypotheses via AMOS 24. The goodness-of-fit statistics of the proposed model revealed that the model could reasonably fit the data ($\varkappa 2$=1538, df=703, $p<0.001$, $\varkappa 2$/df=2,189, NFI=0.916, IFI=0.953, TLI=0.947, CFI=0.953, RMSEA=0.058). While crew (β=0.540, $p<0.001$), yacht (β=0.251, $p<0.001$), gastronomy (β=0.104, $p<0.05$), and activity (β=0.113, $p<0.05$) significantly affect OSQ, CCI (β=0.02, $p>0.05$) does not. Crew is by far the most important factor having an effect on SQ, and yacht ranked second in importance to SQ, following crew. Thus, H1, H2, H3, and H4 were supported, and H5 was rejected. SOC (β=0.464, $p<0.001$) was positively related with CCI. Thus, H6 received strong support. CCI (β=0.161, $p<0.001$), destination (β=0.388, $p<0.001$), and OSQ (β=0.393, $p<0.001$) were significant predictors of CS and thus H7, H8, and H9 were supported. CS (β=0.313, $p<0.001$) and OSQ (β=0.621, $p<0.001$) were positively associated with LY, so H10 and H11 were supported. Moreover, the mediation effect in the model was also tested. The bootstrapping method (bootstrap=2000) was used to test the mediating effects of CS on the relationships between OSQ and LY; the bootstrapping indicated that CS partially mediates the effects of OSQ on LY (β=0.126, $p<0.001$). Thus, H12 was supported. Figure 2 shows the related results.

5. Discussion

In this study, we attempted to evaluate the influence of yacht charter service concept attributes, specifically customer interaction and similarity, on SQ and CS. BV is a relevant research context as its duration and service environment make it possible to gage social interaction between customers and its effect on satisfaction. We put forward 12 hypotheses based on the literature and qualitative research findings, and 11 were supported.

The results revealed that the crew is the most crucial element of overall OSQ, followed by yacht, activities, and gastronomy. In [47], the authors emphasized that employees have sometimes been considered the service itself. Hence, crew' behaviors and competencies have crucial importance for the concept. Moreover, considering the limited-service environment, their receptiveness toward customers' privacy needs will positively affect SQ. The findings also indicate that cabin comfort (i.e., size, air condition, and equipment) is another essential factor of the yacht charter SQ. Moreover, the yacht should have required warnings and information to create a risk-free environment and have sufficient space in shared areas such as the deck and dining table. The food quality onboard is highly essential for customers. Besides, offering activities in various may positively influence OSQ.

In contrast to literature [48], other customers did not significantly affect consumers' SQ perceptions. Rather, the presence of other customers may have had a direct effect on CS. The lack of influence of other customers on the SQ can be explained by considering the type of yacht charter service purchased. In exclusive yacht charter, customers decide on the other participants, which can be family members or friends. Thus, they might consider that since other customers have not been provided by the company, they may not affect the SQ compared with other attributes. However, in cabin charter, customers are unacquainted people who purchase the tour from the yacht company independently. Like in Poland [49], there is price-based competition in the Turkish yacht charter market. Hence, the priority of yacht charter companies is to fill the yacht

Table 2. *Correlations and descriptive statistics*

Constructs	Mean	Standard deviation	1	2	3	4	5	6	7	8	9	10
Gastronomy	5.84	1.19	**1.0**									
Activities	3.48	1.97	.25	**1.0**								
Yacht	5.04	1.48	.57	.47	**1.0**							
Destination	6.10	1.06	.67	.19	.56	**1.0**						
Crew	5.90	1.36	.66	.31	.69	.72	**1.0**					
CCI	6.13	1.19	.44	-.01	.26	.49	.44	**1.0**				
OSQ	5.33	1.53	.62	.41	.74	.55	.79	.31	**1.0**			
SOC	5.69	1.31	.12	-.05	.07	.10	.12	.41	.16	**1.0**		
CS	6.19	1.16	.55	.14	.53	.61	.71	.44	.65	.17	**1.0**	
LY	5.69	1.71	.51	.34	.64	.51	.76	.32	.80	.12	.73	**1.0**

CCI: Customer-to-customer interaction, SOC: Similarity with other customers, LY: Loyalty, OSQ: Overall service quality, CS: Customer satisfaction

Table 3. *Reliability and validity statistics*

Constructs	α	CR	AVE	MSV
Gastronomy	.86	.88	.71	.57
Activities	.86	.86	.68	.29
Yacht	.85	.86	.62	.58
Destination	.87	.87	.64	.60
Crew	.97	.97	.83	.68
CCI	.93	.94	.84	.21
OSQ	.96	.96	.89	.68
SOC	.93	.92	.70	.21
CS	.98	.97	.91	.53
LY	.98	.98	.93	.67

α: Cronbach's alpha, CR: Construct reliability, AVE: Average variance extracted, MSV: Maximum shared variances, CCI: Customer-to-customer interaction, SOC: Similarity with other customers, LY: Loyalty, OSQ: Overall service quality, CS: Customer satisfaction

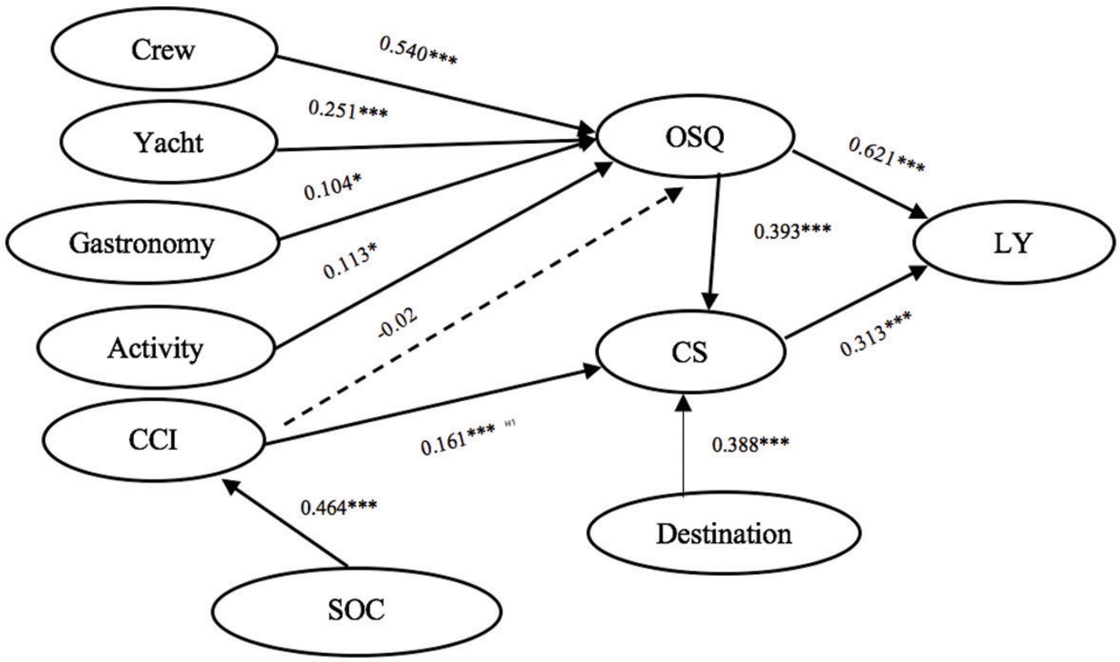

Figure 2. *Structural model results*

**p<0.05, ***p<0.001*

Statistically significant

Statistically insignificant

CCI: Customer-to-customer interaction, SOC: Similarity with other customers, LY: Loyalty, OSQ: Overall service quality, CS: Customer satisfaction

capacity, and it is generally not known which customers will share the same yacht until the last moment. For this reason, cabin charter customers may not have seen this element as a significant factor in their SQ expectations, since they are not provided with clear information on the other customers beforehand.

OSQ served as an antecedent of customer satisfaction and loyalty and had a greater effect on LY than CS. Generally, the opposite is expected, but some prior studies have reached similar results [43]. The BV customer might think that loyalty to service providers depends on the SQ the company provides. Moreover, the authors found that CS partially mediates the effects of overall SQ on LY. Several extant studies also suggest that CS plays a mediating role between SQ and LY [37,38,50].

Moreover, the destination factor is a strong influencer of CS, and this finding is consistent with several studies in the literature e.g., [19,20,51]. The service concept's unique side is the quiet and peaceful bays in the destination. The crowding at the bays might negatively affect destination attractiveness. Hence, managing and controlling the crowding is strongly suggested the service managers. BV destination publicity should be undertaken via brochures or promotional films that inform the voyagers about the destination attractions. Crew training on destination may increase CS.

CCI is a significant factor for CS, which is specifically examined in the study. BV is an interaction-dominant tourism concept that requires living in a limited space with several people for a relatively long period. That is, many interactions occur in the BV service environment, which triggers co-creation of value [2]. These results are in line with studies confirming a strong relationship between CS and CCI [22,25]. Our findings also reveal that the significance of CCI on satisfaction varies depending on the industry. Studies conducted on cruise customers also show that the CCI's effect on satisfaction was implicit [34] or had only an indirect effect [27,12]. There are hardly any studies investigating the service expectations of yacht tourism customers. It can be considered that yacht tourism should be examined under the cruise tourism context. However, while the limited customers experience the service together almost all the time in a small yacht in a yacht charter, thousands of people are hosted on a huge ship in a cruise environment. The yacht charter customers described the components of service experience as a triangle of nature, other people, and the services offered on the yacht. In other service contexts, such as hospitality, restaurant, or cruise, a relationship may only be established with other customers coincidentally. The authors of [34] stated that cruise customers have little interest in socializing with other customers. Nevertheless, meeting new people and developing friendships is essential for yacht customers [11], and the yacht charter provides such an environment where people can get to know other people and introduce themselves like never before. Therefore, a recent study provides a theoretical contribution indicating the sector-specific importance of the CCI concept.

The findings reveal that similarity between customers is positively related to CCI. The authors of [32] suggested that the perception of homogeneity in CS is more important on long trips and the influence of homogeneity on CS will obviously increase. Furthermore, studies on similarity and CCI are rare in the relevant literature and have mostly employed qualitative methods. Our study validates some similarity features in the literature and adds education level and life style as other similarity features that have rarely been tested in prior studies.

Although it is challenging to control, managers should consider that the customer interaction dimension is vital for service satisfaction. As customers' similarity increases, social interaction is enhanced and their satisfaction increases accordingly. The similarity concept involves age, education, and lifestyle for the yachters. Generally, the yachters are well-educated, and they may want to involve intellectual interaction while on the yacht. Furthermore, the yacht charter is a premium type of tourism product; therefore, uniqueness cannot be created solely by physical service elements. The yachters are highly experienced tourists, and they do not want to compromise on fundamentals such as feeling peaceful amidst nature. Customer similarity can establish a more comfortable environment and customers can relax easily under these conditions. Thus, customer segmentation tools can be used to match the most compatible voyagers. For example, online platforms can provide information to voyagers to find other customers having similar characteristics.

Since BV is a high-contact service context, crew training is imperative to provide top-level hospitality. The crew should also handle consumer interactions in the yacht, and they sometimes take on the initiator role to start relationships in the group.

6. Conclusion

Like many other researches in relevant literature, the sample size and customer variety regarding nationality are noticeable limitations of this study. Internationally diverse and larger samples may provide more generalizable insights. Our results emphasize again that voyagers have different expectations, and the yacht market has several segments. Future segmentation studies have the potential to develop better BV services and to design better target marketing practices. Furthermore, the customer similarity scale can be further studied with different characteristics to reach service-specific similarities. Future studies can also investigate the antecedents and outcomes of CCI in other nature-based contexts such as caravan campers.

Ethics

Ethics Committee Approval: Ethics committee approval was obtained from Yaşar University Social Sciences Institute (date: 01/06/2018, no: 5200).

Authorship Contributions

Data Collection or Processing: N. Paker, Analysis or Interpretation: N. Paker, O. Gök, Literature Review: N. Paker, O. Gök, Writing, Reviewing and Editing: N. Paker, O. Gök.

Funding: The authors declared that this study received no financial support.

References

[1] L. Miao, A.S., Mattila and D. Mount, "Other consumers in service encounters: A script theoretical perspective," *International Journal of Hospitality Management*, vol. 30, pp. 933-941, December 2011.

[2] I. Rihova, D. Buhalis, M. Moital and M.B. Gouthro, "Conceptualising customer-to-customer value co-creation in tourism," *International Journal of Tourism Research,* vol.17, pp. 356-363, Jan 2015.

[3] L. Hanks and N. Line, "Perceived similarity in third places: Understanding the effect of place attachment, "*International Journal of Hospitality Management*, vol. 86, pp. 102455, Apr 2020.

[4] A. Alcover, M. Alemany, M. Jacob, M. Payeras, A. Garcia and L.M. Ribes, "The economic impact of yacht charter tourism on the Balearic economy," *Tourism Economics*, vol.17, pp.625-638, Jun 2011.

[5] R. Alkier, "Perspectives of development of luxury nautical tourism in the Republic of Croatia," *Pomorski Zbornik*, vol. 56, pp. 109-124, 2019.

[6] S.A.K. Ioannidis, "An overview of yachting tourism and its role in the development of coastal areas of Croatia," *Journal of Hospitality and Tourism Issues*, vol.1, pp. 30-43, Dec 2019.

[7] M.L. Miller and J. Auyong, "Coastal zone tourism. A potent force affecting envirionment and society," *Marine Policy,* pp.75-99, Mar 1991.

[8] S.C. Chen, M.C. Wu, and C.H. Chen, "Employee's personality traits, work motivation and innovative behavior in marine tourism industry," *J. Service Science & Management,* vol.3, pp.198-205, June 2010.

[9] F. Sevinç and T. Güzel, "Sustainable yacht tourism practices," *Management & Marketing*, vol. 15, pp.61-76, Oct 2018.

[10] M. Orams, *Marine tourism: development, impacts and management,* London & New York: Routlege, 1999.

[11] N. Paker, and C.A. Vural, "Customer segmentation for marinas: evaluating marinas as destinations," *Tourism Management*, vol. 56, pp.156-171, Oct 2016.

[12] B.L. Chua, S. Lee, B. Goh and H. Han, "Impacts of cruise service quality and price on vacationers' cruise experience: moderating role of price sensitivity," *International Journal of Hospitality Management*, vol. 44, pp.131-145, Jan 2015.

[13] V.B. Teye and D. Leclerc, "Product and service delivery satisfaction among North American cruise passengers" *Tourism Management*, vol.19, pp.153-160, Apr 1998.

[14] R.J. Kvortnic, "Shipscape influence on the leisure cruise experience. International Journal of Culture," *Tourism and Hospitality Research*, vol. 2, pp. 289-311, Oct 2008.

[15] H.J. Xie, D.L. Kerstetter and A.S. Mattila, "The attributes of a cruise ship that influence the decision making of cruisers and potential cruisers," *International Journal of Hospitality Management*, vol. 31, pp. 152-159, Mar 2012.

[16] J. Hwang and H. Han, "Examining strategies for maximizing and utilizing brand prestige in the luxury cruise industry," *Tourism Management*, vol. 40, pp. 244-259, Feb 2014.

[17] H. Qu and E.V.Y. Ping, "A service performance model of Hong Kong cruise travelers motivation factors and satisfaction," *Tourism Management*, vol. 20, pp. 237-244, Apr 1999.

[18] K.S. Chon, "Understanding recreational traveler's motivation, attitude and satisfaction," *The Tourist Review*, vol. 44, pp. 3-7, Jan 1989.

[19] Y. Yoon, and M. Uysal, "An Examination of The Effects of Motivation And Satisfaction on Destination Loyalty: A Structural Model," *Tourism Management,* vol. 26, pp. 45-56, Feb 2005.

[20] M. Devesa, M. Laguna and A. Palacios, "The role of motivation in visitor satisfaction: empirical evidence in rural tourism", *Tourism Management*, vol. 31, pp. 547-552, Aug 2010.

[21] E. D. Eris, "Uluslararası pazarlarda Türk marinalarının çekiciligi ve pazarlama Stratejileri," *Ege Akademik Bakıs,* vol.7, pp. 37-55, 2007.

[22] J. Yoo, T.J. Arnold, and G.L. Frankwick, "Effects of positive customer-to-customer service interaction," *Journal of Business Research,* vol. 65, pp. 1313-1320, Sept 2012.

[23] C. Lovelock and L. Wright, *Principles of Service Marketing and Management*. 2nd ed. New Jersey: Prentice Hall, 2002.

[24] C.L. Martin, and C.A. Pranter, "Compatibility management: customer-to-customer relationships in service environments," *Journal of Services Marketing*, vol. 3, pp. 5-15, Mar 1989.

[25] C.H.J. Wu, "The impact of customer-to-customer interaction and customer homogeneity on customer satisfaction in tourism service-The service encounter prospective," *Tourism Management,* vol. 28, pp. 1518-1528, Dec 2007.

[26] W. Wei, Y.T. Lu, L. Miao, L.A. Cai, and C. Wang, "Customer-customer interactions (CCIs) at conferences: an identity approach," *Tourism Management*, vol. 59, pp.154-170, Apr 2017.

[27] J. Huang and C.H.C. Hsu, "The impact of customer-to-customer interaction on cruise experience and vacation satisfaction," *Journal of Travel Research,* vol. 49, pp. 79-92, May 2009.

[28] R. Moore, M.L. Moore, and M. Capella, "The impact of customer-to-customer interactions in a high personal contact service setting," *Journal of Services Marketing,* vol.19, pp.482-491, Dec 2005.

[29] A.D. Brack, and M. Benkenstein, "Responses to other similar customers in a service setting – analyzing the moderating role of perceived performance risk," *Journal of Services Marketing,* vol.28, pp.138-146, May 2014.

[30] H. Kwon, S. Ha and H. Im, "The impact of perceived similarity to other customers on shopping mall satisfaction," *Journal of Retailing and Consumer Services*, vol. 28, pp. 304–309, Jan 2016.

[31] M.V. Thakor, R. Suri and K. Saleh, "Effects of service setting and other consumers' age on the service perceptions of young consumers." *Journal of Retailing,* vol. 84, pp. 137-149, Jun 2008.

[32] E.D. Brocato, C.M. Vooerhees, and J. Baker, "Understanding the influence of cues from other customers in the service experience: a scale development and validation," *Journal of Retailing*, vol.88, pp.384-398, Sept 2012.

[33] S.S. Hyun and H. Han, "Luxury cruise travelers: other customer perceptions," *Journal of Travel Research,* vol. 54, pp. 107-121, Dec 2013.

[34] A. Papathanassis, "Guest-to-guest interaction on board cruise ships: Exploring social dynamics and the role of situational factors," *Tourism Management*, vol. 33, pp. 1148-1158, Oct 2012.

[35] H.H. Hu, J. Kandampully and T.D. Juwaheer, "Relationships and impacts of service quality, perceived value, customer satisfaction, and image: an empirical study, "*The Service Industries Journal*, vol.29, pp.111-125, Feb 2009.

[36] M.D. Richard and A.W. Allaway, "Service quality attributes and choice behavior," *Journal of Services Marketing*, vol. 7, pp. 59-68, Jan 1993.

[37] C-V. Priporas, N. Stylos, L.N. Vedanthachari and P. Santiwatana, "Service quality, satisfaction, and customer loyalty in Airbnb accommodation in Thailand," *International Journal of Tourism Research*, vol. 19, pp. 1-12, Aug 2017.

[38] A. Caruana, "Service loyalty: The effects of service quality and the mediating role of customer satisfaction," *European Journal of Marketing,* vol. 36, pp. 811-828, Aug 2002.

[39] F. Bilika, M.Safari and S. Mansori, "Review of Empirical Studies of Service Quality, Customer Satisfaction, and Loyalty, "*Journal of Marketing Management and Consumer Behavior,* vol.1, no.2, pp.1-11, 2016.

[40] A.G. Woodside, L.L. Frey and R.T. Daly, "Linking Service Quality, Customer Satisfaction, and Behavioral Intention" *Journal of Health Care Marketing,* vol. 9, pp. 5-17, Dec 1989.

[41] J.J. Cronin and S.A. Taylor, "Measuring service quality: a reexamination and extension, "*Journal of Marketing,* vol. 56, pp. 55-68, Jul 1992.

[42] W.A. Elias, F.M. Ahmed and M. Ezzat, "Assessing the tourists satisfaction towards yacht tourism services in the red sea coast, Egypt,", *Minia Journal of Tourism and Hospitality Research*, vol. 9, pp. 157-170, Jun 2020.

[43] T.S. Dagger, J.C. Sweneey and L.W. Johnson, "A hierarchical model of health service quality scale development and investigation of an integrated model," *Journal of Service Research,* vol.10, pp.123-142, Nov 2007.

[44] J.J. Cronin, M.K. Brady and G.T.M. Hult, "Assessing the effects of quality, value, and customer satisfaction on consumer behavioral

intentions in service environments, "*Journal of Retailing*, vol.76, pp.193-218, Summer 2000.

[45] S. Baloglu and M. Uysal, "Market segmentation of push and pull motivations: a canonical correlation approach," *International Journal of Contemporary Hospitality Management*, vol. 8, pp. 32-38, Jun 1996.

[46] G. Fuchs and A. Reichel, "Tourist destination risk perception: the case of Israel," *Journal of Hospitality & Leisure Marketing*, vol. 14, pp. 83-108, Oct 2008.

[47] K. Tajeddini, "Customer orientation, learning orientation, and new service development: an empirical investigation of The Swiss Hotel industry," *Journal of Hospitality & Tourism Research,* vol. 35, pp. 437-468, Nov 2011.

[48] Y.J. Ko, and D.L. Pastore, "A hierarchical model of service quality for the recreational sport industry," *Sport Marketing Quarterly*, vol. 14, pp. 84-97, 2005.

[49] A. Lapko, "Problems of yacht charter companies in Poland," *European Journal of Service Management*, vol. 1, pp. 165-172, 2018.

[50] A. Meesalaa and J.Paul, "Service quality, consumer satisfaction and loyalty in hospitals: thinking for the future," *Journal of Retailing and Consumer Services,* vol. 40, pp. 261-269, Jan 2018.

[51] E. Aydoğan and M. Kadıoğlu, "Yat turizminin turizm sektörü içerisindeki yeri ve önemi," *Journal of Eta Maritime Science*, vol. 6, pp. 243-254, Jul 2017.

ORIGINAL RESEARCH (AR) DOI: 10.4274/jems.2021.88155

Journal of ETA Maritime Science 2021;9(3):168-176

A Sequential Solution with MCDM Methods at the Motor-Yacht Construction Problem

G. Nilay Yücenur

Beykent University, Faculty of Engineering and Architecture, Department of Industrial Engineering, İstanbul, Turkey

Abstract

Yachting is quite popular in recent years and it is defined as an "entertainment and vacation industry in the sea." The yachting industry as parallel to the world economy is developing rapidly in financial, industrial, and physical spaces in the world and in Turkey as well. With this development, yachting provides foreign currency inflow to Turkey in the tourism sector as well as in the construction industry according to the Turkish Statistical Institute's data. Turkey is greatly known in the European yacht and boat market particularly in terms of engine manufacture and specialization, low labor cost, and quality advantages. This study is aimed to determine a suitable shipyard's city to carry out a 30-meter motor yacht. In this research study, a model was suggested for selecting the appropriate shipyard for motor-yacht construction with a proposed solution methodology. In the research methodology, 15 criteria were determined for evaluating 4 shipyards that have different properties and are located in different cities of Turkey. In the first phase of the solution, SWARA was used to obtain the importance weights of the criteria. In the second phase of the solution, alternatives were evaluated with COPRAS according to the calculated importance weights. The proposed model and solution methodology were conducted through an explanatory sample.

Keywords

MCDM, SWARA, COPRAS, Yacht and boat industry, Shipyard location

1. Introduction

In recent years, technological developments in the world and intense competition have greatly influenced the development of the shipbuilding industry. As a result, the structure and capacity of ships have increased. The maritime sector and boat production in the world is among the sectors that governments have prioritized in the development of the industry in many countries, as it produces high-quality employment and added value in the region as well as almost no harm to the environment.

The yachting market, which developed parallel to the maritime sector, has been one of the most popular business areas in recent years due to the characteristics of target customers and market trends. The demand for luxury yachts also affects many economic sectors such as textiles, fashion, jewelry, and furniture. The consumers' desires and demands for new products ensure these supporting sectors to develop themselves as well. Companies with the highest production quality and brand awareness in these sectors create new markets for them as well as strengthen their position and brand image in the richest consumer group in the world. With the developing yachting market, the number of produced yachts increased from 108 to 180 between 2000-2010 in Turkey. Besides this, the share of yacht production in exports of ships and yachts on the basis of goods groups was 11.7%, while the share of the ship sub-industry was 4.8% in 2015-2016. The growing rate of the yacht sub-industry cannot be belittled [1,2].

Therefore, this paper aims to select the most appropriate shipyard among four alternatives, which are in different cities in Turkey for constructing a 30-meter motor yacht. In this study, a sequential methodology consisting of The Stepwise Weight Assessment Ratio Analysis (SWARA) and Complex Proportional Assessment (COPRAS) was proposed.

In the literature review, there are lots of applications in many different areas about SWARA, which determines the

Address for Correspondence: Ganimet Nilay Yücenur, Beykent University, Faculty of Engineering and Architecture, Department of Industrial Engineering, İstanbul, Turkey
E-mail: nilaynil@hotmail.com
ORCID ID: orcid.org/0000-0002-2670-6277

Received: 02.06.2021
Accepted: 17.08.2021

To cite this article: G.N. Yücenur, "A Sequential Solution with MCDM Methods at the Motor-Yacht Construction Problem." *Journal of ETA Maritime Science*, vol. 9(3), pp. 168-176, 2021.

criteria's importance weights. This new method enables researchers to solve real-life problems. For example, with the SWARA method, Rani et al. [3] evaluated the solar panel, Mostafaeipour et al. [4] ranked locations for geothermal energy, Mardani et al. [5] assessed key challenges of digital health interventions, Chen et al. [6] modeled the landslide susceptibility, Naeini et al. [7] analyzed the development of biodiesel production, Mousavi-Nasab and Sotoudeh-Anvari [8] evaluated renewable energy resources, and Balali et al. [9] identified the passive energy consumption.

Likewise, according to the literature review, the COPRAS method, which is applied to evaluate problems according to complex criteria, has been used to solve problems in different fields. For example, with the COPRAS method, Roozbahani et al. [10] planned the water transfer inter-basin, Dhiman and Deb [11] determined hybrid wind farms, Rani et al. [12] applied the method in pharmacological therapy, and Kathamore and Bachchhav [13] classified the bio-based lube oil. Mishra et al. [14] evaluated the healthcare in hazardous waste recycling, Kumari and Mishra [15] selected the green supplier, Garg and Arora [16] made a decision with possibility intuitionistic, and Singh et al. [17] designed brake friction materials.

Even though the solution with these methods is included in the studies of Zarbakhshnia et al. [18], Valipour et al. [19], Yücenur et al. [20], Ansari et al. [21], Mishra et al. [22], and Rani et al. [23] about the selection of a third-party reverse logistics provider, the allocation of risk in water and sewerage projects, selection of city for biogas facility, evaluation of solutions to sustainable remanufacturing supply chain risks, evaluation of bioenergy production process, and selection of sustainable supplier, there is no similar study on yachting and the marine industry available in the literature.

2. Yachting and Boat Industry in Turkey

The yacht and boat manufacturing industry has a very high added value, a high export rate, and provides employment to countries. Various service sectors serve this manufacturing industry. The integration of products like machinery, iron and steel, wood, paint-chemistry, electricity, electronics, textile, decoration, rubber, and plastic are used in shipyards. The yacht and boat industry is different from the shipbuilding industry in terms of both the content and scope and the technology it applies. While the shipbuilding industry needs large investments, long periods, and large seaside locations, the yacht and boat manufacturing industry sometimes can operate in a shorter time and in smaller places with a smaller investment. Although investments in shipyards that build luxury yachts are higher than those made in shipyards that build normal ships with a length of 30 m, depending on the materials used, the technology used, the desired features and demands, the yacht industry is one of the sectors with the highest added value [2].

In terms of the geographical structure of Turkey, the yacht and boat industry has a huge advantage. Besides this geographical advantage, the industry has workmanship and material qualities, cost advantages, owned marinas, yacht locations, and the ability of manufacturers to meet customer demands. With these positive aspects, the sector is quite open to development. Besides these, the training of qualified naval architects with activities of shipbuilding, ship machinery, ship electricity, casting, and profession branches in education activities revised with the contributions of the naval architecture and marine sciences faculties of universities and the shipbuilding industrialists' union is the important advantages of Turkey in this sector. Although Turkey's entry into the sector was very new compared to its competitors in Europe, it has gained an important place in the sector in a short time. Considering the number of boats delivered over 30 meters, Turkey ranked fourth after Italy, the USA, and the Netherlands for 2011 [1].

The Turkish boat and yacht building industry, which has developed rapidly since the 1980s, has become one of the world's leading producers thanks to its workforce, quality manufacturing, modern technology, and superior entrepreneurship spirit.

As the sector grew rapidly in the country, parallel to this, the number of active shipyards, which was 37 in 2002, reached 79 by the end of 2015. These shipyards are concentrated in the Marmara and Western Black Sea regions, and about 23 shipyards are in the investment phase of the country. In addition, 15 new shipyard areas have been identified [2].

In Turkey, superyachts (24 m and above) construction has especially shown a steady increase since 2007. According to data from 2010, Turkey was the third manufacturer in the world due to the quantity and length of delivered superyachts. Turkey was again third in the world with 68 projects and with a total of 3,005 meters in length in 2014. The country was again third in 2016 and maintained its place in the sequencing all over the world according to 2017's data with 3508-meter superyacht orders [2].

The sector is highly influential on the country's economy. Almost all ships built in shipyards in Turkey between 2008-2012 have been exported to the European Union countries and the number of exports of new ships and yachts in 2012 was 813 million dollars [24].

3. Research Problem

While the yacht building industry and used shipyards for yacht building have an important place for the development of Turkey in the maritime sector, the country also has strategic importance for the development of the yacht building industry in Europe. The geographical position, climatic conditions, and production costs provide the country with a great competitive advantage in terms of yacht building.

In this study, the selection of the appropriate shipyard for the construction of a 30-meter motor yacht in the developing yacht industry is carried out by a sequential methodology integrating SWARA/COPRAS.

Figure 1 shows the proposed research model with 15 criteria and 4 alternatives.

3.1. Problem

The problem of this paper is to select the most appropriate alternative shipyard for a 30-meter motor-yacht construction in Turkey.

3.2. Research Criteria

To determine the shipyard to be selected in the construction of the 30-meter motor yacht, 15 criteria were determined according to the literature review and sector experts' opinions. Table 1 shows the evaluation criteria's explanations.

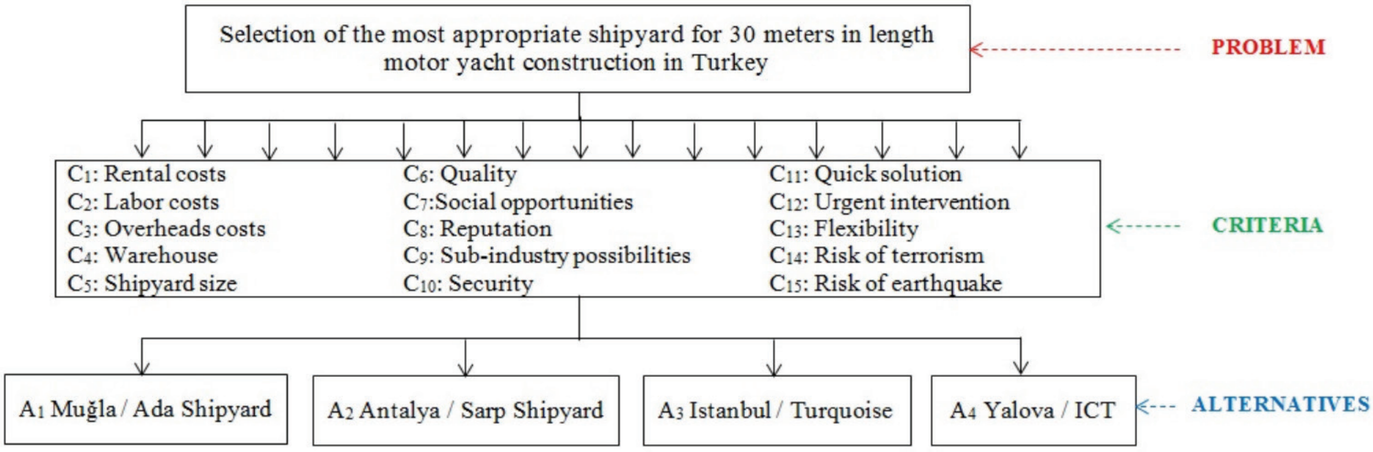

Figure 1. *Proposed research model*

Table 1. *Evaluation criteria and their explanations*

C_1	Rental costs	It is the rental fee requested from companies that want to make the project in the shipyard.
C_2	Labor costs	Depending on the quality of the work done with the city where the shipyard is located, this amount is paid to the qualification worker.
C_3	Overhead costs	Overhead costs are the shipyards' general expenses such as electricity, water, natural gas, and security.
C_4	Warehouse	It is associated with the shipyard area. A storage space can be provided for all shipbuilders, even in different sizes.
C_5	Shipyard size	Shipyard's dimensions. The shipyards' sizes were taken close to each other in calculations for the purpose of the correctness of comparison for all cities.
C_6	Quality	It is the work that the shipyards put out. The quality is proportional to the knowledge, experience, and qualified workforce of shipyards.
C_7	Social opportunities	Activity facilities for blue- and white-collar workers in their off-hours.
C_8	Reputation	The perception depending on the production capacity and quality of the shipyard from the past until today.
C_9	Sub-industry possibilities	The ease of material and labor supply, which is the main component of real manufacturing.
C_{10}	Security	The protection of the shipyard against theft and other crimes.
C_{11}	Quick solution	The duration of remediation of production-related problems in the shipyard by additional labor and/or material supply.
C_{12}	Urgent intervention	Intervention duration and intervention quality level to an accident in the shipyard. It is about the shipyard's location and urban development.
C_{13}	Flexibility	The variety of products that can be done in the shipyard. The manufacturability of wood, composite, aluminum, and steel boats, which are the 4 main materials in yacht manufacturing.
C_{14}	Risk of terrorism	The possibility of a terror attack to the shipyard's city.
C_{15}	Risk of earthquake	The likelihood of an earthquake on the city/residential area where the shipyard is located.

3.3. Research Alternatives

Four shipyards with different characteristics found in different cities where a 30-meter yacht construction can be carried out were determined as alternatives. These shipyards have been preferred because they are the most established companies in their regions, they are of different sizes, and they are located in different regions to use the distinctive features of the criteria. For this purpose, the alternative shipyards that will be considered to solve the problem are found in Muğla, Antalya, İstanbul, and Yalova.

- **A_1 Muğla/Ada Shipyard:** The Ada Shipyard is located in the southwest of Turkey. It has ISO 9001:2008, OHSAS 18001:2007, and ISO 14001:2004 standards about quality, occupational health, and the environment. The shipyard is a reliable shipyard that provides a customer-focused service and attaches importance to quality and detail with years of experience in shipbuilding.

- **A_2 Antalya/Sarp Shipyard:** This shipyard is located in the free zone of Antalya in the south of Turkey. The Sarp shipyard was specifically designed for the construction and refitting of luxury motors and sailing yachts. It also has ISO 9001, ISO 14001, and OHSAS 18001.

- **A_3 İstanbul/Turquoise:** This shipyard was established in 1997 by two Turkish boat companies. The Turquoise Yachts, which is located in İstanbul's most crowded city in Turkey, offers quality turnkey solutions in its facilities to yacht lovers.

- **A_4 Yalova/ICT:** Located in Yalova, the ICT Shipyard was established on a 31,000-square meter seafront land, with a total closed facility of 4,500 square meters. The location of the shipyard has an important advantage by staying out of commercial shipyard areas and being separated from sandblasting and all other negativities.

4. A Proposed Solution Methodology with SWARA & COPRAS

Turkey with its long coasts, yacht tourism facilities, and wealth of culture and history, is an important international market, especially for superyachts. In this paper, a methodological framework has been established to solve the problem of shipyard selection that is suitable for yacht construction due to all these sectoral developments. A solution was proposed in which the alternatives are evaluated according to criteria established by decision makers and two MCDM methods were integrated to find the most appropriate solution to the problem. SWARA was used in the first step of the solution method for weighing of determined criteria. In the second step of the solution method, COPRAS was used to select the most suitable shipyard for the 30-meter motor-yacht construction.

The COPRAS method integrated with SWARA in the study is based on experts' opinions. This proposed integrated method has been chosen because it provides convenience, coordination, and simplicity in the data collection. The fact that complex processes are not needed to evaluate the criteria in the method and that the solution of the problem can be done in a short time are other advantages of this integrated method. Figure 2 shows the integration of this proposed integrated method.

4.1. SWARA

The most important issue in many MCDM problems is to determine the criteria weights. In this paper, SWARA was used for determining the criteria weights. The SWARA method, which is a new method of weight determination and which has been used frequently in recent years, has been put forward by Keršuliene et al. [25]. The method offers the opportunity to evaluate criteria weights

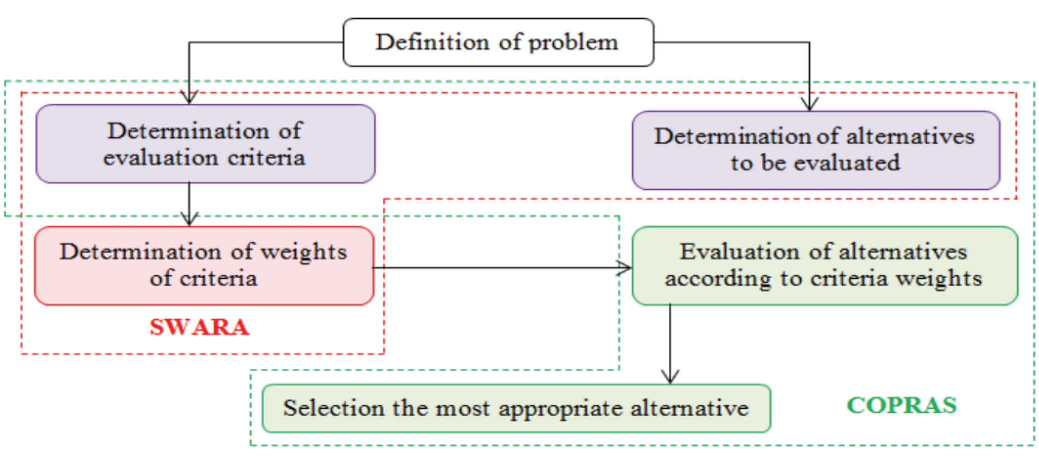

Figure 2. *Decision-making process by the SWARA-COPRAS method*

SWARA: The Stepwise Weight Assessment Ratio Analysis, COPRAS: Complex Proportional Assessment and to use the knowledge and experience of experts in calculations. Thus, experts have a chance to prioritize the criteria based on their needs and target characteristics.

Application steps of SWARA [26]:

Step 1: All criteria are sorted from the most important to the least important one by each decision maker's individual judgment. The same criteria are then sorted again due to fist ranking. p_j^k are obtained ($0 \leq p_j^k \leq 1$) in this sorting. Table 2 shows the first ordering of criteria.

Step 2: The relative average importance scores ($\overline{P_j}$) for all criteria are calculated for all criteria using equation 1. Table 2 shows the second ordering and the $\overline{P_j}$ of criteria.

$$\overline{P_j} = \frac{\sum_{k=1}^{l} p_j^k}{l}; \; j = 1, 2, \ldots, n \tag{1}$$

Here, l is the number of decision makers.

Step 3: Criteria are listed according to the $\overline{P_j}$ in descending order. The s_j values (comparative importance of average value) are obtained as seen in Table 3. According to this table, the order of importance of the criteria was obtained as $C_9>C_1>C_3>C_2>C_5>C_4>C_6>C_8>C_{10}>C_{13}>C_{12}>C_{11}>C_7>C_{15}>C_{14}$.

Step 4: With the binary comparison for all criteria, the coefficient value c_j is obtained using equation 2. $c_j=1$ for the criterion with the greatest s_j.

$$c_j = s_j + 1; \; j = 1, 2, \ldots, n \tag{2}$$

Step 5: For all criteria, the corrected weights s_j' are calculated with equation 3. $s_j'=1$ for the first criterion in ranking.

$$s_j' = \frac{s_{j-1}'}{c_j} \tag{3}$$

Step 6: For all criteria, the final importance weights w_j are obtained with equation 4.

$$w_j = \frac{s_j'}{\sum_{j=1}^{n} s_j'}; \; j = 1, 2, \ldots, n \tag{4}$$

Table 3 shows c_j, s_j', and w_j values for 15 criteria.

As seen in Table 3, C_9 (with a score of 9.5%) is the most important criterion according to the proposed model and experts' opinion. C_1 (with a score of 9.1%) and C_3 (with a score of 9.0%) follow this criterion, while the least important one is C_{14} (with a score of 4.1%).

4.2. COPRAS Method

After the calculation of criteria weights with SWARA, COPRAS is used to evaluate the alternatives. It is not possible for a single criterion to express the entirety of objectives being watched by the users. For this reason, COPRAS was developed by the researchers [27]. COPRAS includes the phasing and ranking of alternatives based on the importance and utility of the criteria. At the same time, the method can easily be applied to complex criteria and problems involving numerous alternatives.

***Table 2**. First and second ordering and $\overline{P_j}$ of fifteen criteria*

		Decision makers				Decision makers				
Criteria		DM_1	DM_2	DM_3	DM_4	DM_1	DM_2	DM_3	DM_4	$\overline{P_j}$
C_1	Rental cost	4	1	3	2	0.85	1.00	0.85	0.90	0.90
C_2	Labor cost	3	2	4	3	0.90	0.95	0.80	0.85	0.88
C_3	Overhead costs	2	3	1	4	0.95	0.90	1.00	0.70	0.89
C_4	Warehouse	6	7	7	5	0.75	0.60	0.60	0.65	0.65
C_5	Shipyard size	5	5	6	6	0.80	0.75	0.65	0.60	0.70
C_6	Quality	7	6	10	7	0.70	0.70	0.40	0.50	0.58
C_7	Social opportunities	13	13	12	13	0.20	0.20	0.25	0.15	0.20
C_8	Reputation	8	8	5	8	0.65	0.50	0.70	0.40	0.56
C_9	Sub-industry possibilities	1	4	2	1	1.00	0.85	0.95	1.00	0.95
C_{10}	Security	10	9	8	11	0.55	0.45	0.55	0.25	0.45
C_{11}	Quick solution	11	12	13	12	0.50	0.25	0.15	0.20	0.28
C_{12}	Urgent intervention	12	10	11	9	0.45	0.40	0.30	0.35	0.38
C_{13}	Flexibility	9	11	9	10	0.60	0.35	0.45	0.30	0.43
C_{14}	Risk of terrorism	15	15	14	15	0.05	0.10	0.10	0.05	0.08
C_{15}	Risk of earthquake	14	14	15	14	0.15	0.15	0.05	0.10	0.11

Application steps of COPRAS [21,23]:

Step 1: m (number of alternatives-$i = 1, 2, \ldots, m$) and n (number of evaluation criteria-$j = 1, 2, \ldots, n$) values are determined.

Step 2: With equation 5, the decision matrix is formed. Here, C_j shows the decision criteria, w_j shows the importance weights of criteria that were calculated by the SWARA method, A_i shows alternative shipyards, and x_{ij} shows the value of alternative i according to criterion j ($i = 1, 2, \ldots, m$ and $j = 1, 2, \ldots, n$).

$$D = \begin{array}{c} \\ \\ A_1 \\ A_2 \\ A_3 \\ \vdots \\ A_m \end{array} \begin{array}{c} \begin{array}{cccccc} C_1 & C_2 & C_3 & C_4 & \cdots & C_n \\ w_1 & w_2 & w_3 & w_4 & \cdots & w_n \end{array} \\ \begin{bmatrix} x_{11} & x_{12} & x_{13} & \cdots & x_{1n} \\ x_{21} & x_{22} & x_{23} & \cdots & x_{2n} \\ x_{31} & x_{32} & x_{33} & \cdots & x_{3n} \\ \vdots & \vdots & \vdots & \vdots & \vdots \\ x_{m1} & x_{m2} & x_{m3} & \cdots & x_{mn} \end{bmatrix} \end{array} \tag{5}$$

Table 4 shows the decision matrix for the subjective and objective criteria assessment of the application problem.

Table 3. *$\bar{P}_j$, c_j, s'_j and w_j values*

Criteria		$\bar{P}_j$	c_j	s'_j	w_j
C_9	Sub-industry possibilities	0.95	1.00	1.00	0.095
C_1	Rental cost	0.90	1.05	0.95	0.091
C_3	Overhead costs	0.89	1.01	0.94	0.090
C_2	Labor cost	0.88	1.01	0.93	0.089
C_5	Shipyard size	0.70	1.18	0.79	0.076
C_4	Warehouse	0.65	1.05	0.75	0.072
C_6	Quality	0.58	1.08	0.70	0.067
C_8	Reputation	0.56	1.01	0.69	0.066
C_{10}	Security	0.45	1.11	0.62	0.059
C_{13}	Flexibility	0.43	1.03	0.61	0.058
C_{12}	Urgent intervention	0.38	1.05	0.58	0.055
C_{11}	Quick solution	0.28	1.10	0.53	0.050
C_7	Social opportunities	0.20	1.08	0.49	0.047
C_{15}	Risk of earthquake	0.11	1.09	0.45	0.043
C_{14}	Risk of terrorism	0.08	1.04	0.43	0.041

The objective information that is essential for the criteria, "C_1-*Rental cost*," "C_2-*Labor cost*," and "C_5-*Shipyard size*" are obtained.

Step 3: The normalization procedure of the decision matrix D is performed by equation 6 and the normalized decision matrix that is seen in equation 7 is obtained.

$$\tilde{x}_{ij} = \frac{x_{ij}}{\sum_{i=1}^{m} x_{ij}} \tag{6}$$

$$\tilde{D} = \begin{array}{c} \\ A_1 \\ A_2 \\ A_3 \\ \vdots \\ A_m \end{array} \begin{array}{c} \begin{array}{cccccc} C_1 & C_2 & C_3 & C_4 & \cdots & C_n \\ w_1 & w_2 & w_3 & w_4 & \cdots & w_n \end{array} \\ \begin{bmatrix} \tilde{x}_{11} & \tilde{x}_{12} & \tilde{x}_{13} & \cdots & \tilde{x}_{1n} \\ \tilde{x}_{21} & \tilde{x}_{22} & \tilde{x}_{23} & \cdots & \tilde{x}_{2n} \\ \tilde{x}_{31} & \tilde{x}_{32} & \tilde{x}_{33} & \cdots & \tilde{x}_{3n} \\ \vdots & \vdots & \vdots & \vdots & \vdots \\ \tilde{x}_{m1} & \tilde{x}_{m2} & \tilde{x}_{m3} & \cdots & \tilde{x}_{mn} \end{bmatrix} \end{array} \tag{7}$$

Step 4: The weighted decision matrix D^* that is seen in equation 8 is obtained by multiplying the normalized decision matrix and criteria importance weights. The importance weights of the criteria are obtained with SWARA for this application. Table 5 shows the weighted decision matrix.

$$D^* = \begin{array}{c} \\ A_1 \\ A_2 \\ A_3 \\ \vdots \\ A_m \end{array} \begin{array}{c} \begin{array}{ccccc} C_1 & C_2 & C_3 & \cdots & C_n \end{array} \\ \begin{bmatrix} d_{11} & d_{12} & d_{13} & \cdots & d_{1n} \\ d_{21} & d_{22} & d_{23} & \cdots & d_{2n} \\ d_{31} & d_{32} & d_{33} & \cdots & d_{3n} \\ \vdots & \vdots & \vdots & \vdots & \vdots \\ d_{m1} & d_{m2} & d_{m3} & \cdots & d_{mn} \end{bmatrix} \end{array} \tag{8}$$

Step 5: With equation 9, criteria are defined as useful (*max*) and useless (*min*). Useful criteria are placed in front of the matrix. Table 6 shows this matrix.

$$D^* = \begin{array}{c} \\ A_1 \\ A_2 \\ A_3 \\ \vdots \\ A_m \end{array} \begin{array}{c} \begin{array}{ccccccc} C_{max1} & C_{max2} & \cdots & C_{maxk} & \cdots & C_{\min(k+1)} & \cdots & C_{minn} \end{array} \\ \begin{bmatrix} d_{11} & d_{12} & \cdots & d_{1k} & \cdots & d_{1(k+1)} & \cdots & d_{1n} \\ d_{21} & d_{22} & \cdots & d_{2k} & \cdots & d_{2(k+1)} & \cdots & d_{2n} \\ d_{31} & d_{32} & \cdots & d_{3k} & \cdots & d_{3(k+1)} & \cdots & d_{3n} \\ \vdots & \vdots & \vdots & \vdots & & \vdots & \vdots & \vdots \\ d_{m1} & d_{m2} & \cdots & d_{mk} & \cdots & d_{m(k+1)} & \cdots & d_{mn} \end{bmatrix} \end{array} \tag{9}$$

Table 4. *Evaluating alternatives*

Criteria	C_1	C_2	C_3	C_4	C_5	C_6	C_7	C_8	C_9	C_{10}	C_{11}	C_{12}	C_{13}	C_{14}	C_{15}
Min/max	**min**	**min**	**min**	**max**	**max**	**max**	**max**	**max**	**max**	**max**	**max**	**max**	**max**	**min**	**min**
Weights	0.091	0.089	0.090	0.072	0.076	0.067	0.047	0.066	0.095	0.059	0.050	0.055	0.058	0.041	0.043
A_1	4000	3000	65	95	1000	40	100	70	40	40	40	35	40	50	50
A_2	7000	7000	100	90	950	80	100	80	80	100	80	80	80	45	20
A_3	6000	6000	80	100	1050	100	85	100	100	80	100	100	100	60	80
A_4	5000	4000	40	100	1000	65	50	95	70	45	65	60	70	40	100
min: Minimum, max: Maximum															

Table 5. *Weighted decision matrix*

Criteria	C_1	C_2	C_3	C_4	C_5	C_6	C_7	C_8	C_9	C_{10}	C_{11}	C_{12}	C_{13}	C_{14}	C_{15}
Min/max	min	min	min	max	max	max	max	max	max	max	max	max	max	min	min
A_1	0.017	0.013	0.021	0.018	0.019	0.009	0.014	0.013	0.013	0.009	0.007	0.007	0.008	0.011	0.009
A_2	0.029	0.031	0.032	0.017	0.018	0.019	0.014	0.015	0.026	0.022	0.014	0.016	0.016	0.009	0.003
A_3	0.025	0.027	0.025	0.019	0.020	0.024	0.012	0.019	0.033	0.018	0.018	0.020	0.020	0.013	0.014
A_4	0.021	0.018	0.013	0.019	0.019	0.015	0.007	0.018	0.023	0.010	0.011	0.012	0.014	0.008	0.017
min: Minimum, max: Maximum															

Table 6. *Replacing of useful and useless criteria*

Criteria	Useful criteria										Useless criteria				
	C_4	C_5	C_6	C_7	C_8	C_9	C_{10}	C_{11}	C_{12}	C_{13}	C_1	C_2	C_3	C_{14}	C_{15}
Min/max	max	max	max	max	max	max	max	max	max	max	min	min	min	min	min
A_1	0.018	0.019	0.009	0.014	0.013	0.013	0.009	0.007	0.007	0.008	0.017	0.013	0.021	0.011	0.009
A_2	0.017	0.018	0.019	0.014	0.015	0.026	0.022	0.014	0.016	0.016	0.029	0.031	0.032	0.009	0.003
A_3	0.019	0.020	0.024	0.012	0.019	0.033	0.018	0.018	0.020	0.020	0.025	0.027	0.032	0.013	0.014
A_4	0.019	0.019	0.015	0.007	0.018	0.023	0.010	0.011	0.012	0.014	0.018	0.018	0.008	0.008	0.017
min: Minimum, max: Maximum															

Step 6: With the help of equation 10 and equation 11, S_{i+} and S_{i-} values are obtained respectively for useful and useless criteria and the results are shown in Table 7.

$$S_{i+} = \sum_{j=1}^{k} d_{ij}, \; j = 1, 2, \ldots, k \tag{10}$$

$$S_{i-} = \sum_{j=(k+1)}^{n} d_{ij}, \; j = k+1, k+2, \ldots, n \tag{11}$$

Step 7: With equation 12, the relative importance weight Q_i is obtained for each alternative and shown in Table 7.

$$Q_i = S_{i+} \oplus \frac{\sum_{i=1}^{m} S_{i-}}{S_{i-} \otimes \sum_{i=1}^{m} \frac{1}{S_{i-}}} \tag{12}$$

Step 8: The alternative with the highest Q_i is chosen as the best (equation 13 is below).

$$Q_{\max} = \max_i \{Q_i\} \; i = 1, 2, \ldots, m \tag{13}$$

According to Table 7, the "*A_3 - Turquoise*" is the best shipyard alternative with a value of 0.282.

Table 7. *Q_i values*

	A_1	A_2	A_3	A_4
S_{i+}	0.122	0.184	0.209	0.154
S_{i-}	0.069	0.104	0.102	0.075
Q_i	0.230	0.256	0.282	0.253

Step 9: Using equation 14, the performance index of all alternatives P_i is obtained. For the best alternative, P_{best}=100. Table 8 shows the P_i values and ranking of alternatives.

$$P_i = \frac{Q_i}{Q_{\max}} \otimes 100\% \tag{14}$$

According to the research model, the "*A_3 - Turquoise*" was found to be the most suitable shipyard for the 30-meter motor yacht construction in Turkey by its performance index value, which is *100.00*. The "*A_2 - Sarp Shipyard*" was the second best shipyard with a performance index value of *90.61* and the last shipyard was the "*A_1 - Ada Shipyard*" with a performance index value of *81.51*. According to the results given in Table 8, the ranking of the shipyards in which a 30-meter motor yacht can be constructed according to the proposed research model in this paper is İstanbul, Antalya, Tuzla, and Muğla.

5. Conclusion

The yacht and boat industry is different from the shipbuilding industry with its content, terminology, investment, operation, and technology in Turkey, same as with all over the world. The only common aspect of the shipbuilding industry and the yacht building industry is

Table 8. *P_i values and ranking of alternatives*

	A_1 - Muğla Ada Shipyard	A_2 - Antalya Sarp Shipyard	A_3 - İstanbul Turquoise	A_4 - Tuzla ICT
P_i	81.51	90.61	100.00	89.55
Ranking	4	2	1	3

that their products swim in the sea. While the shipbuilding industry needs large investments, long periods of time, and large areas near the sea, the yacht and boat manufacturing industry can be managed without much need for smaller investments, shorter times, smaller places, and the seaside.

Compared to the length of the coast with the number of boats per capita, Turkey has great potential in the boat and yacht industry.

In this point, a sequential solution methodology that consists of the SWARA and COPRAS was proposed for choosing the most suitable shipyard in constructing a new motor yacht, and alternatives were evaluated by determining the weights of the criteria determined within the proposed model. For solving the most suitable shipyard to the 30-meter motor-yacht construction problem in Turkey, four alternatives with different characteristics in different cities of the country were evaluated. As a result of the proposed method, the Turquoise Yachting from İstanbul was found to be the most appropriate shipyard.

Although this paper can contribute to the literature and guide to future studies, the most important limitation of this study is the subjective criteria used in the scope of the study. Even though attempts were made to minimize the number of subjective criteria in the study, only 3 out of 15 criteria were evaluated with definite numbers. At this point, besides the knowledge and experience of decision makers, it is also not possible to predict the instinct factor that will be effective in their decision-making process. Another limitation of the study the avoidance of computational complexity. According to the experts' opinion, only four shipyards were selected and evaluated among all shipyards located in Turkey. In the future, it is possible to eliminate this limitation with the evaluation of all shipyards located in Turkey for motor-yacht construction. In addition, it will be possible to evaluate all shipyards in the direction of the needs of the manufacturing companies that want to produce a similar production worldwide with the proposed research model.

As a result, when developed countries are examined, it can be seen that these countries are going forward in the maritime industry. Moreover, their economies have made the greatest contribution from the maritime industry and they have adopted the maritime industry as a culture. With this understanding, it should not be forgotten that the number of amateur seafarers in developed countries is high and that amateur maritime cultures have been adopted by society since childhood. The dissemination of this culture in Turkey is quite important for the development of the maritime sector. The most basic starting point for the development of the maritime economy of Turkey with maximum benefit will be the adoption of the maritime culture.

Funding: The author declared that this study received no financial support.

References

[1] West Mediterranean Development Agency, "Yatçılık sektör raporu," 2012, [Online]. Available: https://baka.gov.tr/uploads/1357649647YATCiLiK-SEKTORU-RAPORU-5ARALiK.pdf. [Accessed: Jul. 31, 2021]

[2] Turkish Chamber of Commerce, "Rakamlarla denizcilik sektörü ve istatistikler," 2017. İMEAK. [Online] Available: https://www.denizticaretodasi.org.tr/Media/SharedDocuments/DenizTicaretiDergisi/mart_ek_2017.pdf. [Accessed: Jul. 28, 2021].

[3] P. Rani, A.R. Mishra, A. Mardani, F. Cavallaro, D. Streimikiene and S.A.R. Khan, "Pythagorean fuzzy SWARA–VIKOR framework for performance evaluation of solar panel Selection." *Sustainability*, vol. 12, pp. 1-18, May 2020.

[4] A. Mostafaeipour, S.J.H. Dehshiri and S.S.H. Dehshiri, "Ranking locations for producing hydrogen using geothermal energy in Afghanistan." *International Journal of Hydrogen Energy,* vol. 45, pp. 15924-15940, Jun 2020.

[5] A. Mardani, M.K. Saraji, A.R. Mishra and P. Rani, "A novel extended approach under hesitant fuzzy sets to design a framework for assessing the key challenges of digital health interventions adoption during the COVID-19 outbreak." *Applied Soft Computing*, vol. 96, pp. 106613, Nov 2020.

[6] W. Chen, X. Chen, J. Peng, M. Panahi and S. Lee, "Landslide susceptibility modeling based on ANFIS with teaching-learning-based optimization and Satin bowerbird optimizer." *Geoscience Frontiers*, vol. 12, pp. 93-107, Jan 2021.

[7] M.A. Naeini, M. Zandieh, S. E. Najafi, and S.M. Sajadi, "Analyzing the development of the third-generation biodiesel production from microalgae by a novel hybrid decision-making method: The case of Iran." *Energy,* vol. 195, pp. 116895, Mar 2020.

[8] S. Mousavi-Nasab and A. Sotoudeh-Anvari, "An extension of best-worst method with D numbers: application in evaluation of renewable energy resources." *Sustainable Energy Technologies and Assessments*, vol. 40, pp. 100771, Aug 2020.

[9] A. Balali, A. Hakimelahi and A. Valipour, "Identification and prioritization of passive energy consumption optimization measures in the building industry: An Iranian case study." *Journal of Building Engineering*, vol. 30, pp. 101239, Jul 2020.

[10] A. Roozbahani, H. Ghased and M.H. Shahedany, "Inter-basin water transfer planning with grey COPRAS and fuzzy COPRAS techniques: a case study in Iranian Central Plateau." *Science of The Total Environment*, vol. 726, pp. 138499, Jul 2020.

[11] H.S. Dhiman and D. Deb, "Fuzzy TOPSIS and fuzzy COPRAS based multi-criteria decision making for hybrid wind farms." *Energy*, vol. 202, pp. 117755, Jul 2020.

[12] P. Rani, A.R. Mishra, and A. Mardani, "An extended Pythagorean fuzzy complex proportional assessment approach with new entropy and score function: application in pharmacological therapy selection for type 2 diabetes." *Applied Soft Computing,* vol. 94, pp. 106441, Sep 2020.

[13] P.S. Kathamore and B.D. Bachchhav, "Grade classification of bio-based lube oil by multi attribute decision making methods." *Materialstoday: Proceedings*, vol. 43, pp. 760-768, Jul 2020.

[14] A.R. Mishra, P. Rani, A. Mardani, K.R. Pardasani, K. Govindan and M. Alrasheedi, "Healthcare evaluation in hazardous waste recycling using novel interval-valued intuitionistic fuzzy information based on complex proportional assessment method." *Computers & Industrial Engineering*, vol. 139, pp. 106140, Jan 2020.

[15] R. Kumari and A.R. Mishra, "Multi-criteria COPRAS method based on parametric measures for ıntuitionistic fuzzy sets: application of green supplier selection." *Iranian Journal of Science and Technology, Transactions of Electrical Engineering,* vol. 44, pp. 1645-1662, Jan 2020.

[16] H. Garg and R. Arora, "Algorithms based on COPRAS and aggregation operators with new ınformation measures for possibility ıntuitionistic fuzzy soft decision-making." *Mathematical Problems in Engineering,* pp. 1563768, 2020.

[17] T. Singh, A. Patnaik, G. Fekete, R. Chauhan and B. Gangil, "Application of hybrid analytical hierarchy process and complex proportional assessment approach for optimal design of brake friction materials." *Polymer Composites*, vol. 40, pp. 1602-1608, 2019.

[18] N. Zarbakhshnia, H. Soleimani and H. Ghaderi, "Sustainable third-party reverse logistics provider evaluation and selection using fuzzy SWARA and developed fuzzy COPRAS in the presence of risk criteria." *Applied Soft Computing,* vol. 65, pp. 307-319, Apr 2018.

[19] A. Valipour, N. Yahaya, N.M.D. Noor, I. Valipour and J. Tamosaitiene, "A SWARA-COPRAS approach to the allocation of risk in water and sewerage public-private partnership projects in Malaysia." *International Journal of Strategic Property Management*, vol. 23, pp. 269-283, 2019.

[20] G.N. Yücenur, Ş. Çaylak, G. Gönül and M. Postalcıoğlu, "An integrated solution with SWARA&COPRAS methods in renewable energy production: city selection for biogas facility." *Renewable Energy*, vol. 145, pp. 2587-2597, Jan 2020.

[21] Z.N. Ansari, R. Kant, and R. Shankar, "Evaluation and ranking of solutions to mitigate sustainable remanufacturing supply chain risks: a hybrid fuzzy SWARA-fuzzy COPRAS framework approach." *International Journal of Sustainable Engineering,* vol. 13, pp. 473-94, May 2020.

[22] A.R. Mishra, et al. "Novel multi-criteria ıntuitionistic fuzzy SWARA–COPRAS approach for sustainability evaluation of the bioenergy production process." *Sustainability,* vol. *12,* pp. 4155, May 2020.

[23] P. Rani, et al. "Hesitant fuzzy swara-complex proportional assessment approach for sustainable supplier selection (HF-SWARA-COPRAS)." *Symmetry*, vol. *12*, pp. 1152, Jul 2020.

[24] Republic of Turkey Ministry of Commerce, "General Directorate of Export," [Online]. Available: https://ticaret.gov.tr/data/5b87000813b8761450e18d7b/Gemi_%C4%B0n%C5%9Fa_%20Sanayii.pdf. [Accessed: Jul. 30, 2021]

[25] V. Keršuliene, E.K. Zavadskas, and Z. Turskis, "Selection of rational dispute resolution method by applying new step-wise weight assessment ratio analysis (SWARA)." *Journal of Business Economics and Management,* vol. 11, pp. 243-258, Mar 2010.

[26] V. Keršuliene and Z. Turskis, "Integrated fuzzy multiple criteria decision making model for architect selection." *Technological and Economic Development of Economy*, vol. 17, pp. 645-666, Oct 2011.

[27] E. K. Zavadskas, A. Kaklauskas and T. Vilutiene T, "Multicriteria evaluation of apartment blocks maintenance contractors: Lithuanian case study." *International Journal of Strategic Property Management*, vol. 13. pp. 319-338, Sep 2009.

ORIGINAL RESEARCH (AR)

DOI: 10.4274/jems.2021.25582

Journal of ETA Maritime Science 2021;9(3):177-191

Effects of Exhaust Backpressure Increment on the Performance and Exhaust Emissions of a Single Cylinder Diesel Engine

Yiğit Gülmez[1,2], Güner Özmen[3]

[1]Dokuz Eylül University, Graduate School of Natural and Applied Sciences, Department of Marine Transportation Systems Engineering, İzmir, Turkey
[2]İskenderun Technical University, Barbaros Hayrettin Naval Architecture and Maritime Faculty, Hatay, Turkey
[3]Dokuz Eylül University, Maritime Faculty, Department of Marine Engineering, İzmir, Turkey

Abstract

Exhaust gas aftertreatment systems and exhaust gas waste heat recovery systems are main solutions to decrease the environmental impact and increase the efficiency of diesel engines. However, any system installed on the exhaust pipe of diesel engines is a source of exhaust backpressure. Moreover, increasing the exhaust backpressure has negative effects on the performance and environmental impact of diesel engines. The study aims to investigate the negative impacts of exhaust backpressure increment on performance indicators, fuel consumption and exhaust emissions of a diesel engine. The experimental study was performed on a test bench comprising a single cylinder diesel engine, a dynamometer and various measurement equipment. The backpressure was increased by adding various sized orifices on the exhaust pipe of the test engine and the test engine was run under six different engine loads at an engine speed of 1600 rpm. Subsequently, the impacts of backpressure increment on the brake specific fuel consumption (BSFC), brake thermal efficiency, volumetric efficiency, mean effective pressures, mechanical efficiency, and exhaust emissions were determined. The study results showed that backpressure increment causes retarding of combustion phases up to a crank angle of 4°, decrease in the indicated mean effective pressure, and decrease in the peak cylinder pressure from 78.36 to 70.7 bar at the maximum available engine load. From fuel consumption perspective, backpressure increment caused an increase in the BSFC approximately up to 3.29% at 24.66 kPa backpressure. On the other hand, the results showed that increasing the backpressure caused a significant increment in the pumping mean effective pressure and a remarkable decrease in the volumetric efficiency. The findings of this study have significant implications for evaluating the negative impacts of any system installed on the exhaust pipe of a diesel engine.

Keywords

Exhaust backpressure, Cylinder pressure, Engine performance parameters, Exhaust emissions, Four-stroke diesel engine

1. Introduction

Diesel engines are the most widespread option for transportation of goods owing to their low operational and maintenance costs, high energy efficiency, and durability. However, the environmental impact of diesel engines and legal requirements to protect the environment from the negative impacts of engines have forced engine manufacturers to develop more environmental-friendly engines. Legal requirements to avoid air pollution requires to reduce the brake specific exhaust emissions, i.e., the quantity of pollutants emitted per unit of energy output. There are a few methods to decrease the brake specific exhaust emissions caused by diesel engines. Some of the methods such as using a type of exhaust gas after treatment systems and exhaust heat regeneration systems require to install an additional system on exhaust pipe of the engine. However, any system installed on the exhaust pipe of an internal combustion engines largely results an increase in the exhaust backpressure due to increasing the resistance against the flow of exhaust gas.

The negative impact of backpressure due to the characteristics of any system installed on exhaust pipes for

Address for Correspondence: Yiğit Gülmez, Dokuz Eylül University, Graduate School of Natural and Applied Sciences, Department of Marine Transportation Systems Engineering, İzmir, Turkey
E-mail: yigit.gulmez@iste.edu.tr
ORCID ID: orcid.org/0000-0003-1955-6706

Received: 07.05.2021
Accepted: 30.06.2021

To cite this article: Y. Gülmez and G. Özmen, “Effects of Exhaust Backpressure Increment on the Performance and Exhaust Emissions of a Single Cylinder Diesel Engine.” *Journal of ETA Maritime Science*, vol. 9(3), pp. 177-191, 2021.

any purpose has been extensively discussed. In response to strict regulations to decrease the amount of harmful emissions in flue gas, as solution, there are a number of aftertreatment systems that can be installed on the exhaust outlet of diesel engines. As an effective NO_x reducing aftertreatment solution [1], selective catalytic reduction (SCR) systems have negative impacts on the performance of diesel engines due to increasing exhaust backpressure. A few studies have investigated the negative impact of SCR systems on backpressure. For instance, Zhang et al. [2] designed a new mixer for an SCR system to decrease the negative impact on engine performance. In the study, the exhaust backpressure was investigated as a performance indicator of the engine. The study has important results for the interaction between backpressure and SCR mixer design. However, the study did not investigate the effect of backpressure on combustion performance and exhaust emissions.

Diesel particulate filters (DPFs) are yet another aftertreatment system installed on diesel engines. These systems help filtrate the particles in the flue gas. However, the exhaust backpressure increases as the particles are captured within its matrix [3]. Backpressure increment of diesel engines is the main factor affecting the sizing of DPF systems in real world applications [4]. Several studies have described the effects of the type, design, and material selection of DPF systems on backpressure increment in internal combustion engines. Li et al. [5] compared diesel oxidation catalyst +DPF and electric diesel particulate trap systems considering the effects of both systems on exhaust backpressure and particulate trapping efficiency. In another study [6], the interactions between DPF and particulate oxidation catalyst were investigated in terms of the filtration and backpressure. D'Aniello et al. [7] developed a 0D model to investigate the aspect of the system with adding a catalytic silicon carbide wall flow DPF on the exhaust pipe of a diesel engine. In the study, the exhaust backpressure was considered as one of the characteristics of the system. These studies [5-7] have made contributions toward understanding the effects of DPF system characteristics on backpressure increments. However, these papers did not report any result on the negative impacts of backpressure on engine performance, fuel consumption, or brake specific exhaust emissions.

A DPF can accumulate a large volume of particle matters (PM) which causes high-pressure drop in the filter [8] and high backpressure increment in exhaust pipe. Investigating the impact of increasing PM accumulation on the performance of a diesel engine is a crucial point for researchers. Chiavola et al. [9] studied the loading process of a DPF filter considering to limit exhaust backpressure increment. In another study [10], the effects of residual ash in a DPF on trapping performance of the filter and backpressure increment in exhaust line of the diesel engine have been investigated. Although increased ash accumulation is known to cause an increase in the backpressure [9,10], there has been no study on the effect of increasing backpressure on diesel engine performance. Zhang et al. [11] conducted a study to estimate the impact of ash accumulation on DPF-related fuel penalty. Similarly, Wang et al. [12] investigated the effects of ash inside a platinum-based catalyst DPF on regulated and unregulated exhaust emissions of a diesel engine. The results of the studies [11,12] are important to analyze the effect of backpressure increment on exhaust emissions.

Waste heat recovery (WHR) systems enable to produce energy by utilizing the waste heat of the engine. However, adding any type of WHR system on the exhaust outlet of an engine is a source of exhaust backpressure. Any loss in engine brake power due to backpressure increment may even decrease the total efficiency of the system. Extensive studies have investigated the effect of increasing backpressure on the system efficiency. Wu et al. [13] made a model design to maximize the Organic Rankine Cycle (ORC) system energy output by considering to limit the negative impact of the system to vehicle performance. Similarly, Baldasso et al. [14] proposed a model for the optimal design of an ORC system mounted on exhaust line of a marine engine by considering the effect of increased backpressure on the performance of both engine and ORC. The results of the studies [13,14] considered the brake specific fuel consumption (BSFC) of complete system including the test engine and ORC system, and thus, the power output included the power generated by the ORC system. Zhao et al. [15] investigated the effect of ORC system operating conditions on the performance of the diesel engine. Similarly, in another study [16], the negative impact of an exhaust ORC system on diesel engine fuel economy for off-highway vehicles was investigated. The study evaluated positive and negative impacts of increasing backpressure, increasing heat exchanger weight and the effects of all variables on fuel consumption of the engine and power regeneration of the ORC system. Di Battista et al. [17] developed a mathematical model by sizing the two heat exchangers of a standard ORC system. In the study the effect of the backpressure on BSFC of the engine was calculated via a correlation. The study did not investigate the effect of backpressure on exhaust emissions. The studies [13-17] have investigated the negative impact of attaching a waste heat system heat exchanger on the exhaust pipe of diesel engines. Some of the studies have investigated effect of such an appendage on fuel consumption as well. However, these studies have considered the system as a whole with both the engine and waste heat system. Thus, the negative impact solely on the engine side could be analyzed incomprehensively.

Few have investigated the effect of backpressure increment on the performance of a diesel engine in detail. Tourlonias and Koltsakis [18] conducted a model-based study to compare the performance of aftertreatment emission reducing systems. In the study the performance indicator was selected as fuel consumption. The results of the study provide fuel penalties from heat-up strategy, filter regeneration and filter loading, and increasing backpressure situations. The study has important results on the effect of different aftertreatment technologies on fuel consumption increment of the engine. However, in the study, the effect of different aftertreatment technologies and backpressure increment on exhaust emissions and performance of the diesel engine has not been investigated. Sapra et al. [19] conducted an experimental investigation of the performance of a marine diesel engine equipped with underwater exhaust system against dynamic back pressure at varying sea-states. A turbocharged marine diesel engine was tested against different backpressures produced by a butterfly valve at the exhaust gas outlet of the turbocharger. The study found that the negative impacts of dynamic backpressure were less influential than static backpressure increment. The study has important implications on the effects of operational dynamics of governor and turbocharger on the fuel penalty due to backpressure increment. However, the study did not investigate the negative impact of backpressure on in-cylinder pressure rise characteristics of the test engine. Sivaram et al. [20] investigated the importance of the exhaust pipe length on fuel economy and volumetric efficiency of a single cylinder diesel engine. The study showed that increased exhaust pipe length and the corresponding increase in the backpressure can lead to increased fuel consumption and decreased volumetric efficiency. In another study [21], marine diesel engine performance against static backpressure was investigated experimentally and via a simulation. In the study, a turbocharged diesel engine was tested under different loads and various static backpressure. Besides, in the study, a simulation model was generated and used to analyze the performance of the engine against high back pressures. Cong et al. [22] studied the effect of backpressure increment on conventional and low-temperature combustion characteristics of diesel engines. A naturally aspirated single cylinder diesel engine was used as the test engine. The study results showed that increased backpressure does not affected the initial cool flame combustion reactions. However, the backpressure increment caused retarding of the main combustion phase and increased the combustion process. Fernoaga et al. [23] investigated the effect of exhaust backpressure on the power generation characteristics of a diesel engine. In the study, the maximum available shaft power of the engine under different loads and engine speeds was mainly considered as the performance parameter of the engine. The experimental results were used to generate a machine learning algorithm for predicting the maximum available engine power generation under different exhaust backpressures, engine speeds, and engine loads. In another study, [24] a few muffler designs were compared due to backpressure generation characteristics. In the study, computational fluid dynamics software was used to estimate the backpressure increments. Kim and Bae [25] examined the feasibility of replacing the conventional high-pressure loop/low-pressure loop exhaust gas recirculation with a combination of internal and low-pressure loop exhaust gas recirculation system. The aim of such a strategy was to have the availability to retard intake valve closing without the concern of backpressure increment due to the high-pressure loop exhaust gas recirculation. The study has important results for the effect of exhaust backpressure on turbocharger efficiency of the engine. The study mainly focused on the impacts of changing EGR strategy, retarding intake valve closing timing, and negative valve overlap configuration. Thus, the study did not investigate the effect of backpressure on combustion performance, BSFC and exhaust emissions. In another study [26], the characteristics of exhaust gas pressure waves under different engine loads have been investigated. The result showed that the pressure wave in the exhaust line of the engine during the exhaust valves were opened was affected by both the backpressure in the line and in-cylinder pressure. The study results are crucial to understanding the effect of backpressure on the exhaust gas discharge characteristics of a diesel engine. Kasprzyk et al. [27] investigated the effect exhaust backpressure on the operation of exhaust gas oxygen content sensor. The study determined the sensitivity of the sensor to the exhaust pressure under different operational conditions of the test engine. The measurement results of excess air sensor were compared with exhaust gas analysis. Based on the data analysis in the study, a new empirical calculation methodology for the exhaust backpressure compensation correlation for diesel engines was proposed. Andwari et al. [28] investigated the effects of ORC and turbo-compound system integration on a diesel engine. In the study, two WHR strategies were modeled and simulated through a 1D simulation by using GT-Power. The strategies were evaluated in terms of their WHR and BSFC reduction capabilities. A rise in the exhaust backpressure increased the fuel consumption so much that the system was unable to regenerate sufficient power to compensate for the power loss in the engine at lower speeds. The study has important implications on proving the negative impact of backpressure on engine performance. The study investigated only the negative impacts of backpressure on the BSFC of the engine. However, the backpressure may have many other negative impacts such as increased exhaust emissions, poor composition quality, and deteriorating engine combustion. Michos et al. [29] investigated the effect of an ORC system on the exhaust backpressure of a turbocharged heavy duty marine engine. Ricardo WAVE software was used in the study for the investigation of different turbocharging strategies and the effect of different ORC configurations. The study investigated the effect of backpressure (0-100 mbar) on the engine mass flow rate, BSFC, effective pressure, turbine inlet and compressor pressure, air mass flow rate, and exhaust gas mass flow rate. The study has remarkable results on the effect of exhaust backpressure for engines using different turbocharging strategies. The result showed that the fuel consumption and effective pressure increases, while the air mass flow rate decreases by increasing backpressure for the engine with a fixed turbocharged exhaust system. The results of the study are very critical to understand the effect of backpressure on the performance of an engine with different turbocharging strategies. The study mainly focused on the interaction between engine performance indication parameters, backpressure, and turbocharging strategies [30]. However, the study did not investigate the effects of backpressure on the combustion performance and exhaust emissions. In another study, Lu et al. [31] presented a hypothesis about NO_2 formation process in a dual-fuel engine and investigated the effect of methanol proportion in fuel, exhaust gas recirculation, and exhaust backpressure on nitric oxide emissions. The exhaust backpressure was increased by 3, 6, and 9 kPa, respectively. In the study, ppm levels of nitric oxide emission were compared for four different backpressure levels and the study determined that NO_x emissions were increased by increasing backpressure. However, the exhaust backpressure affects the volumetric efficiency of an engine which thus wise would affect exhaust gas mass flow rate. Therefore, the exhaust gas mass flow rate would not be constant for different backpressure levels. Thus, the comparison of NO_x emissions according to ppm levels would not reflect the effect of backpressure on NO_x emissions level. Making the comparison in terms of the brake specific NO_x emissions levels for various backpressure levels would be more appropriate.

The literature review has shown that any system installed on the exhaust pipe of a diesel engine cause an increase in exhaust backpressure. Increasing backpressure has negative impacts on the performance of an engine. Previous studies on the effects of exhaust backpressure on the performance and exhaust emissions of diesel engines investigated the negative impact of backpressure increment on the BSFC. However, much uncertainty still exists about the relationship between the exhaust backpressure and diesel engine performance indicators such as the volumetric efficiency, mechanical efficiency, combustion characteristics, and environmental impact of diesel engines.

In the current study, the effects of exhaust backpressure increment on the BSFC, volumetric efficiency, mechanical efficiency, brake specific exhaust emissions, and combustion characteristics have been investigated. For this purpose, a single cylinder diesel engine with a dynamometer was used as a test stand, and the exhaust backpressure of the engine was increased by adding different sizes of orifices on the exhaust pipeline of the engine. This study aims to contribute to a deeper understanding of the negative impacts of exhaust backpressure on the efficiency, combustion characteristics, and environmental impact of diesel engines. The results are important to analyze the effect of backpressure increment on the performance of diesel engines, help understand the relationship between exhaust backpressure and in-cylinder pressure, and can be used as a guide to predict the negative impact of installing any type of WHR or aftertreatment system on the exhaust pipe of an engine on the combustion performance. Finally, the study provides suggestions on minimizing the negative impact of backpressure increment.

2. Materials and Methods

2.1. Experimental Setup

In this study, a test bench was used to analyze the effects of exhaust backpressure on the performance and exhaust emissions of a diesel engine experimentally. Figure 1 illustrates the detailed schematic of the test bench.

As shown in Figure 1, the experimental setup comprises a diesel engine, an electric dynamometer, a fixed orifice housing, a fuel tank, and various measurement devices. The test engine was a single cylinder, direct injection, naturally aspirated, air cooled diesel engine. Table 1 provides the other properties of the test engine. A 20 kW DC dynamometer was used for loading the engine to any load for any engine speed.

In the experiments, the backpressure was increased by adding orifices of various diameters one by one to the

Table 1. *Properties of the test engine*

Items	Specifications
Displacement volume - Compression ratio	817 cm^3-17:1
Bore × Stroke	102 mm×100 mm
Rated Speed	3000 rpm
Maximum Power (kW) (ISO 1585)	13 kW @ 3000 rpm
Maximum Torque (Nm)	48 Nm @ 1600 rpm

housing on the exhaust pipe. The orifices were square edged and concentric bored and made of 2 mm thick, grade AISI-304 stainless steel material. The bore sizes of the orifices in diameter were 28, 24, 20, 16, and 12 mm, respectively. The diameter of the exhaust pipe without using any orifice was 32 mm.

A Coriolis type flowmeter was used to measure the mass flow rate, temperature, and density of fuel instantaneously. The maximum error rate of the device for mass flow rate measurement was <±0.1% for liquids. Similarly, a vortex type flowmeter was used to measure the mass flow rate, temperature, and humidity of intake air. The equipment was connected to the engine suction air inlet via a flexible pipe to avoid equipment damage due to engine vibration and balancing the flow in the measurement device. The maximum error rate of the device for mass flow rate measurement was less than ±2% for air. The engine load and torque were calculated using the force value measured by a load cell installed on the dynamometer.

The exhaust gas temperature and the rates of CO_2, O_2, CO, NO_X, and SO_X were measured by an exhaust gas analyzer. The measurement accuracy of the device was in accordance with MARPOL Annex VI and NO_x Technical Code requirements. Exhaust gas backpressure was measured by using a pressure sensor.

The in-cylinder pressure was measured using a piezoelectric pressure sensor and an appropriate charge amplifier. Additionally, an rpm counter was used simultaneously to measure the engine speed and timing of the top dead center (TDC). TDC timing enabled to determine instantaneous crank angle of the test engine. The in-cylinder pressure and derived crank angle values were used to create open indicator diagrams, which were used to the assess in-cylinder combustion performance.

2.2. Experimental Procedure

The experiments were conducted at an engine speed of 1600 rpm, under six different set points of engine torques, and with five different sized orifices. First, the largest sized orifice was attached on the orifice housing. Subsequently, the test engine was run at an engine speed of 1600 rpm under engine torque loads of 8, 16, 24, 32, and 40, and 48 Nm. The experimental procedure was repeated by adding orifices of different diameters. The only difference on engine loading procedure with different orifice sizes was the value of maximum engine torque. The maximum producible engine torque was 48 Nm at 1600 rpm engine speed.

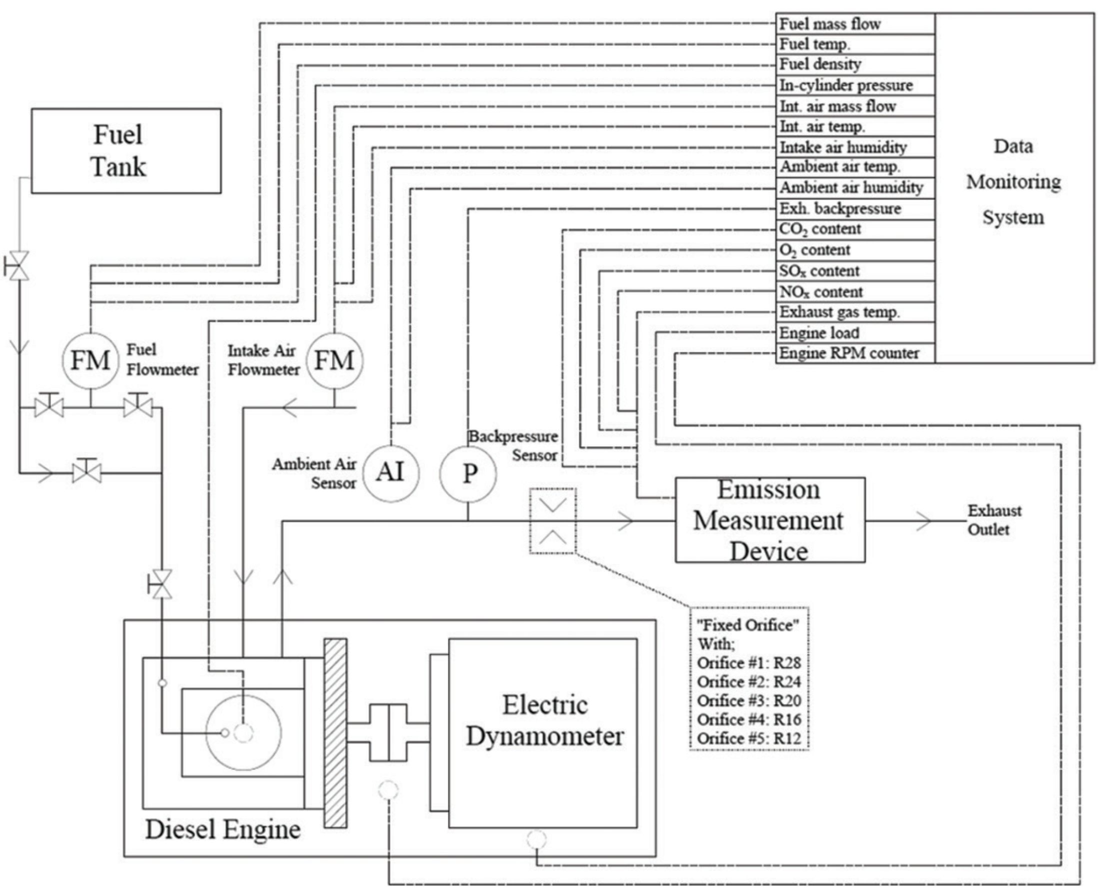

Figure 1. *Experimental setup*

However, decreasing the orifice size caused a decrease in the maximum producible engine torque value linearly to 46.43 Nm with orifice #5. Thus, the experiments were conducted for the maximum available engine torque in place of 48 Nm with smaller orifices. All the measurement equipment in the test setup were calibrated according to the instruction books, before starting the experiments. It is ensured that all parameters, except for the variables changed for tests, were fixed during the experiments. During the tests, all the measurements were taken 3 min after the exhaust gas temperature would rise or drop to a constant level.

Fuel flowmeter, intake air flowmeter, ambient air sensor, engine rpm counter, crank angle encoder, load cell, and emission measurement device were "ready to use" measurement devices. Thus, the results of the measurements were converted to a suitable measurement unit by the device itself. For these devices, the measurement results were filtered for noise reduction by device, and the results were read from the device monitor manually for all measurements. Dissimilarly, the in-cylinder pressure sensor and exhaust backpressure measurement sensor have analog outputs and the results of the measurements were collected and converted to a suitable measurement unit by data monitoring system. Additionally, for the two sensors, the noise reduction filtering of measurement results was made by authors using specially designed filters. For this purpose, the output of the in-cylinder pressure sensor with more than 3000 measurement points for each cycle was smoothed using a fifth order Savitsky-Golay filter with a frame length of 73 samples. Data processing for the in-cylinder pressure measurement was made by four steps. Level correction, angle referencing, cycle averaging and filtering. The signal processing was optimized by a step-by-step offline application methodology in accordance with the methods proposed by Payri et al. [32]. Finally, the noise reduction of the exhaust backpressure sensor was made using a second-order low-pass Butterworth filter with a cut off frequency of 200 Hz.

During the experiments, the test engine was loaded to a specified engine torque at a specified engine speed. Following the appropriate conditions occur, the fuel temperature and mass flow rate, air temperature and mass flow rate, ambient air conditions, volumetric exhaust emission rates and exhaust temperature at measurement point have been read from the monitor of related sensors and recorded. Subsequently, the outputs from exhaust backpressure, crank angle, and in-cylinder pressure sensors were taken, manipulated, and recorded by the data monitoring system. Each measurement was repeated thrice at different times, and the test result value was accepted as the average of the three values. The difference between the average of the three measurements and the end measurement values was found to be <3% of the measured value.

2.3. Calculations

The test bench enables to measure engine speed, in-cylinder pressure, crank angle, fuel and air properties, exhaust backpressure, exhaust temperature, the force applied to the dynamometer shaft and proportional contents of emissions in the raw exhaust gas. These are measurable parameters. However, the engine torque, brake power, indicated power, any types of the average indicated mean effective pressure (IMEP), BSFC, brake thermal efficiency, volumetric efficiency, mechanical efficiency, and brake specific exhaust emissions cannot be measured directly. These parameters can be derived using one, two, or more of the measured parameters. The engine torque and brake power were derived from the force applied to dynamometer shaft and engine speed. BSFC was calculated by the rate of hourly fuel consumption to energy produced per hour. The net IMEP ($IMEP_n$), gross IMEP ($IMEP_g$) and pumping mean effective pressure (PMEP) were calculated by using indicated power values which were gathered by integrating the in-cylinder pressure-volume closed diagram.

Volumetric efficiency (η_v) of the engine was calculated by the following formula. In the formula, m'_{air} is the mass flow rate of the intake air, ρ_{air} is the density of the intake air, V_s is the stroke volume, n is the engine speed and i is the number of cycles per one revolution of the engine shaft. Formula 1 is below;

$$\eta_v = \frac{\dot{m}_{air}}{\rho_{air} V_s n i} \quad (1)$$

The brake thermal efficiency (η_{bt}) was calculated using the ratio of the brake power (ρ_b) to the fuel energy. The fuel energy was calculated by multiplying the mass flow rate (m'_{fuel}) and lower heating value (Q_{LC}) of the fuel. Formula 2 is below;

$$\eta_{bt} = \frac{P_b}{\dot{m}_{fuel} Q_{LC}} \quad (2)$$

The mechanical efficiency (η_m) was calculated by the ratio of the brake mean effective pressure (BMEP) to $IMEP_n$. The BMEP was derived from the brake power and engine displacement volume (V_d). Formula 3 is below;

$$BMEP = \frac{P_b}{V_d n i} \quad (3)$$

Finally, brake specific exhaust emissions were derived from volumetric rates of exhaust components in raw exhaust gas according to techniques presented in NO_x Technical Code [33]. For the calculation, the air humidity, density of the exhaust gas (derived from the exhaust temperature and volumetric rates of exhaust components), air flow rate, and fuel flow rate were also used.

3. Findings and Discussion

In the study, the effects of backpressure on the performance of a diesel engine were investigated. For this purpose, different sized orifices were added to the exhaust pipe of the engine to increase the backpressure on the exhaust outlet of the engine. Table 2 illustrates the backpressure increment values with different sized orifices under different engine loads. The last column of the table shows the backpressure value with the maximum available torque value. As shown, increasing the engine load has a positive effect on the backpressure values in general. It is probably related with increasing exhaust gas temperature due to increasing engine load. Decreasing orifice radius caused a significant increase in exhaust backpressure.

In the current study, the effects of backpressure increment on the in-cylinder pressure-volume diagrams have been investigated in detail. Figure 2a, b, c and d illustrate the open and closed in-cylinder pressure diagrams with maximum available engine torque.

As shown in Figure 2c, increasing the backpressure caused a decrease in the peak pressure from 78.36 bar to 70.7 bar. The ignition delay period was increased, the angle of peak pressure was retarded by some 4° crank angle, and dp/dθ in the rapid pressure rise phase decreased significantly. Details about Figure 2 are provided in Table 3. Cong et al.

Table 2. *Measured exhaust backpressure vs engine load and different sized orifice (Orifices #1 to #5 correspond to diameters of 28, 24, 20, 16 and 12 mm, respectively)*

Orifice no. load (Nm)	Exhaust backpressure (kPa)					
	8	16	24	32	40	Max. available torque
Orifice #1	1.2748	1.2748	1.2759	1.2842	1.2852	1.2921 at 48.02 Nm
Orifice #2	1.7640	1.7582	1.7866	1.7791	1.7800	1.799 at 47.97 Nm
Orifice #3	2.9425	2.9423	2.9706	3.0115	3.0290	3.0853 at 47.89 Nm
Orifice #4	6.9356	7.0395	7.2912	7.3523	7.3214	7.4822 at 47.62 Nm
Orifice #5	24.1057	24.3849	25.0422	25.3891	25.9458	26.2589 at 46.43 Nm

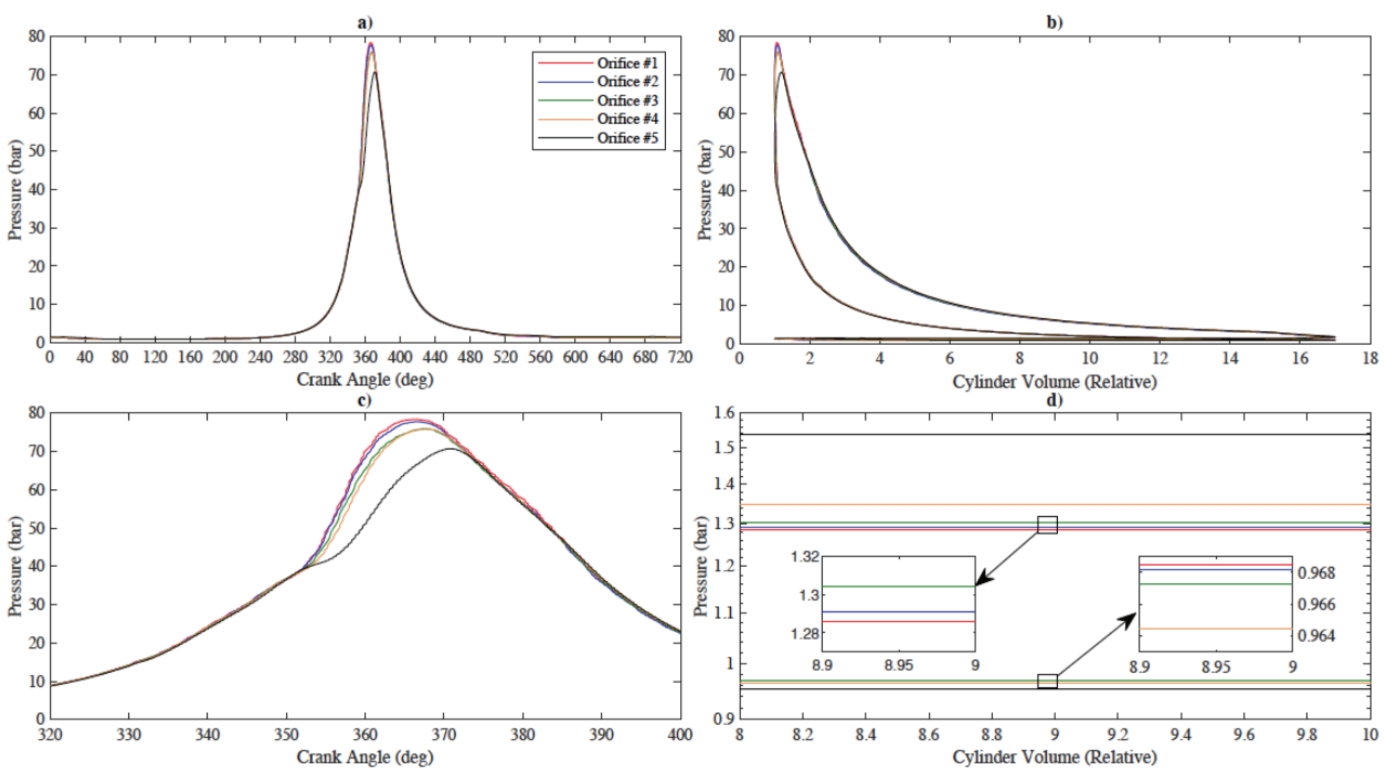

Figure 2. *In-cylinder pressure with different orifices under maximum available engine load a) Open indicator diagram, b) Closed indicator diagram, c) Open indicator diagram (detailed view) and d) Intake and exhaust strokes in detail*

[22] investigated in-cylinder pressure for two backpressure scenarios. The results of that study indicated that a higher backpressure caused a retarding of the combustion phases, decrease in combustion duration, and decrease in maximum pressure at 2500 rpm engine speed, 16 mg/cycle fuel consumption, and 30° crank angle injection advance. The current study showed similar results. However, the previous study investigated the effect of backpressure increment on in-cylinder pressures at constant fuel consumption and thus under different engine loads. The results of the current study enable to understand the impact of backpressure increment on in-cylinder pressures at constant engine load.

Clearly, from Table 3, the maximum available engine torques decrease with increasing backpressure. The brake power, net indicated power, and BMEP also decreased. Notably, the PMEP and BSFC values increase with increasing backpressure. In literature, many studies investigated the BSFC increment caused by increasing backpressure. And the results of the current study in accordance with the literature [18-31]. However, no study has investigated the effects of backpressure increment on the mean effective pressure values. There is a small decrease in $IMEP_n$ and $IMEP_g$ with increasing backpressure. It may not be a distinct change because these values may decrease when decreasing the engine torque. However, the increment in PMEP values may be good sign to observe the negative impact of backpressure increase. As seen from the table, PMEP values increase with decreasing orifice radius significantly. Conceivably, this is directly related to the resistance against exhaust gas flow due to higher pressure in the exhaust pipe. An increase in PMEP decreased exhaust gas discharge efficiency in exhaust stroke and relatedly decreased the volumetric efficiency. In the literature, Hield [34] has investigated PMEP increase effect of exhaust backpressure increment in diesel engines. However, according the result of that study, backpressure increment caused a slight increase in PMEP values once compared with the results of the current study. This may be due to the test engine in the study was a turbocharged engine, and thus, the PMEP increase effect of backpressure increment may has been absorbed by turbocharger.

In Figure 2 and Table 3, the maximum available torque values decrease with decreasing orifice radius. This may cause a comparison of the effect of backpressure on performance parameters such as indicated mean effective pressure values under non-equivalent conditions. To make an assessment under equal circumstances, engine torque values were equalized to some 40 Nm value. Figure 3 a, b, c and d show open and closed indicator diagrams under 40 Nm engine torque, 1600 rpm engine speed and with five different sized orifices.

In Figure 3, the effects of backpressure increment on the in-cylinder pressure rise characteristics are similar to those shown in Figure 2. However, the only difference is that, Figure 3 enables to make a comparison on the effect of backpressure increment on BSFC, IMEP, PMEP, and friction mean effective pressure (FMEP) under equal engine torque levels. Details about Figure 3 are provided in Table 4.

Table 4 shows the results obtained from the analysis of the pressure-volume diagram shown in Figure 3. Data from this table can be compared with the data listed in Table 3. Decreasing the engine torque caused a decrease in the brake power and mean effective pressure values. However, the BSFC values slightly increase. Once the effect of increasing backpressure on the performance parameters is compared under same engine torque conditions, it can be clearly seen that increased backpressure causes a slight decrease

Table 3. *Performance parameters at maximum available engine torque*

Orifice #	1	2	3	4	5
Engine speed (rpm)	1604	1602	1601	1591	1593
Torque (Nm)	48.02	47.97	47.89	47.62	46.43
Brake power (kW)	8.07	8.05	8.03	7.94	7.75
Net indicated power (kW)	9.09	9.06	9.05	8.91	8.68
$IMEP_n$	8.32	8.31	8.30	8.22	8.00
$IMEP_g$	8.64	8.63	8.63	8.63	8.52
PMEP	0.32	0.32	0.33	0.40	0.52
FMEP	0.26	0.26	0.27	0.29	0.26
BMEP	7.39	7.38	7.37	7.33	7.14
BSFC (g/kW.h)	255.92	255.84	257.23	259.08	265.78
Crank angle at maximum pressure (deg)	366.6	366.6	367.4	367.7	370.6
Maximum pressure (bar)	78.36	77.75	75.92	75.82	70.70

$IMEP_n$: Net indicated mean effective pressure, $IMEP_g$: Gross indicated mean effective pressure, PMEP: Pumping mean effective pressure, FMEP: Friction mean effective pressure, BMEP: Brake mean effective pressure, BSFC: Brake specific fuel consumption in $IMEP_n$ under all orifice sizes. Because $IMEP_n$ is equal to the difference between $IMEP_g$ and PMEP, increase in PMEP causes a decrease the $IMEP_n$ values. Once the change in BSFC values is investigated, it can be assumed that increasing backpressure increases BSFC of the engine. Considering the backpressure values in Table 2 and BSFC values in Table 4, it can be deduced that a backpressure increase of 0.49 kPa caused an increase of 0.34% in BSFC, 6.04 kPa backpressure increase caused an increase of 1.05% in BSFC, and 24.66 kPa backpressure increase caused an increase of 3.29% in BSFC. Interestingly, from Table 3, $IMEP_g$ values vary with increasing backpressure. $IMEP_g$ values decrease with increasing backpressure value up to 3.029 kPA with orifice#3. However, increasing the backpressure from 3.029 kPa to 7.3214 kPa caused an increase in $IMEP_g$ value. Thereafter, the increasing trend continues with increasing

Table 4. *Performance parameters at 40 Nm engine torque*

Orifice #	1	2	3	4	5
Engine speed (rpm)	1602	1593	1600	1592	1605
Torque (Nm)	40.42	40.27	40.29	40.32	40.25
Brake power (kW)	6.78	6.72	6.75	6.72	6.76
Net indicated power (kW)	7.80	7.71	7.74	7.69	7.71
$IMEP_n$	7.15	7.11	7.10	7.09	7.05
$IMEP_g$	7.43	7.40	7.39	7.45	7.54
PMEP	0.28	0.29	0.29	0.36	0.48
FMEP	0.37	0.39	0.35	0.37	0.29
BMEP	6.22	6.19	6.20	6.20	6.19
BSFC (g/kW.h)	259.10	259.97	259.95	261.83	267.64
Crank angle at maximum pressure (deg)	365.5	365.7	367.2	367.5	370.1
Maximum pressure (bar)	74.72	75.00	73.39	72.62	69.02

$IMEP_n$: Net indicated mean effective pressure, $IMEP_g$: Gross indicated mean effective pressure, PMEP: Pumping mean effective pressure, FMEP: Friction mean effective pressure, BMEP: Brake mean effective pressure, BSFC: Brake specific fuel consumption

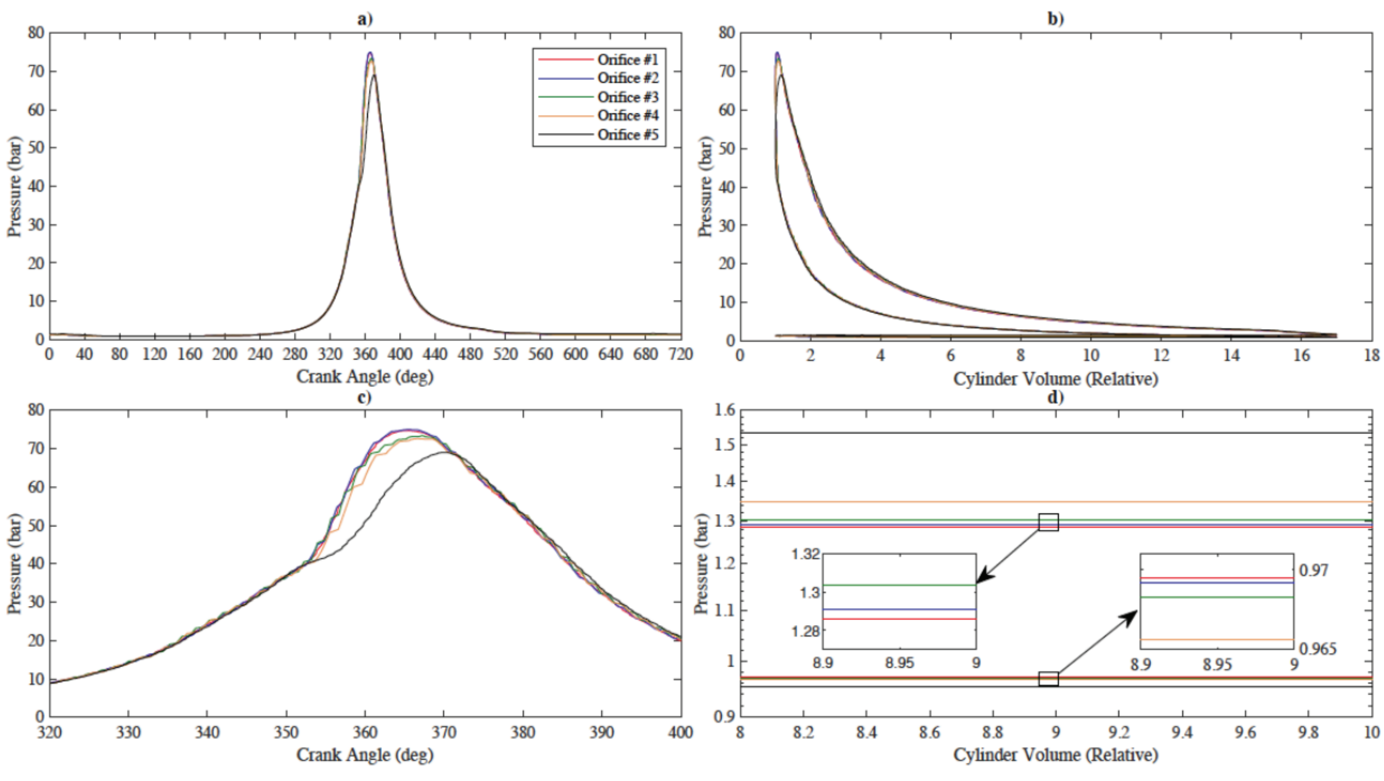

Figure 3. *In-cylinder pressure with different orifices at an engine load of 40 Nm: a) Open indicator diagram, b) Closed indicator diagram, c) Open indicator diagram (zoomed in view) and d) Intake and exhaust strokes in detail*

backpressure after that. As shown, $IMEP_n$ data increase steady, however IMEPg data fluctuate. The difference may be caused due to the gas exchange process. Moreover, the fluctuations in the mechanical efficiency originate from the change in the volumetric efficiency.

$IMEP_n$, $IMEP_g$, PMEP and FMEP values are affected by increasing backpressure under 40 Nm engine torque as illustrated in Table 4. Decreasing the engine torque to lower values also has similar trends in mean effective pressure values. Figure 4a, b, c and d show the changes in mean effective pressure values with increasing backpressure under different engine loads.

Figure 4 shows the effect of different engine torques and increasing backpressure on the mean effective pressure values of test engine at an engine speed of 1600 rpm. As shown in Figure 4a, b and d, the changing trends are similar to the trends under an engine torque of 40 Nm. Decreasing the engine load caused a decrease in $IMEP_n$ and $IMEP_g$ due to the decrease in power production. In PMEP values, there is also a similar trend in the plot. As Figure 4d investigated, it can be stated that at all engine loads, 25.1 kPa backpressure increment with orifice #5 caused some 50% PMEP increase while 7.3 kPa increment with orifice #4 and 3.2 kPa backpressure increment with orifice #3 caused 28.6% and 3.2% PMEP increments respectively. In the literature, Michos et al. [29] measured some 15% PMEP increase at 10 kPa backpressure using a fixed turbocharged diesel engine. The variation may be caused by the difference between test engines. In that study, a turbocharged diesel engine was used as the test engine, and a fixed turbocharger may lead to absorption of a part of the negative impact of backpressure increment on the pumping work of the engine.

Mean effective pressure values are critical indicators of the fuel economy and efficiency of the test engine. However, there are other performance indicators such as mechanical efficiency (η_m), brake thermal efficiency (η_{bt}), volumetric efficiency (η_v) , and BSFC. Figure 5a, b, c and d illustrate the effect of increasing backpressure and changing engine load on engine performance parameters.

Figure 5 shows that increasing the backpressure causes a significant increase in the BSFC. BSFC increased averagely 3.2% at approximately 25.1 kPa backpressure, %1.2 at approximately 7.2 kPa backpressure and %0.4 at approximately 3 kPa backpressure. In the literature, many studies [11,16,18,29,31] investigated BSFC penalty of backpressure increment. The results of the current study are similar to results of that studies. For instance, Zhang et al. [11] has found that BSFC increased 4.57% at 25.1 kPa backpressure, while an increment was observed as 0.73% at 7.8 kPa and 0.44% at 4.5 kPa backpressure. In another

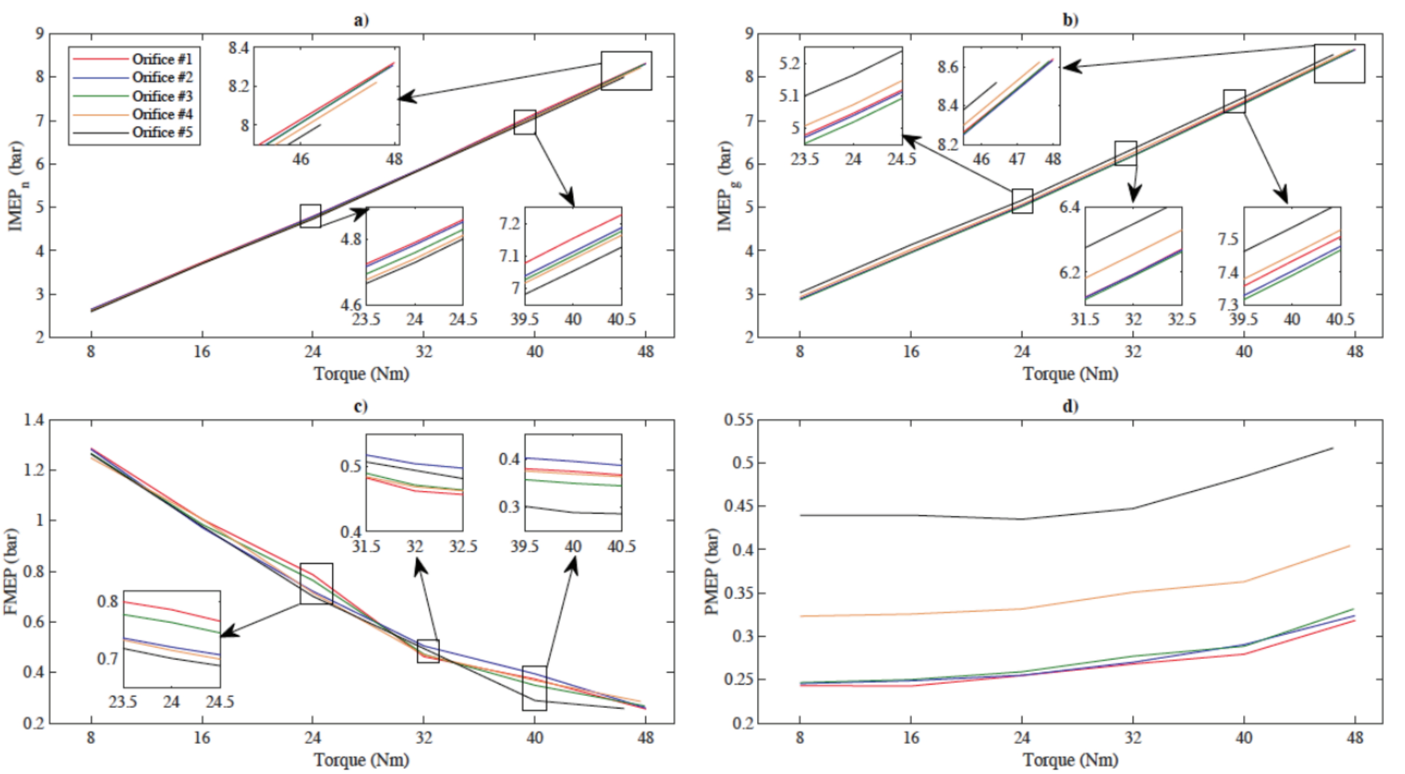

Figure 4. *Mean effective pressure values a) $IMEP_n$, b) $IMEP_g$, c) FMEP and d) PMEP*

$IMEP_n$: Net indicated mean effective pressure, $IMEP_g$: Gross indicated mean effective pressure, PMEP: Pumping mean effective pressure, FMEP: Friction mean effective pressure

study, Karvountzis-Kontakiotis et al. [16] have stated that BSFC increased 2% with 25 kPa and 0.5% with 10 kPa backpressure increment. However, no published study has attempted to investigate the mechanism between backpressure increment and BSFC increase. As shown in Figure 2 and Figure 3, the backpressure increment caused retarding of the combustion phases. As the backpressure increases, the angle of ignition start and the angle of maximum pressure were retarded significantly. Besides, dp/dθ on rapid pressure rise phase has decreased. In the literature, many studies which investigated the effects of fuel injection timing on combustion of diesel engines [35-38] have found that advancing fuel injection timing caused retarding of combustion phases and a decrease in dp/dθ on rapid pressure rise phase as similar to negative impacts of increasing backpressure. Thus, when running the engine against high exhaust backpressure, retarding the injection timing may result in an abatement in the fuel penalty. This may be a new research topic for researchers.

One of the most apparent impact of backpressure increment on the performance parameters of a diesel engine is the impact on the volumetric efficiency, as shown in Figure 5b. As shown in the figure, changing load also affected the volumetric efficiency. For instance, with orifice#4, volumetric efficiency was increased from 82.97% at 8 Nm torque to 84.68% at maximum engine load. However, increasing backpressure clearly decreased the volumetric efficiency of the engine. For example, at an engine load of 40 Nm, the volumetric efficiency decreased from 86.56% with orifice#1 to 83.39% with orifice#5. This was probably due to the increased pumping work required for the test engine. In exhaust stroke, exhaust gas discharging efficiency was decreased due to backpressure increment. Increasing the quantity of the remained gas in the cylinder caused a decrease in the intake air quantity aspirated in the intake stroke. As illustrated in Figure 5c, the brake thermal efficiency is directly related with BSFC, and decreasing the BSFC causes an increase in the brake thermal efficiency and vice versa.

In Figure 5d, the effect of backpressure increment on mechanical efficiency of test engine was illustrated. As seen, backpressure increment has a slight positive effect on mechanical efficiency. For instance, at 40 Nm engine load, the mechanical efficiency increased from 86.98% with orifice#1 to 87.51% with orifice#5. This may be a secondary result of decreased maximum in-cylinder pressure and IMEP due to backpressure increment.

Figure 6a, b, c and d illustrate the effect of backpressure increment on CO and NO_x emissions. Figure 6a and 6b shows the emissions in volumetric ratio. Figure 6c and 6d shows the emissions as brake specific exhaust emissions.

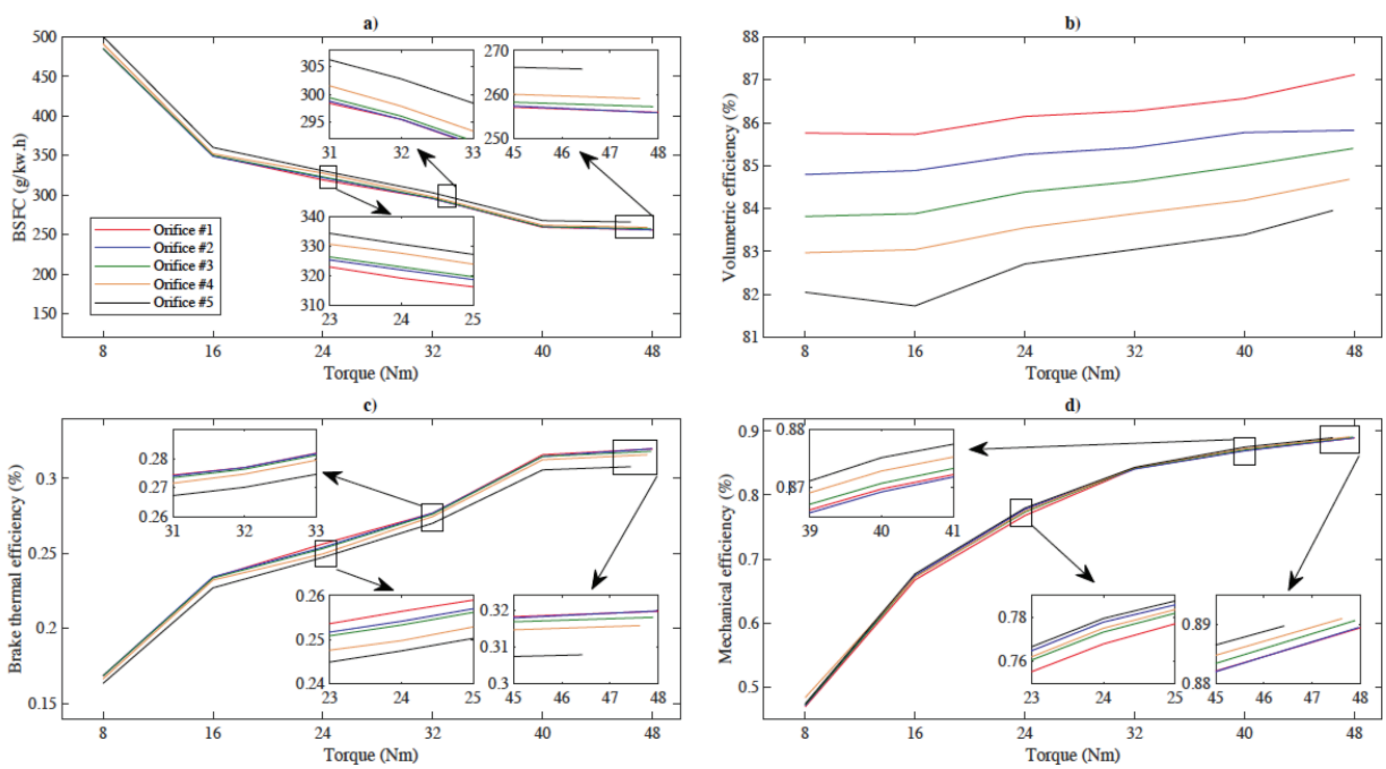

Figure 5. *Efficiency values under different loads a) BSFC, b)* η_v *c)* η_{bt} *and* η_m

BSFC: Brake specific fuel consumption

As shown in Figure 6a and 6-c, which presents increasing backpressure up to 3 kPa with orifice#3, there is no significant change under any loading. Increasing backpressure from approximately 1.28 to 1.78 kPa has caused a slight decrease in brake specific CO emissions as shown in Figure 6c. For example, at an engine torque of 40 Nm, brake specific CO emissions decreased from 5.1565 to 5.1405 g/kW.h. From another view, increasing the backpressure to approximately 3 kPa has also resulted a decrease from 5.1565 to 5.0692 g/kW.h in brake specific CO emissions. Dissimilarly, increasing the backpressure to 7.2 kPa and 25.1 kPa with orifice #4 and orifice #5, respectively, caused a significant increase in brake specific CO emissions. At 40 Nm engine load, the brake specific CO emissions increased to 5.85 and 6.38 g/kW.h respectively. It is almost similar for volumetric CO emissions. On the other hand, increasing backpressure also caused a decrease in NO_x emissions as shown in Figure 6d. At an engine torque of 40 Nm, brake specific NO_x emissions decreased from 10.17 g/kW.h to 9.99, 10.01, 9.6, and 9.32 g/kW.h values with decreasing orifice size. The reason behind the decreasing trend is probably related to the decreasing in-cylinder pressure with increasing backpressure, as shown in Figure 2 and Figure 3. According to Zeldovich [39] Mechanism and Fenimore [40] Mechanism the generation of nitric oxides is directly related with in-cylinder pressure and in-cylinder temperatures. Thus, increasing the backpressure causes decrease of in-cylinder pressure and temperatures and thus it results a significant decrease in brake specific NO_x emissions.

4. Conclusion

The current study was designed to determine the effect of backpressure increment on the performance parameters of a diesel engine. In the experimental study, the exhaust backpressure was increased by installing different sized orifices on the exhaust pipe.

The impacts of backpressure increment on in-cylinder pressure characteristics, mechanical efficiency, brake thermal efficiency, BSFC, volumetric efficiency, and exhaust emissions of the engine were analyzed. From the experimental results, the following conclusions can be drawn:

Increasing exhaust backpressure caused increase in time (as crank angle) for ignition delay. This can be attributed to the retarding of the combustion phases such as rapid pressure rise and main combustion. In addition, the angle of peak pressure was retarded, and the peak cylinder pressure decreased.

The BSFC of the engine increased with backpressure increment. The BSFC increasing characteristics obtained in the current study is similar to the results in previous studies. However, no published study has attempted to find the relationship between BSFC increment and in-cylinder pressure characteristics. In the current study, it was

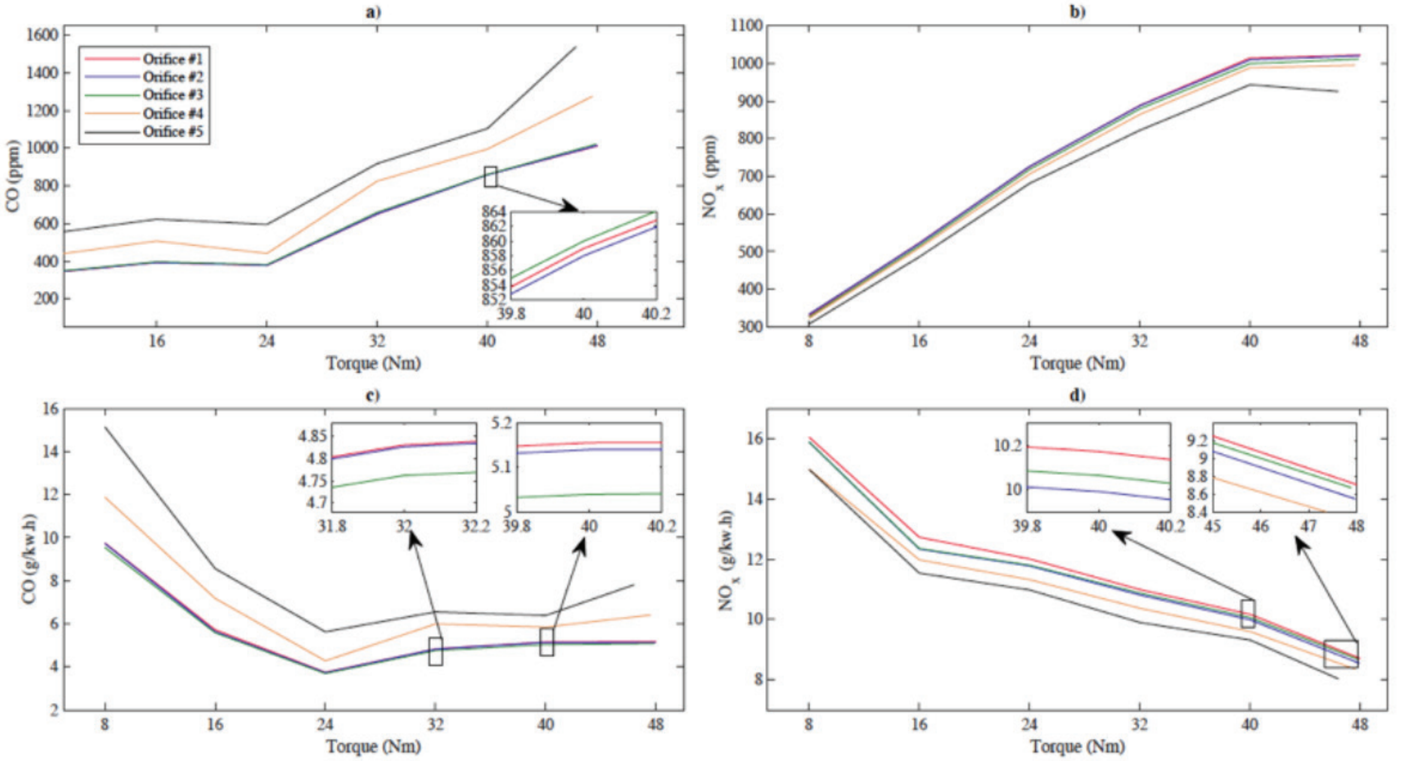

Figure 6. *Exhaust emissions under different loads and backpressures: a) CO (ppm), b) NO_x (ppm) c) CO (g/kW.h), d) NO_x (g/kW.h)*

found that the combustion phases were retarded because of the backpressure increment. Given that retarding the combustion phases causes an increase in BSFC, as a suggestion, some part of BSFC increment penalty may be possibly abated by advancing the fuel injection timing and thus advancing combustion phases. The question raised by the current study may be a new research goal for further studies.

$IMEP_n$ values was decreased with backpressure increment. The main reason behind such a reduction was the increasing trend in the PMEP values, which significantly increased with increasing backpressure. This was an expected outcome due to the strong correlation between the difference in the exhaust and intake manifold pressures and the pumping losses.

The volumetric efficiency of the test engine decreased with increasing backpressure. As the volumetric efficiency is the measure of breathing ability of an engine, probably the increasing flue gas quantity remained in-cylinder after exhaust stroke caused such a reduction. The mechanical efficiency of the engine increased with increasing backpressure. The main reason behind this positive result may be the negative impact of decreasing the force applied to piston and bearings.

The backpressure increment caused an increase in CO emissions especially with higher backpressure. However, a small increment in the backpressure caused a slight decrease in CO emissions. On the other hand, the emissions of nitric oxides (in ppm) decreased with increasing backpressure.

The backpressure increment caused a decrease in the maximum available torque values. Thus, the engine torque decreased to 46.4 Nm from 48 Nm under high backpressure.

The current study has some limitations, e.g., the generalizability of the results. For instance, the effects of backpressure increment for the current test engine was studied in detail and the results of the study is repeatable for the specific test engine. However, no experimental study was conducted using different engine models or under different operational conditions. Notwithstanding these limitations, the study suggests that the backpressure increment causes a decrease in almost all performance indicators of diesel engines. The findings will be useful for studies to be conducted on estimating the level of negative impact of installing any system on exhaust pipe of an engine such as aftertreatment or WHR systems. Further researches can be conducted to optimize the engine operational parameters to minimize the negative impact of backpressure increment on engine performance. The study can be reproduced in a different engine testing laboratory with a different test engine to make generally accepted evaluation about the role of backpressure increment on the performance of diesel engines.

Authorship Contributions

Concept design: Y. Gülmez, G. Özmen, Data Collection or Processing: Y. Gülmez, Analysis or Interpretation: Y. Gülmez, G. Özmen, Literature Review: Y. Gülmez, Writing, Reviewing and Editing: Y. Gülmez, G. Özmen.

Funding: The authors declared that this study received no financial support.

References

[1] M. Naseri, C. Aydin, S. Mulla, R. Conway and S. Chatterjee, “Development of emission control systems to enable high NO_x conversion on heavy duty diesel engines,” *SAE International Journal of Engines*, vol. 8, pp. 1144-11451, Apr 2015.

[2] C. Zhang, C. Sun, M. Wu, and K. Lu, “Optimisation design of SCR mixer for improving deposit performance at low temperatures,” *Fuel*, vol. 237, pp. 465-474, Feb 2019.

[3] A.J. Martyr and M.A. Plint, “Engine exhaust emissions,” in Engine Testing (Fourth Edition), A.J. Martyr and M.A. Plint, Eds. Oxford: Butterworth-Heinemann, 2012, pp.407-450. [Online]. Available: Science Direct, https://doi.org/10.1016/B978-0-08-096949-7.00016-9. [Accessed: May 5, 2021].

[4] A. M. Stamatellou and A. Stamatelos, “Overview of diesel particulate filter systems sizing approaches,” *Applied Thermal Engineering*, vol. 121, pp. 537-546, Jul 2017.

[5] Z. Li, K. Jue, D. Lou, X. Zhong, and Y. Zhang, “Effect of electric diesel particulate trap on particulate emission characteristics of light-duty diesel engine,” *IOP Conference Series Earth Environmental Science*, vol. 510, 2020.

[6] I. Rounce, M. Bogarra, J. M. Herreros, F. J. Martos Ramos, and A. Tsolakis, “Understanding the effects of catalytic partial flow filters on particle removal efficiency,” *Results in Engineering*, vol. 4, Sep 2019.

[7] F. D’Aniello, B. Rossomando, I. Arsie, and C. Pianese, “Development and experimental validation of a control oriented model of a catalytic DPF,” SAE Technical Paper 2019-01-0985. pp. 1-14, Apr 2018.

[8] J. He, K. Chen and J. Xu, “Urban air pollution and control,” in Encyclopedia of Sustainable Technologies, M.A. Abraham, Eds. Cambridge: Elsevier, 2017, pp. 243-257.

[9] O. Chiavola, G. Chiatti, and N. Sirhan, “Impact of particulate size during deep loading on DPF management,” *Applied Sciences*, vol. 9, 2019.

[10] Y. Cui, et al. “Combustion and emission characteristics of wood pyrolysis oil-butanol blended fuels in a DI diesel engine,” *International Journal of Automotive Technology*, vol. 19, no. 5, pp. 759–769, 2018, [Online]. Available: Springer Link, https://doi.org/10.1007/s12239. [Accessed: May 5, 2021].

[11] J. Zhang, V. W. Wong, S. Shuai, Y. Chen and A. Sappok, “Quantitative estimation of the impact of ash accumulation on diesel particulate filter related fuel penalty for a typical modern on-road heavy- duty diesel engine” *Applied Energy*, vol. 229, pp. 1010-1023, Nov 2018.

[12] H. Wang, et al. "The effects of ash inside a platinum-based catalyst diesel particulate filter on particle emissions, gaseous emissions, and unregulated emissions," *Environmental Science and Pollution Research,* vol. 25, pp. 33736-33744, Oct 2018.

[13] X. Wu, J. Chen, and L. Xie, "Optimal design of organic Rankine cycles for exhaust heat recovery from light-duty vehicles in view of various exhaust gas conditions and negative aspects of mobile vehicles," *Applied Thermal Engineering*, vol. 179, Oct 2020.

[14] E. Baldasso, M. E. Mondejar, J. G. Andreasen, K. A. T. Rønnenfelt, B. Ø. Nielsen, and F. Haglind, "Design of organic Rankine cycle power systems for maritime applications accounting for engine backpressure effects," *Applied Thermal Engineering*, vol. 178, pp. 115527, Sep 2020.

[15] M. Zhao, M. Wei, P. Song, Z. Liu, and Z. Wang, "Effects of the ORC operating conditions on the engine performance for an engine-ORC combined system," *Energy Procedia*, vol. 105, pp. 662-667, May 2017.

[16] A. Karvountzis-Kontakiotis, I.Pesmazoglou, and L. Tocci, "*Effect of an ORC waste heat recovery system on diesel engine fuel economy for off-highway vehicles,*" SAE Technical Paper 2017-01-0136, [Online]. Available: SAE Mobilus, https://doi.org/10.4271/2017-01-0136. [Accessed: May 5, 2021].

[17] D. Di Battista, M. Di Bartolomeo, C. Villante, and R. Cipollone, "A model approach to the sizing of an ORC unit for WHR in transportation sector," *SAE International Journal of Commercial Vehicles*, vol. 10, pp. 608-617, Apr 2017.

[18] P. Tourlonias and G. Koltsakis, "Model-based comparative study of Euro 6 diesel aftertreatment concepts, focusing on fuel consumption," *International Journal of Engine Research,* vol. 12, pp. 238-251, June 2011.

[19] H.D. Sapra, J. Singh, C. Dijksta, P. de Vos and K. Visser, "*Experimental investigations of marine diesel engine performance against dynamic back pressure at varying sea-states due to underwater exhaust systems,*" in ASME 2019 Internal Combustion Engine Division Fall Technical Conference, ICEF 2019, 20 October 2019 - 23 October 2019, [Online]. Available: https://asmedigitalcollection.asme.org/ICEF/ICEF2019/volume/59346, [Accessed: June 6, 2021].

[20] A. R. Sivaram, R. Rajavel, N. Jayakumar and M. Vinothkumar "Exhaust back pressure effect on the performance features of a diesel engine," *ARPN Journal of Engineering and Applied Sciences,* vol. 12, pp. 5353-5356, Oct 2017.

[21] H. D. Sapra, M. Godjevac, K. Visser, D. Stapersma and C. Dijksta, "Experimental and simulation-based investigations of marine diesel engine performance against static back pressure" *Applied Energy*, vol. 204, pp. 78-92, Oct 2017.

[22] S. Cong, G.P. McTaggart-Cowan and C. P. Garner, "*The effects of exhaust back pressure on conventional and low temperature diesel combustion" in IMechE's Internal Combustion Engines: Performance*, Fuel Economy and Emissions Conference, London, 8 December 2009 - 9 December 2009, [Online]. Available: https://journals.sagepub.com/doi/10.1177/09544070JAUTO1577, [Accessed: June 6, 2021].

[23] V. Fernoaga, V. Sandu and T. Balan, "Artificial intelligence for the prediction of exhaust back pressure effect on the performance of diesel engines," *Applied Sciences,* vol. 10, pp. 7370, Sep 2020.

[24] S. Thirumurugaveerakumar, "Design and optimization of muffler back pressure" in International Conference on Physics and Chemistry of Materials in Novel Engineering Applications AIP Conf. Proc. 2270, 120001-1–120001-7, 2020, [Online]. Available: https://doi.org/10.1063/5.0019700, [Accessed: June 6, 2021].

[25] J. Kim and C. Bae, "Emission reduction through internal and low-pressure loop exhaust gas recirculation configuration with negative valve overlap and late intake valve closing strategy in a compression ignition engine," *International Journal of Engine Research*, vol. 18, pp. 973-990, Feb 2017.

[26] Z. Yang, S. et al. "Preliminary investigation of exhaust pressure waves in a single cylinder diesel engine and the impacts on aftertreatment sprays," *SAE International Journal of Engines*, vol. 10, pp. 636-645, April 2017.

[27] P. Kasprzyk, J. Hunicz, A. Rybak, M. S. Geca and M. Mikulski, "Excess air ratio management in a diesel engine with exhaust backpressure compensation" *Sensors,* vol. 20, pp. 1-16, Nov 2020.

[28] A. M. Andwari, A. Pesyridis, V. Esfahanian, A. Salavati-Zadeh, and A. Hajialimohammadi, "Modelling and evaluation of waste heat recovery systems in the case of a heavy-duty diesel engine," *Energies,* vol. 12, pp. 1397, Apr 2019.

[29] C. N. Michos, S. Lion, I. Vlaskos, and R. Taccani, "Analysis of the backpressure effect of an Organic Rankine Cycle (ORC) evaporator on the exhaust line of a turbocharged heavy duty diesel power generator for marine applications," *Energy Conversion Management*, vol. 132, pp. 347-360, Jan 2017.

[30] Y. Choi, A. Negash, and T. Y. Kim, "Waste heat recovery of diesel engine using porous medium-assisted thermoelectric generator equipped with customized thermoelectric modules," *Energy Conversion and Management,* vol. 197, pp. 111902, Oct 2019.

[31] H. Lu, A. Yao, C. Yao, C. Chen, and B. Wang, "An investigation on the characteristics of and influence factors for NO2 formation in diesel/methanol dual fuel engine," *Fuel,* vol. 235, pp. 617-626, Jan 2019.

[32] F. Payri, J.M. Luja´n, J. Martı´n and, A. Abbad, "Digital signal processing of in-cylinder pressure for combustion diagnosis of internal combustion engines," *Mechanical Systems and Signal Processing*, vol. 24, pp. 1767-1784, Aug 2010.

[33] International Maritime Organization Marine Environment Protection Committee, "Resolution MEPC.177(58) NOx Technical Code," 2008, [Online]. Available: https://wwwcdn.imo.org/localresources/en/KnowledgeCentre/IndexofIMOResolutions/MEPCDocuments/MEPC.177(58).pdf. [Accessed: May. 5, 2021].

[34] P. Hield, "The effect of backpressure on the operation of diesel engines," MA: Australia Government, Department of Defence, Maritime Platform Division, 2011. [Online]. Available: https://apps.dtic.mil/sti/pdfs/ADA542137.pdf. [Accessed: May. 5, 2021].

[35] E. F. Pehlivan and İ. Altın, "Biyodizel pilot püskürtmeli doğalgaz yakıtıyla çalışan bir dizel motorda silindir basıncı değişiminin stokastik reaktör model kullanılarak incelenmesi," *Journal of Eta Maritime Science*, vol. 5, pp. 5-17, 2017.

[36] A.K. Agarwal, et al, "Effect of fuel injection pressure and injection timing of Karanja biodiesel blends on fuel spray, engine performance, emissions and combustion characteristics,"

Energy Conversion and Management, vol. 91, pp. 302-314, Feb 2015.

[37] A. Yousefi, H. Guo and M. Birouk, "Effect of diesel injection timing on the combustion of natural gas/diesel dual-fuel engine at low-high load and low-high speed conditions," *Fuel,* vol. 235, pp. 838-846, 2019.

[38] K. Bayramoğlu and M. Nuran, "Analyzing the effect of fuel injection timing and injection duration on performance and emissions in diesel engines" *Journal of Eta Maritime Science*, vol. 8, pp. 38-52, 2020.

[39] Y.B. Zeldovich, "The oxidation of nitrogen in combustion and explosions" *in Selected Works of Yakov Borisovich Zeldovich, Volume I Chemical Physics and Hydrodynamics*, G. I. Barenblatt and Rashid Alievich Sunyaev, Eds. Oxford: Princeton University Press, 1992, pp. 364-403.

[40] C. P. Fenimore, "Formation of nitric oxide in premixed hydrocarbon flames," *Symposium (International) on Combustion,* vol. 13, pp. 373-380, 1971.

ORIGINAL RESEARCH (AR)

DOI: 10.4274/jems.2021.24654

Journal of ETA Maritime Science 2021;9(3):192-199

Numerical Self-Propulsion Assessment of a Generic Submarine Model at Various Forward Speeds

Taner Çoşgun

Yıldız Technical University, Department of Naval Architecture and Marine Engineering, İstanbul, Turkey

Abstract

In this study, we use computational fluid dynamics (CFD) to investigate the self-propulsion characteristics of a submarine model. Predicting a marine vehicle's self-propulsion features, and as a result, determining the thrust force required to drive the ship with a constant forward speed is critical for the propulsive system and main engine selection. A Reynolds-Averaged-Navier-Stokes Equations based numerical methodology has been applied to the flow field around the Defense Advanced Research Projects Agency suboff geometry to predict the self-proportion characteristics of a marine vehicle. First, the model's self-propulsion characteristics were determined for a relatively lower hull speed (5.35 knots), and the results were compared with those of other studies and experiments. The study was then extended to include higher forward speeds ranging from 5.93 to 17.79 knots. The results reveal that the propeller rotation rate at the model's self-propulsion point rises as the vessel speed and the power requirement increase. Similarly, the advance coefficient remains nearly unaffected by the Froude Number. The resistance components, propulsion characteristics, flow field surrounding the model, and the wake structure in the propeller slipstream were also evaluated for the determined self-propulsion points.

Keywords

Self-propulsion estimation, DARPA, Submarine, Resistance, Computational fluid dynamics

1. Introduction

Determining the propulsion performance is one of the key features of the initial design stage of marine vehicles. As the performance of a propeller behind a hull generally differs from that of open water tests, self-propulsion assessments provide valuable information in ensuring that a ship equipped with the propeller can operate with the requisite forward speed. Therefore, in the recent decade, numerous research efforts have been focused on the high-fidelity self-propulsion predictions of surface ships and submarines [1-5].

The conventional method for evaluating the hydrodynamic performance of marine vehicles is to conduct model testing. Although model tests produce reliable data, they are time-consuming and expensive. Computational fluid dynamics (CFD) has been gaining attention as an effective and reliable alternative tool for investigating the hydrodynamics and flow details around floating bodies. For self-propulsion investigations and other fields of numerical marine hydrodynamics, numerical simulations, such as virtual towing tank tests, have become a common technique. Carrica et al. [6] numerically presented a method for predicting the self-propulsion point of three benchmark ship geometries. They aimed at satisfying the thrust-resistance equilibrium by controlling the propeller rotational speed. Using CFD calculations, Castro et al. [7] predicted the full-scale self-propulsion computations of the KRISO Container Ship (KCS) hull. They concluded that the propeller operates more efficiently in full scale than in model scale calculations. Shen et al. [8] investigated the self-propulsion and maneuvering of KCS using the open-source CFD tool OpenFOAM with the dynamic overset grid technique. Gaggero et al. [9] considered the same KCS test case to apply the coupled Boundary Element

Address for Correspondence: Taner Çoşgun, Yıldız Technical University, Department of Naval Architecture and Marine Engineering, İstanbul, Turkey
E-mail: tcosgun@yildiz.edu.tr
ORCID ID: orcid.org/0000-0002-1364-0133

Received: 28.06.2021
Accepted: 02.08.2021

To cite this article: T. Coşgun, "Numerical Self-Propulsion Assessment of a Generic Submarine Model at Various Forward Speeds." *Journal of ETA Maritime Science*, vol. 9(3), pp. 192-199, 2021.

Method/Reynolds Averaged Navier-Stokes (RANS) approach to obtain self-propulsion characteristics. He et al. [10] performed a gradient-based design optimization of self-propulsion for a Japanese bulk carrier (JBC). Their study focused on using the proposed method that considers the hull-propeller interaction and allows the use of a large number of design variables to optimize the shape of the stern region of the hull. Bakica et al. [11] used OpenFOAM to calculate the self-propulsion characteristics of the JBC hull and investigate the wake field of the KCS hull. Feng et al. [12] proposed a new body force method coupled with the blade element momentum theory to estimate the self-propulsion performance of the KCS hull. They reported that while preserving the body force method's computational efficiency, the new model considers the three-dimensional viscous effects to improve the fidelity of the predictions. Sezen et al. [13] investigated the self-propulsion characteristics of a full-scale vessel. They also examined the scale impact on the results and put the 1978 International Towing Tank Conference (ITTC) performance prediction method to the test. Several researchers have also studied the self-propulsion performance of ships at full scale [14-16].

Predicting the propulsion characteristics of submarines, like surface ships, has been the subject of several studies. Chase [17] developed an inhouse CFD solver to investigate the effects of the turbulence models on the self-propulsion performance and wake field of the Defense Advanced Research Projects Agency (DARPA) submarine model. Zhang and Zhang [18] investigated the self-propulsion characteristics and resistance of a submarine model operating close to a free surface. Sezen et al. [19] applied RANS based numerical methodology on analyzing a benchmark submarine's self-propulsion performance. They compared the body force (actuator disc) method's results with the self-propelled submarine model calculations. Kinaci et al. [20] estimated a submarine's self-propulsion points and two surface ship models. They also performed the same calculations using a classical engineering approach in addition to the CFD analysis. They compared the results of different methodologies with those of other researchers. Carrica et al. [21] investigated the self-propulsion characteristics of a generic Joubert BB2 submarine model in free surface proximity conditions. Their study also included waves' effect on the propulsion performance and wake in the propeller slipstream.

In this paper, we discuss the numerical estimation of the self-propulsion characteristics of the DARPA submarine model. A RANSE based commercial finite volume solver, Siemens Star CCM+, was used in the computations. Self-propulsion features of the model were calculated at a relatively lower forward speed first to compare and validate the present results with other studies. The study was then extended to include higher hull velocities. The submarine model's self-propulsion points and power requirements were calculated for various forward speeds. Furthermore, both self-propelled and towed cases were subjected to resistance analysis. Limited wake stricter investigations were presented to understand the change in the resistance components.

2. Materials and Methods

2.1. Numerical Modeling

This section presents the numerical modeling details. Below are the descriptions of the benchmark submarine model's geometrical features, numerical methodology, and grid topology.

2.2. Geometry of the Problem

The computations are conducted on the benchmark submarine model introduced by DARPA. The DARPA's submarine form had two configurations at first: AFF-1 and AFF-8. The fundamental distinction between both forms is that AFF-8 has appendages like rudders and sail, whereas AFF-1 is a bare hull form with no appendages. For the current numerical simulations, the AFF-8 submarine hull form shown in Figure 1 is selected. Table 1 lists the main dimensions of the model. Ref. [22] and [23] provide more details about the AFF-8 submarine form. The self-propulsion computations used an INSEAN E1619 propeller. The propeller has seven blades and is 0.262 m in diameters. The propeller's details can be found in [24].

Table 1. *The main properties of the DARPA submarine model*

Parameter	Dimension
L_{OA} (m)	4.356
L_{BP} (m)	4.261
D_{max} (m)	0.508
S (m^2)	6.348
∇ (m^3)	0.706
DARPA: Defense Advanced Research Projects Agency	

2.3. Governing Equations and Solution Strategy

The velocity and pressure fields were obtained using a numerical solution of the time-dependent Navier-Stokes equations and the continuity equation. The equations 1 and 2 are:

$$\frac{\partial u_i}{\partial x_i} = 0 \quad (1)$$

where u_i is the time-averaged velocity, p is the pressure, ρ is the density, and μ is the dynamic viscosity. The last term on the right-hand side of Eq. 2 denotes the Reynolds stress tensor, representing the turbulence effects on the mean momentum.

$$\rho\left(\frac{\partial u_i}{\partial t}+u_j\frac{\partial u_i}{\partial x_j}\right)=-\frac{\partial p}{\partial x_i}+\frac{\partial}{\partial x_j}\left(\mu\frac{\partial u_i}{\partial x_j}-\rho\overline{u_i'u_j'}\right) \quad (2)$$

A commercial CFD tool, Star CCM+, is used in the computations. The solver implements the finite volume method for discretizing the governing equations. To improve the accuracy of the solution, a temporal and spatial discretization was done using a second-order scheme. The SIMPLE algorithm is used for velocity-pressure coupling.

The turbulent field is modeled using the realizable k-e turbulence model with the wall-function approach. The turbulence model is described in detail in the solver's documentation [25].

The rotational motion of the propeller was modeled using the rigid body motion (RBM) method, often known as the sliding interface technique. Simulations were first initialized steadily with the moving reference frame method, which simulates the quasi-steady flow around the propeller. After the steady simulations had converged, the numerical procedure was switched to unsteady. Here, the aim is to provide preliminary data for the unsteady simulations.

2.4. Computational Domain and Boundary Conditions

The flow around the submarine model was solved using a rectangular-shaped computational domain. Numerical predictions were performed in a Cartesian coordinate system with the negative x-axis in the incoming flow direction and the positive +z-axis pointing upwards. The origin of the coordinate system was located in the submarine model's aft peak. The submarine model was placed at the 2LBP and 5LBP, away from the inlet and outlet boundaries. The solution domain's sidewalls were extended to a length of 2LBP from the submarine hull's center. These dimensions were selected to be large enough to capture all flow field changes while complying with the ITTC recommendations [26].

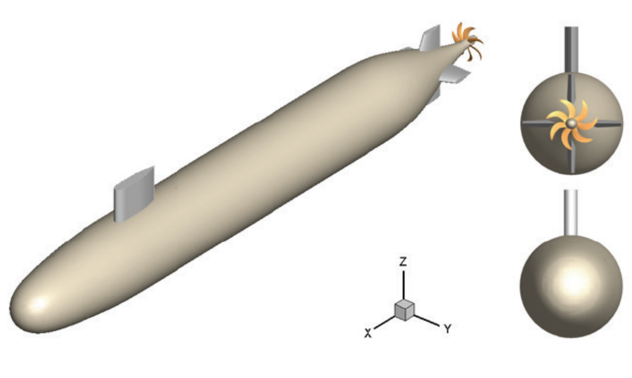

Figure 1. *Geometry of the DARPA submarine model*

DARPA: Defense Advanced Research Projects Agency

A uniform velocity profile was imposed on the solution domain inlet boundary. The study tested seven distinct inflow velocities: 2.75, 3.05, 5.14, 6.10, 7.16, 8.23, and 9.15 m/s, which corresponds to 5.35, 5.93, 10.00, 11.85, 13.92, 16.00, and 17.79 knots, respectively. Pressure outlet boundary condition is used for the outlet boundary, whereas the submarine hull was treated with a no-slip wall condition. The rest of the domain surfaces were treated with a symmetry condition.

2.5. Grid Structure

The solution domain was constructed using unstructured hexahedral elements. Figure 2 depicts the general view of the grid topology. When generating the surface grid, special care was taken to ensure the high curvature of the appendages and propeller blades are well represented. Prismatic layers were used on the solid surfaces along the submarine hull to capture the boundary layer adequately. Positive y+ values are kept in the range of 30<y+<300 on the submarine hull to comply with the RANS closure's standard wall-function approach ($y+=u_\tau y/\nu$, where u_τ is the friction velocity, y is the height of the first cell on the wall and ν is the kinematic viscosity).

A couple of refinement regions were created on some parts of the solution domain. First, the computational grid was refined around the submarine hull. Furthermore, local grid refinements were applied to the wake region and the appendages for accurate modeling of the possible flow separations and high-velocity gradients. The other refinement was achieved in the propeller slipstream. Additionally, attention is paid to providing a smooth mesh transition and alignment between the inside and outside of the interface boundary around the rotating propeller zone to avoid any other numerical error. The simulations used 2.31 M elements after conducting a grid dependency study.

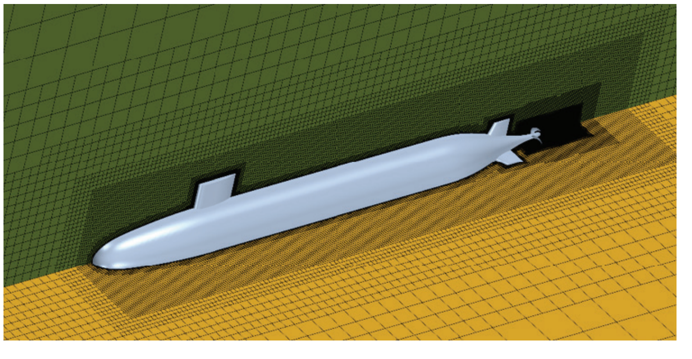

Figure 2. *Grid structure around the submarine model*

3. Numerical Results

The self-propulsion points, resistance components, and wake structure of the DARPA Suboff at different velocities were determined using CFD. First, a validation of the numerically obtained results was conducted against the related experimental data. As shown in Figure 3, resistance analysis of the DARPA geometry was performed for various velocities and compared with Liu and Huang's [23] experimental measurements. As seen from the figure, numerical results for all data points are in excellent agreement with the experimental results. The maximum relative error between the two sets of results is approximately 2%.

Table 2 presents the self-propulsion characteristics for the DARPA submarine model at V=5.35 knots forward speed and compares it with the results of other studies. In Table 2, Oscillating Water Column (OWC) denotes the open water curve. The calculated thrust coefficient has been placed at the matched point of the propeller's open water performance curve to obtain the corresponding advance coefficient at that self-propulsion point. The thrust and torque coefficients were calculated using the thrust and torque values from the self-propelled CFD analysis. The calculation 3 and 4 are as follows;

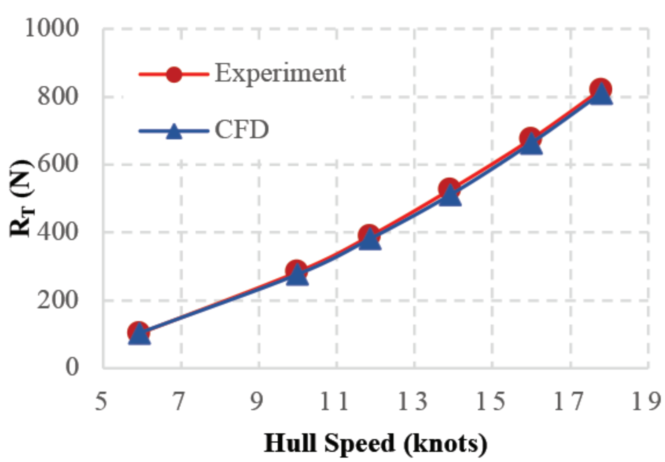

Figure 3. *Total resistance calculations for DARPA hull*

DARPA: Defense Advanced Research Projects Agency, CFD: Computational fluid dynamics

$$K_T = \frac{T}{\rho n^2 D^4} \quad (3)$$

$$K_Q = \frac{Q}{\rho n^2 D^5} \quad (4)$$

here T and Q denote the trust and torque values, respectively. D is the propeller diameter. The advance ratio of the propeller is calculated using the axial velocity V_A that the propeller receives and the rotation rate n;

$$J = \frac{V_A}{n.D} \quad (5)$$

the open water propeller efficiency is;

$$\eta_0 = \frac{T.V_A}{2\pi.n.Q_0} \quad (6)$$

here Q_O represents the open water propeller torque. As shown in Table 2, the results of this numerical methodology are close to those of other studies. The advance coefficient and the trust values are remarkably similar to the results presented by Chase and Carrica [24] using experimental OWC. The open water efficiency is within the range of other studies' CFD results, although slightly lower than the experimental OCW predictions. Figure 4 illustrates the DARPA suboff geometry's self-propulsion characteristics determined at higher hull speeds. As shown, the predicted propeller rotation rate values are in good agreement with those of other researchers. The propeller rotational speed (rps- rotation per second) required to drive the hull at a given forward velocity increases with the hull speed. The propeller rotation rates curve at the self-propulsion point has a linear trend. In contrast, the variation of other characteristics to changing hull speed is nearly constant. Similar findings were reported by Kinaci et al. [27]. They numerically investigated the self-propulsion performance of the benchmark DTC hull and showed that J, K_T, and K_Q remain nearly unchanged, whereas the propeller rotation rate increases with increasing Froude Number.

Table 2. *Self-propulsion results at V=5.35 knots*

	J	K_T	K_Q	η_0
Chase and Carrica [24] - Using Experimental OWC	0.7659	0.2342	0.0435	0.6602
Chase and Carrica [24] - Using CFD OWC	0.7498	0.2342	0.04558	0.6115
Kinaci et al. [20] - Self propelled CFD	0.7774	0.2312	0.0461	0.6202
Özden and Çelik [28] - Self propelled CFD	0.7280	0.2416	0.0464	0.6030
Sezen et al. [19] - Using CFD OWC	0.8146	0.2363	0.0454	0.6752
Present - Using CFD OWC	0.7632	0.2321	0.0449	0.6315

CFD: Computational fluid dynamics, OWC: Oscillating Water Column

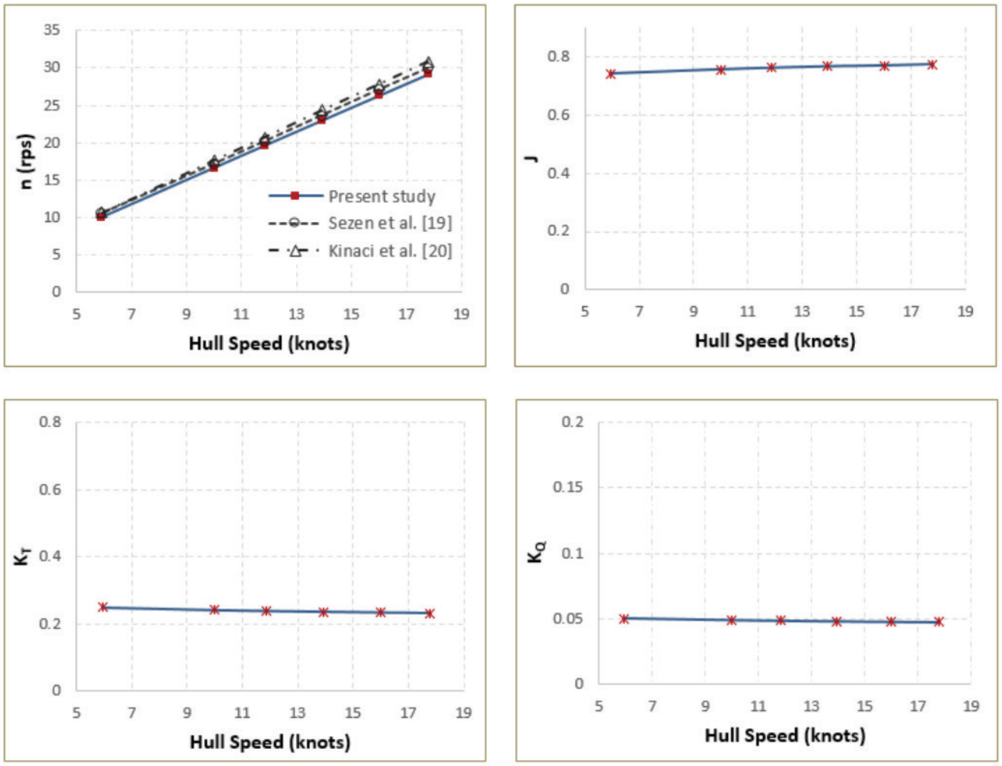

Figure 4. *Self-propulsion characteristics of DARPA suboff at different forward velocities*

DARPA: Defense Advanced Research Projects Agency

Figure 5 shows the power estimation of the DARPA suboff for determined self-propulsion points. The figure includes the effective power (P_E) that is required to pull the hull at a constant speed and the power delivered to the propeller (P_D). The effective power is computed as follows:

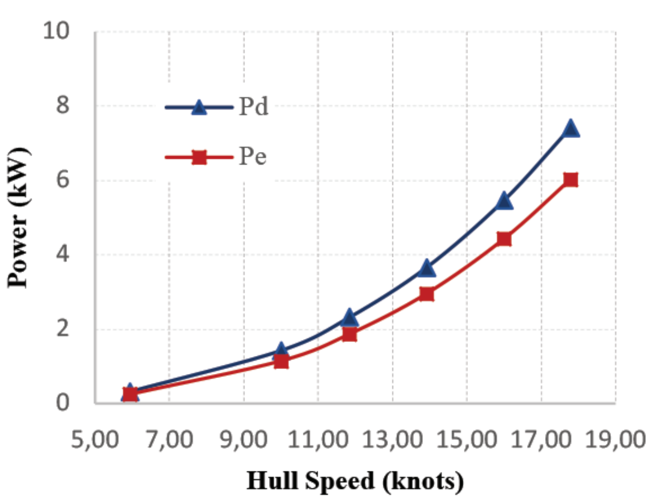

Figure 5. *Required power predictions of DARPA hull*

DARPA: Defense Advanced Research Projects Agency

$$P_E = R_T . V_S \quad (7)$$

where R_T is the total resistance of the hull and V_S is the given hull velocity. Then the power delivered to the propeller is calculated as:

$$P_D = \frac{P_E}{\eta_D} \quad (8)$$

In Equation 8, η_D represents the propulsion efficiency and can be calculated as: $\eta_D = \eta_H . \eta_0 . \eta_R$, where the hull efficiency η_H, and the relative rotation efficiency η_R, is:

$$\eta_R = \frac{Q_0}{Q} \quad (9)$$

$$\eta_H = \frac{1-t}{1-w} \quad (10)$$

In Eq. 10, the thrust reduction factor t can be obtained using the total towed resistance of the hull and the thrust generated by the propeller using $t = T - R_T / T$. The nominal wake coefficient W can be calculated using the axial velocity that the propeller receives and the hull velocity: $w = V_s - V_A / V_S$. Figure 5 shows that at relatively lower hull speeds, the effective and delivered power values are very close to each other at the self-propulsion points. As the forward velocity increases, the effective power falls below the delivered power value owing to the propulsion efficiency in Equation 8. In reality, the propulsion efficiency does not deviate significantly for varying hull velocities, but the increasing effective hull resistance and power values for higher forward speeds are responsible for this discrepancy.

The resistance features of the DARPA hull for the towed and self-propelled cases are also investigated, as Figure 6 depicts. As expected, an increase in the hull's forward speed gives rise to the resistance forces. Considering the total resistance R_T, the towed and the self-propelled submarine results are similar. The disparity in the calculations increases with increasing hull velocity. When we examine the resistance components in the two scenarios, the friction resistance values are almost equal. However, the computed viscous pressure resistance values show an increasing discrepancy with rising hull speed. We can conclude that the difference between the total resistance values of towed and self-propelled cases is owing to the pressure-related forces.

The normalized axial velocities around the submarine hull are presented in Figure 7 to investigate the flow field around the submarine model. The figure shows the upper and the lower bounds of the investigated hull velocity range. The normalized axial velocity value is non-dimensionalized using the hull velocity $u^* = u/V_S$ and then presented with the threshold value $u^* \leq 1$ to examine the boundary layer distribution. For higher and lower forward speeds, the normalized axial velocity distributions around the submarine hull are similar. Notably, these velocity values are the normalized values, and as the vessel speed increase, the dimensional axial velocities rise in value. Owing to the symmetrical geometry of the submarine model, the axial velocity distribution and boundary layer thickness along the hull do not show a strong variation in the streamwise direction, except in the wake region of the sail. The sail's wake seems to vanish toward the aft of the hull. According to Sezen et al. [19] the resistance and self-propulsion analyses of the benchmark DARPA Suboff with E1619 propeller have been done using Computational Fluid Dynamics (CFD, the sail' wake still exists in the propeller plane and slightly accelerates the flow. Compared with the bare form of the DARPA submarine model, they reported that the other appendages also affect the velocity distribution on the propeller plane. Furthermore, Dogrul's [29] revealed that the appendages of the present investigated model had an effect on and raised the resistance and form factor values.

Figure 8 demonstrates the tangential velocity distribution in the propeller's slipstream. The tangential velocity around the submarine hull is mainly concentrated in the propeller slipstream, allowing the propeller wake extension information to be accessible. The tangential velocity values for the lower hull speed are relatively lower and rapidly decreasing with increasing distance from the propeller. As the hull speed increases, the close and far cross-sections tangential velocities from the propeller rises. From Figure 4, the required propeller rotational speed increases to overcome the increasing hull drag for higher forward speeds. As the propeller rotates at higher rps, the propeller wake penetrates through a broader region for high hull speeds. Consquently, a wider wake alters the pressure distribution around the submarine. In contrast to the towed cases, there is no propeller rotation to influence the velocity and pressure distribution on the hull's wake. In the self-propelled cases, a stronger propeller wake with high forward speed possibly causes the discrepancy in the pressure resistance results in Figure 6.

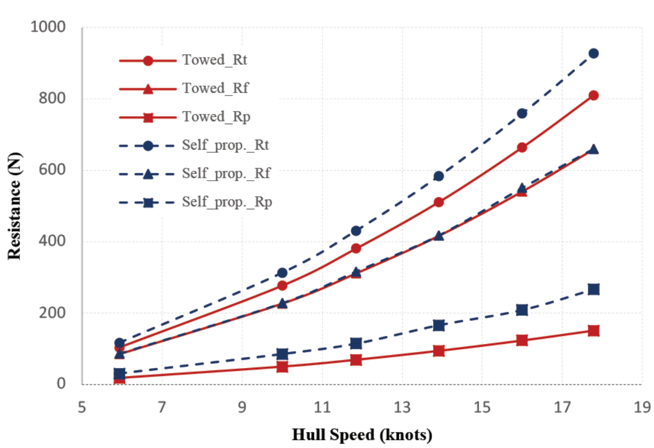

Figure 6. *Resistance components of DARPA hull for towed and self-propelled cases*

DARPA: Defense Advanced Research Projects Agency

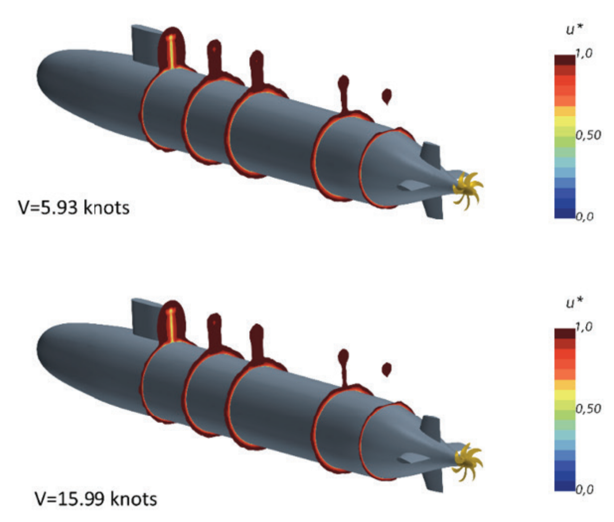

Figure 7. *Normalized axial velocities around the hull*

4. Conclusion

This study presents the self-propulsion estimation and resistance analysis of the DARPA submarine model. A RANSE based CFD methodology was used to calculate the flow field around the towed and the self-propelled submarine hulls. The propeller rotation for the self-propulsion computations was modeled using the RBM method. The study aims to assess the submarine model's self-propulsion characteristics for various higher forward speeds and investigate the resistance components variation. The self-propulsion performance of the DARPA suboff for a relatively lower hull speed was calculated and compared to the predictions of other researchers for validation. The results of reported calculations agreed well with that of other studies. Then, using the same methodology, the self-propulsion points for increasing hull forward velocities were estimated. The results reveal that the propeller rotation rate (rps) increases for higher hull speeds, while the advance coefficient (J) remains nearly constant. The power analysis showed a growing disparity between the delivered and the effective powers as the hull speed increased.

The self-propelled hull's total resistance is higher than the towed cases. Considering the resistance components, the frictional resistance values of the two cases are very close; however, the viscous pressure resistance values diverge with increasing hull speed. For the self-propelled cases, the tangential velocity distribution in the propeller slipstream shows a stronger wake with increasing hull speeds. The resistance discrepancies of the towed and self-propelled cases have been attributed to the influence of the propeller rotation on the velocity and pressure distribution on the wake region.

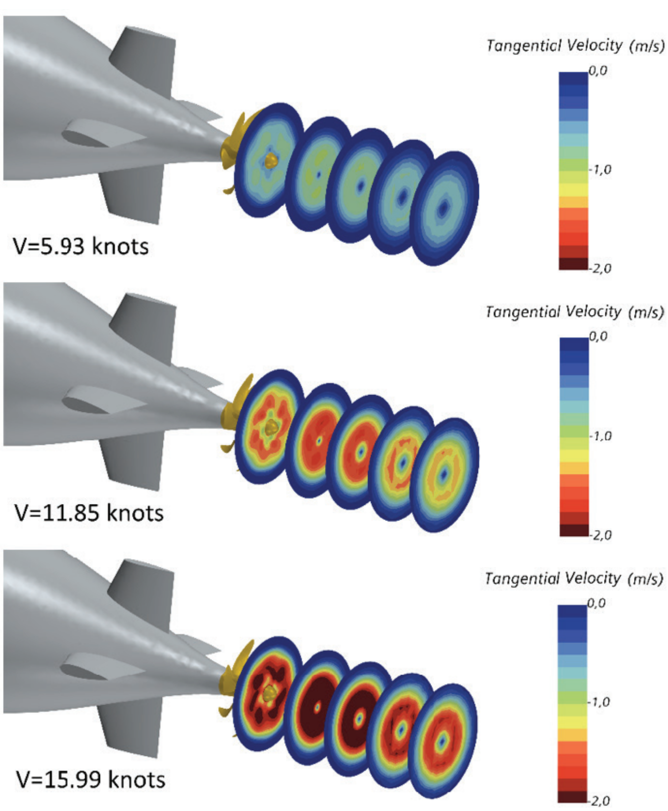

Figure 8. *Tangential velocity distributions in the propeller slipstream*

Acknowledgments

The authors wish to thank Dr. Mario FELLI and INSEAN for sharing the geometry and the experimental data of the INSEAN E1619 submarine propeller.

Funding: The author declared that this study received no financial support.

References

[1] C. Guo, X. Wang, C. Wang, Q. Zhao, and H. Zhang, "Research on calculation methods of ship model self-propulsion prediction," *Ocean Engineering*, vol. 203, pp. 107232, May 2020.

[2] L. Zhang, Y. Wei, Y. Deng, H. Yin, Y. Shang and J. Zhang, "A comparative investigation of fixed and free-running CFD self-propulsion models on a waterjet-propelled trimaran," *Ocean Engineering*, vol. 232, pp. 109081, Jul 2021.

[3] A.M. Bassam, A. B. Phillips, S. R. Turnock, and P. A. Wilson, "Experimental testing and simulations of an autonomous, self-propulsion and self-measuring tanker ship model," *Ocean Engineering*, vol. 186, pp. 106065, Aug 2019.

[4] D. Villa, S. Gaggero, T. Gaggero, G. Tani, G. Vernengo, and M. Viviani, "An efficient and robust approach to predict ship self-propulsion coefficients," *Applied Ocean Research,* vol. 92, pp. 101862, Nov 2019.

[5] F. Jiang, Y. Li, and J. Gong, "Study on the manoeuvre characteristics of a trimaran under different layouts by water-jet self-propulsion model test," *Applied Ocean Research,* vol. 108, pp. 102550, March 2021.

[6] P.M. Carrica, A. M. Castro, and F. Stern, "Self-propulsion computations using a speed controller and a discretized propeller with dynamic overset grids," *Journal Marine Science Technology*, vol. 15, pp. 316-330, Dec 2010.

[7] A. M. Castro, P. M. Carrica, and F. Stern, "Full scale self-propulsion computations using discretized propeller for the KRISO container ship KCS," *Computers & Fluids*, vol. 51, pp. 35-47, Dec 2011.

[8] Z. Shen, D. Wan, and P. M. Carrica, "Dynamic overset grids in OpenFOAM with application to KCS self-propulsion and maneuvering," *Ocean Engineering,* vol. 108, pp. 287-306, Nov 2015.

[9] S. Gaggero, D. Villa, and M. Viviani, "An extensive analysis of numerical ship self-propulsion prediction via a coupled BEM/RANS approach," *Applied Ocean Research,* vol. 66, pp. 55-78, Jun 2017.

[10] P. He, G. Filip, J.R.R.A. Martins, and K. J. Maki, "Design optimization for self-propulsion of a bulk carrier hull using a discrete adjoint method," *Computers & Fluids*, vol. 192, pp. 104259, Oct 2019.

[11] A. Bakica, I. Gatin, V. Vukcevic, H. Jasak, and N. Vladimir, "Accurate assessment of ship-propulsion characteristics using CFD," *Ocean Engineering*, vol. 175, pp. 149-162, Mar 2019.

[12] D. Feng, J. Yu, R. He, Z. Zhang, and X. Wang, "Improved body force propulsion model for ship propeller simulation," *Applied Ocean Research,* vol. 104, pp. 102328, Nov 2020.

[13] S. Sezen, C. Delen, A. Dogrul, and M. Atlar, "An investigation of scale effects on the self-propulsion characteristics of a submarine," *Applied Ocean Research,* vol. 113, pp. 102728, Aug 2021.

[14] C. Delen, U. Can, and S. Bal, "Prediction of Resistance and Self-Propulsion Characteristics of a Full-Scale Naval Ship by CFD-Based GEOSIM Method," *Journal of Ship Research*, pp. 1-16, Oct. 2020.

[15] W. Sun, Q. Hu, S. Hu, J. Su, J. Xu, J. Wei and G. Huang, "Numerical Analysis of Full-Scale Ship Self-Propulsion Performance with Direct Comparison to Statistical Sea Trail Results," *Journal Marine Science Engineering,* vol. 8, pp. 24, Jan 2020.

[16] H. Jasak, V. Vukcevic, I. Gatin, and I. Lalovic, "CFD validation and grid sensitivity studies of full scale ship self propulsion," *International Journal of Naval Architecture Ocean Engineering*, vol. 11, pp. 33-43, Jan 2019.

[17] N. Chase, *Simulations of the DARPA suboff submarine including self-propulsion with the E1619 propeller*, İowa: University of Iowa, 2012.

[18] N. Zhang and S.L. Zhang, "Numerical simulation of hull/ propeller interaction of submarine in submergence and near surface conditions," *Journal of Hydrodynamics* vol. 26, pp. 50-56, Feb 2014.

[19] S. Sezen, A. Dogrul, C. Delen, and S. Bal, "Investigation of self-propulsion of DARPA suboff by RANS method," *Ocean Engineering,* vol. 150, pp. 258-271, Feb 2018.

[20] O.K. Kinaci, M.K. Gokce, A.D. Alkan, and A. Kukner, "On self-propulsion assessment of marine vehicles," *Brodogradnja*, vol. 69, pp. 29-51, Dec 2018.

[21] P.M. Carrica, Y. Kim, and J.E. Martin, "Near-surface self propulsion of a generic submarine in calm water and waves," *Ocean Engineering*, vol. 183, pp. 87-105, Jul 2019.

[22] N.C. Groves, T.T. Huang, and M. S. Chang, "Geometric characteristics of DARPA suboff models (DTRC model nos. 5470 and 5471) (No. DTRC/SHD-1298-01)," 1989.

[23] H.L. Liu and T.T. Huang, "Summary of DARPA suboff experimental program data (No. CRDKNSWC/HD-1298-11)," Final Rep. Jun 1998.

[24] N. Chase and P.M. Carrica, "Submarine propeller computations and application to self-propulsion of DARPA Suboff," *Ocean Engineering,* vol. 60, pp. 68-80, Mar 2013.

[25] Siemens, "Star-CCM+ User Guide version 14.02.010" 2019.

[26] ITTC, "Recommended Procedures and Guidelines Practical Guidelines for Ship CFD Applications," 2011. Available from: https://www.scribd.com/document/177879513/ITTC

[27] O.K. Kinaci, M.K. Gokce, and C. Delen, "Resistance experiments and self-propulsion estimations of Duisburg Test Case at 1/100 scale," *Ship Technology Research,* vol. 67, pp. 109-120, May 2020.

[28] Y.A. Özden and F. Çelik, "Numerical investigation of the effects of underwater aft cone angle and length-to-beam ratio on hull efficiency," *Gemi ve Deniz Teknolojisi*, pp. 71-88, Jul 2017.

[29] A. Doğrul, "Hydrodynamic investigation of a submarine moving under free surface," *Journal of Eta Maritime Science*, vol. 7, pp. 212-227, 2019.

ORIGINAL RESEARCH (AR)

DOI: 10.4274/jems.2021.87049

Journal of ETA Maritime Science 2021;9(3):200-209

Analytical and Numerical Analysis of the Strength Performance of a Novel Ship Construction Profile

Ahmet Taşdemir[1], Serkan Nohut[2], Mehmet Akman[3]

[1]Piri Reis University, Maritime Faculty, Department of Marine Engineering, İstanbul, Turkey
[2]Piri Reis University, Faculty of Engineering, Department of Mechanical Engineering, İstanbul, Turkey
[3]Muğla Sıtkı Koçman University, Department of Motor Vehicles and Transportation Technologies, Muğla, Turkey

Abstract

Construction profiles in different shapes such as bulb flats, tees, channels, and angles are widely used in the shipbuilding industry. During the ship construction process, these conventional profiles are joined to the plates as stiffeners and are dimensioned according to class rules. This article investigates the structural performance of a novel construction profile, the so-called TP profile, that can be used in the hull construction of ships and of which form is inspired by the human bone geometry. The cross-sectional area and the weight of the TP profile are designed to be equal to those of the conventional HP profile and commercial T profile. Strength performances of these profiles are compared via analytical and numerical analyses. The plate joint profiles are modeled under various loading and boundary conditions and the finite element method is used for the calculation of stress components and deflections. The TP profile has a high potential to be used in the shipbuilding industry.

Keywords

Ship construction, TP profile, HP profile, Finite element analysis, Ship strength

1. Introduction

Maritime transportation has a significant role in world trade and the capacity of seaborne trade keeps growing. It is reported [1] that the world's seaborne trade in 2014 was about 50 times larger in terms of tonnage compared to its value in 1975. Moreover, there are about 53,000 [2] merchant ships trading internationally as of 2019. Proportional to the maritime transportation growth, the ship sizes and the number of ship types are also increasing due to economic reasons. In the last decade, the average container ship and bulk carrier capacities have shown an increase of almost 100% [3]. Despite some depressed periods, a total of about 90 million CGT was constructed and delivered in 2018 [4]. Based on the market size and growth, the consumption of construction materials is one of the primary concerns for the shipbuilding industry to save building costs and to achieve fuel saving. It was stated [5] that the steel cost used in hull construction is about 8%-15% of the total cost of a commercial ship. Moreover, the weight of the lightship over the total weight is about 14% for tankers, 30% for bulk carriers, 35% for container ships, and 41% for ro-ro carriers [6]. Therefore, the design and optimization of a ship hull have become important to minimize material, labor, and operational costs.

Structural design rules for ships are mostly based on empirical and experience-based formulations regulated by classification societies [7]. However, these rules mainly target a safe design rather than an optimum one. Specifically, the constructional profile types and numbers and the plate thickness used in the hull structure directly affect the weight and cost of newly built ships. This makes cost efficiency a key factor in the ship design phase. As a result, the development of novel strengthening construction profiles that will decrease the costs or increase the structural reliability plays an important role in the optimized hull design. At the end of the 1800s, a comprehensive study was performed in which

Address for Correspondence: Ahmet Taşdemir, Piri Reis University, Maritime Faculty, Department of Marine Engineering, İstanbul, Turkey
E-mail: atasdemir@pirireis.edu.tr
ORCID ID: orcid.org/0000-0002-7414-2525

Received: 25.04.2021
Accepted: 12.08.2021

To cite this article: A. Taşdemir, S. Nohut and M. Akman, "Analytical and Numerical Analysis of the Strength Performance of a Novel Ship Construction Profile." *Journal of ETA Maritime Science*, vol. 9(3), pp. 200-209, 2021.

different profiles (so-called German Profiles) for rolling iron were introduced taking into account the requirements of theory, construction, and rolling technology by the commission of the Association of German Architects and Engineers' Associations and the Association of German Engineers, on whose behalf, Heinzerling and Intze published the German Normal Profile Book [8]. However, these profiles were not fully used in industrial applications. In the following years, construction profiles in different shapes such as bulb flats, tees, channels, and angles have been started to be used in the analysis for shipbuilding.

In recent years, numerical methods have been widely used for the design of ship hulls. The finite element method (FEM) is one of the most preferred tools to solve constructional problems where standardized bulb flats, tees, angles, channels, and rectangular profiles are widely used to stiffen the plates and panels. Nohut and Tasdemir [9] applied a FEM in POSEIDON to accelerate the modeling ship's hull and to analyze the structural hulls, where T-shaped and bulb flats are used in the sections of a car carrier and a multi-purpose vessel. Patel et al. [10] discussed a method based on FEM to assess the strength in service of the loss of surface material due to the corrosion and erosion of marine structures. They reported that the developed code enables handling irregular shapes and differential corrosion thicknesses. Paik et al. [11] developed a novel formulation to analyze the ultimate strength performance of the ship hull including bulb flat stiffened panels. Moreover, they compared the results of the analysis with those of the FEM. Abubakar and Dow [12] analyzed the bulb flats stiffened double bottoms experimentally and numerically to investigate the grounding damage. They proved that the FEM-based results are agreeable with experimental results. Prabowo et al. [13] simulated the grounding behavior of a double bottom stiffened with bulb flats using FEM. Ahmadi et al. [14] used FEM and artificial neural network to analyze and predict the ultimate strength of cracked pitted plates under different geometrical and crack size dimensions. Storheim and Amdahl [15] simulated the effect of the slope of the stress-strain curve (i.e., strain rate), strain localization, and crack propagation during ship collisions using non-linear finite element analysis. Paik et al. [16] carried out benchmark studies for the ultimate limit state assessment of unstiffened plates, stiffened panels, and hull girders stiffened with three different T-shaped profiles using FEM. Xia et al. [17] conducted a numerical study on the strength behaviors of ship hull plates under cyclic loads using FEM. Tasdemir and Nohut [18] investigated the fatigue behaviors of a vertical side web constructed with T-shaped and bulb flat profiles, connected to the main deck of a vessel using three types of finite element analyses. As a result of the study, they recommended weld toe grinding, TIG dressing, or hammer peening to increase the fatigue life of the analyzed part. Gledic et al. [19] used FEM to calculate the strength parameters of the midship including bulb flat stiffened plates under 50 random damage scenarios, where low-cycle fatigue damage is predicted. Shen et al. [20] analyzed the spring-back and cold forming process of hull plates using implicit and dynamic explicit FEM. Rao and Wan [21] studied the wave-plate interaction resulting from the slamming force using the moving particle semi-implicit FEM. Niklas and Kozak [22] analyzed the stress and strain behaviors of toe and root notches on panels using 2D and 3D elements. To sum up, studies related to the ship construction in the literature are based on strength analyses, fatigue estimations, and material and method research along with numerical and experimental investigations of hull sections including standard constructional profiles.

In this study, apart from studies in the literature, the strength performance of a novel construction profile, the so-called TP profile, is investigated and the performance parameters are compared with those of the commonly used conventional bulb flat (HP) and T-shaped profiles. Two cases are set up for the strength performance investigation of the profile joints with plates. In the first case, a beam is fixed from one of its ends and a uniformly distributed load acts normal to the plate. In the second case, the beam is fixed from both ends under a uniformly distributed load, which has the same magnitude and direction as those of Case 1. Euler-Bernoulli beam equations and Timoshenko theory-based beam elements are used for evaluating the bending, shear, and Von-mises stresses along with deflections under cases including different loading and boundary conditions. Moreover, solid elements are used for advanced numerical investigations at the same conditions to analyze the behaviors of the beams under three-dimensional forces.

2. Methodology

Bulb flats and T sections, the most commonly used profiles in ship hulls, are suitable for areas where bending moments are dominant [23]. Cross-sectional dimensions of these profiles are generally 160 mm to 430 mm in width, and the thickness of the profiles varies between 7 mm and 20 mm. Within the scope of this article, a novel profile, of which form mimics the bone geometry of living things, is introduced. Figure 1 shows a typical human femur bone [24] and the bone geometry-inspired, dimensionally parametric TP profile.

The top end of the bone consists of nearly symmetrical and curvilinear bulbs next to the centered small channel, which increase the moment of inertia of the geometry relative to the lateral axis as shown in Figure 1. The main

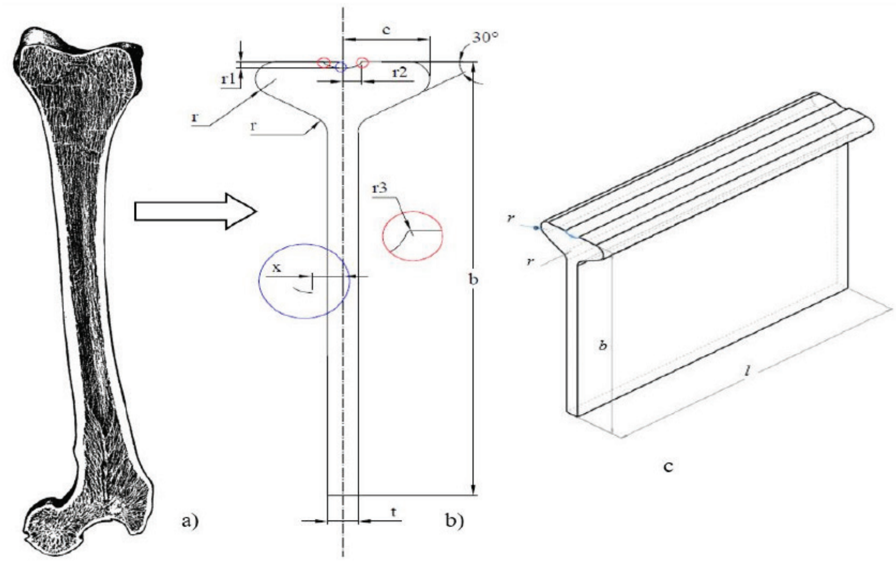

Figure 1. *Geometry of (a) a femur (Blaisedell, 1898), (b) TP - front, TP - isometric view*

aim for increasing the moment of inertia is to decrease the stresses and deformations on the profile. This principle is used for the form determination of the novel TP profile. In literature, there are many studies on the bone strength analysis supporting the subject including the ultimate strength, buckling, and fatigue investigations particularly in the human femur and tibia bones [25-29].

Dimensions of the TP profile section are scalable by the needs and limits of the thickness (t), height (b), bulb width (c), and radius (r, r_1, r_2), which are t=[3,20] mm, b=[80, 450] mm, c=[18, 85] mm, r=[4, 20] mm, r_1=[1, 10], r_2=[1, 20], and r_3=[1, 5]. The similarity of TP with the bone is restricted by the shape at the top end, which is the key factor to increase the moment of inertia due to its distance from the neutral axis. As used in the ship construction process, the flat plates are joint to the HP, T, and TP profiles and modeled for the loading cases. Figure 2 shows the cross sections of HP, T, and TP-joint plates.

Cross-sectional areas and weights are selected to be the same for all profiles and plates. The profile-joint plates are modeled as beams in the YZ plane. Structural steel is used and the geometrical and material properties of the profile-joint plates are shown in Table 1.

In addition to common dimensional parameters given in Table 1, other dimensions of the TP profile are r=5.5 mm, r_1=2 mm, r_2=5 mm, and c=23 mm. The strength performances of the three profile-joint plates are investigated under two common cases. In Case 1, one end has a fixed support, while the other end is free. In addition, a 40-kN/m distributed load is applied along the z-axis. In Case 2, both ends have fixed supports and a

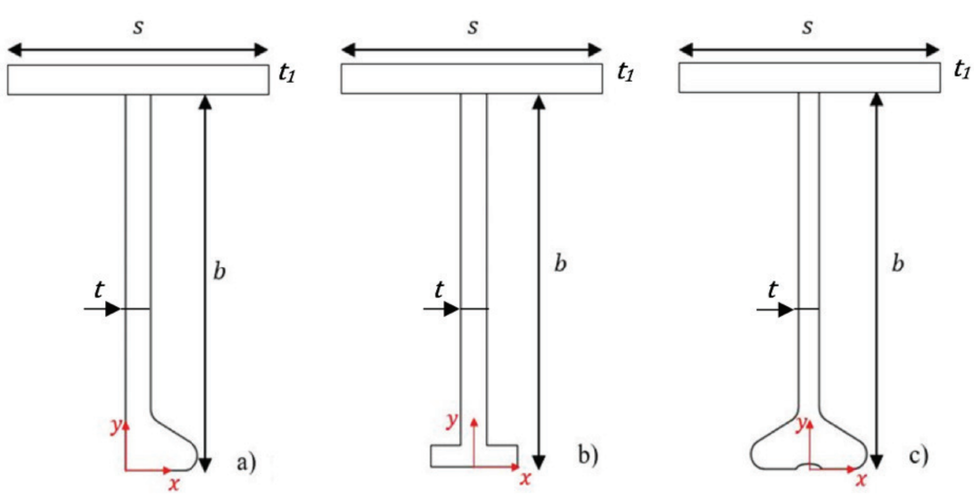

Figure 2. *Cross sections of the (a) HP-joint plate, (b) T-joint plate, and (c) TP-joint plate*

***Table 1.** Geometrical (G) and material (M) properties of the HP, T, and TP-joint plates*

Properties		HP Plate	T Plate	TP Plate
G	Height - *b* [mm]	140	140	140
	Width - *s* [mm]	250	250	250
	Thickness of plate - t_1 [mm]	10	10	10
	Thickness of profile - *t* [mm]	10	10	8.24
	Length - *l* [mm]	500	500	500
	Cross-sectional area - *A* [mm^2]	4163	4163	4163
	Distance of the neutral axis from *x*-axis [mm]	111.11	111.91	107.43
	Distance of the neutral axis from *y*-axis [mm]	5.82	0	0
	Moment of inertia - I_x [mm^4]	1.036e7	1.002e7	1.211e7
	Moment of inertia – I_y [mm^4]	1.308e7	1.306e7	1.311e7
	Polar moment of inertia - *J* [mm^4]	2.344e7	2.308e7	2.522e7
M	Density - ρ [kg/m^3]	7850	7850	7850
	Weight [kg]	16.34	16.34	16.34
	Tensile-compressive yield strength [MPa]	235	235	235
	Young's modulus - *E* [GPa]	200	200	200
	Shear modulus - *G* [GPa]	79.3	79.3	79.3

40-kN/m distributed load is applied along the z-axis. Moreover, the profile-connected plates are modeled as rigid bodies.

3. Finite Element Model

The Euler-Bernoulli beam theory is widely used for long and slender body strength analysis, assuming that the cross-section of the beam is rigid, remains plane after deformation, and remains normal to the deformed axis [30]. On the other hand, the Timoshenko beam theory, where transverse shear stresses are taken into account, is a first-order shear deformation theory, including that the cross-section of the beam remains plane and undistorted after deformation [31]. The numerical procedure first starts using the BEAM188 element, which is based on the Timoshenko beam theory to compare the results of stresses and deflections with those of the analytical solutions. Cross sections are modeled in the ANSYS 14.5 Static Structural module according to the data given in Figure 2 and Table 1. Line bodies are created and the beam is divided into 100 pieces of BEAM188 elements. BEAM188 is a two-node element in space, providing relationships between transverse shear stresses and strains in the elastic region and can be used for slender beams [32,33]. The element uses linear shape functions resulting in all element solutions along the length being constant. On the other hand, plate-profile connections and weld effects are ignored in 3D models. The profile and the plates are designed separately and formed in one part in the design modeler module of ANSYS. Therefore, the profile-connected plates behave like a one-piece solid body in FEM models. SOLID186 and SURF154-type elements are used during the 3D meshing process. The SOLID186 element is a high-order three-dimensional 20-node network element that has three degrees of freedom per node and the element is used in cases of plasticity, hyperelasticity, creep, high stresses, and high deflection [33]. Apart from BEAM188, SOLID186 is used for high-order theories including various load distributions in 3D applications. Moreover, SURF154 is used for solving problems under different load and surface effects in 3D structural analyses. SURF154 is overspread onto the face of 3D elements that are determined by four to eight nodes and the material's properties. Besides, the plane force over the unit length is used for calculating the stress stiffness matrix and load vectors [33]. Figure 3 shows the meshed plates.

The number of elements used is 49410, 42960, and 62062 for the HP plate, T plate, and TP plate, respectively. The aspect ratio of the elements is selected to be less than 5 for stress and less than 10 for the deformation analyses to increase the accuracy of the results [34]. Therefore, the maximum aspect ratios of HP, T, and TP plates are 2.06, 1.76, and 4.96, respectively. On the other hand, the minimum orthogonal quality of HP, T, and TP plates are 0.71, 0.81, and 0.74, respectively.

4. Results and Discussion

The bending, shear, and equivalent Von-Mises stresses along with the deflections are calculated under two cases. Analytical calculations are verified using beam elements.

After, the two cases are modeled by 3D elements to include the shear forces.

4.1 Numerical Simulations with Beam Elements

Numerical solutions show that the maximum bending stress is obtained at a fixed support as indicated in Table 2. Since the center of mass of the investigated profiles is at different locations, the vertical distances of the neutral axis from the origin in the cross sections and the moments of inertia are different. As a result, different bending stresses are obtained. The maximum bending stresses are calculated as 53.6 MPa, 55.8 MPa, and 44.4 MPa for HP, T, and TP profiles, respectively. Although the maximum stress in HP and T profiles are very close to each other, the maximum bending stress of the TP is quite different. Here, the maximum bending stresses are obtained at the bottom side of the sections. The values for the top side of the cross sections are 18.8 MPa, 19 MPa, and 17.6 MPa for HP, T, and TP profiles, respectively. Similar to the bending stress distribution, the maximum deflection is obtained in the section of the T profile as 0.155 mm. The deflection of the TP profile is about 0.13 mm, which is about 13% less than that of the HP and T sections. Table 2 shows the numerical and analytical results.

It is seen that the analytical and numerical stress and deflection results are very close to each other. This is based on the beam approach and slender models that decrease the deviations.

4.2. Numerical Simulations with 3D Elements

The cross sections are extruded in the z-axis to analyze the strength performances of 3D bodies. Solid elements are used for advanced numerical analysis. The loading and boundary conditions of the models are the same as those of the previous section. Figure 4 shows the representation of the loading and boundary conditions on the 3D model. Due to the occurrence of some singularities at points of constraints, two-section planes (XY plane) are introduced at 5% and 50% of the total length of the models to evaluate the maximum values. The presented stress distributions are taken at 0.05l (Plane C in Figure 4) and the deflections are based on the XY plane at 0.5l (Plane B in Figure 4) or free ends.

4.2.1. Case 1

In Case 1, the structure is fixed at one end and a 40-kN/m uniformly distributed load is applied on the top surface of the plate. The maximum bending stress occurred at the fixed point of the structure. The maximum bending stresses (normal stress in the z-axis) are obtained at the bottom of

Table 2. *Numerical and analytical results for the sections (N for numerical, A for analytical)*

Solution	Parameter	Case 1			Case 2		
		HP	T	TP	HP	T	TP
N	Max. moment [kNm]	5	5	5	0.833	0.833	0.833
	Max. bending stress [MPa]	53.612	55.803	44.381	8.936	9.308	7.399
	Max. deflection in y-axis [mm]	0.1544	0.1553	0.1296	0.0032	0.0033	0.0027
A	Max. moment [kNm]	5	5	5	0.833	0.833	0.833
	Max. bending stress [MPa]	53.618	55.806	44.351	8.936	9.301	7.391
	Max. deflection in y-axis [mm]	0.1508	0.1550	0.1290	0.0031	0.0032	0.0026

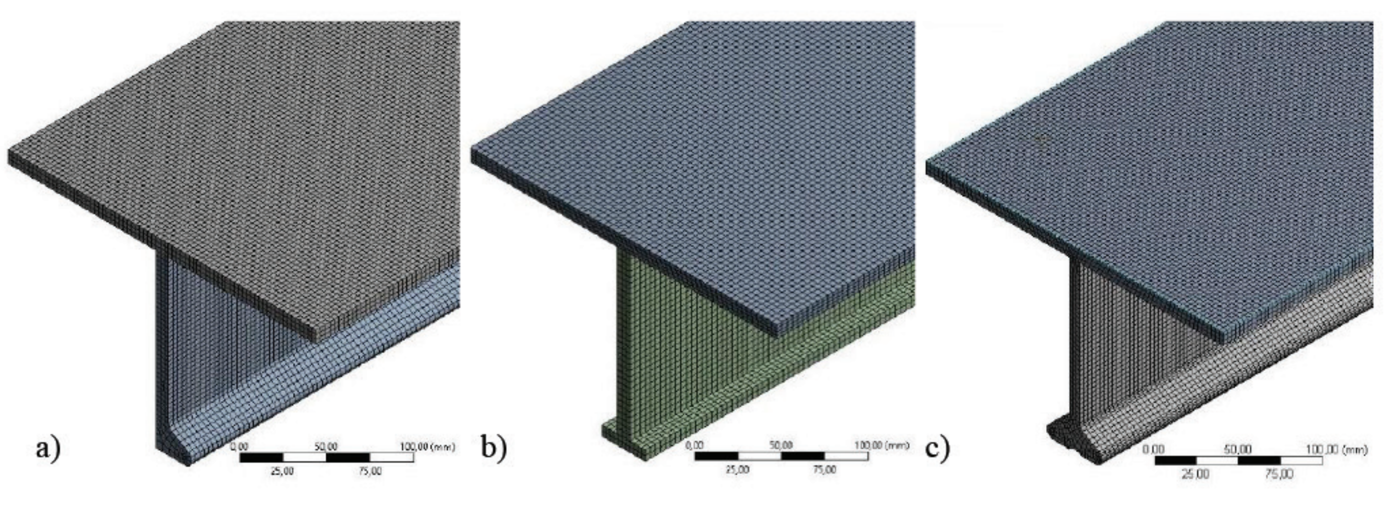

Figure 3. *Meshed (a) HP, (b) T, and (c) TP-joint plates*

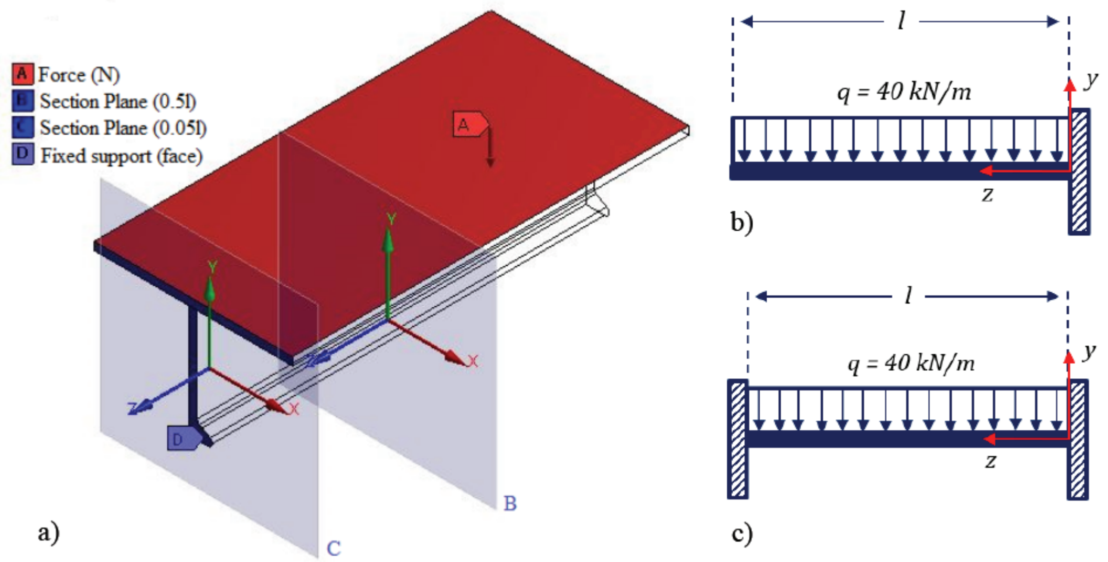

Figure 4. *(a) 3D model and the representation of the loading and boundary conditions for (b) Case 1 and (c) Case 2*

the profiles. The maximum stresses are recorded as 64.8 MPa, 51.9 MPa, and 44.9 MPa for HP, T, and TP profiles, respectively. This shows that the maximum bending stress that occurs in the TP profile is lower than those of the other two profiles. Furthermore, it should be stated that the HP is an asymmetrical profile and its centroid is 5.82 mm away from the y-axis. Therefore, the profile is exposed to the torsion around the z-axis. Besides, the shear stresses are very small in comparison with the bending stresses. The cross sections had nearly uniform shear stress distributions, where the shear stress is concentrated at the corners and fillets of the profiles. Note that the average shear stress in the TP section is higher than that of the HP and T. Figure 5 shows the equivalent Von-Mises stresses at the profile cross sections.

Similar to the bending stress concentration, the maximum Von-Mises stress is 64.8 MPa at the bottom corner region of the HP profile, which is larger than that of the symmetrical T and TP profiles. Close to the plate region, the Von-Mises stresses are decreasing and the obtained maximum Von-Mises stress at the TP section is 23.9 MPa. Note that the obtained maximum values are less than the yield limit of the

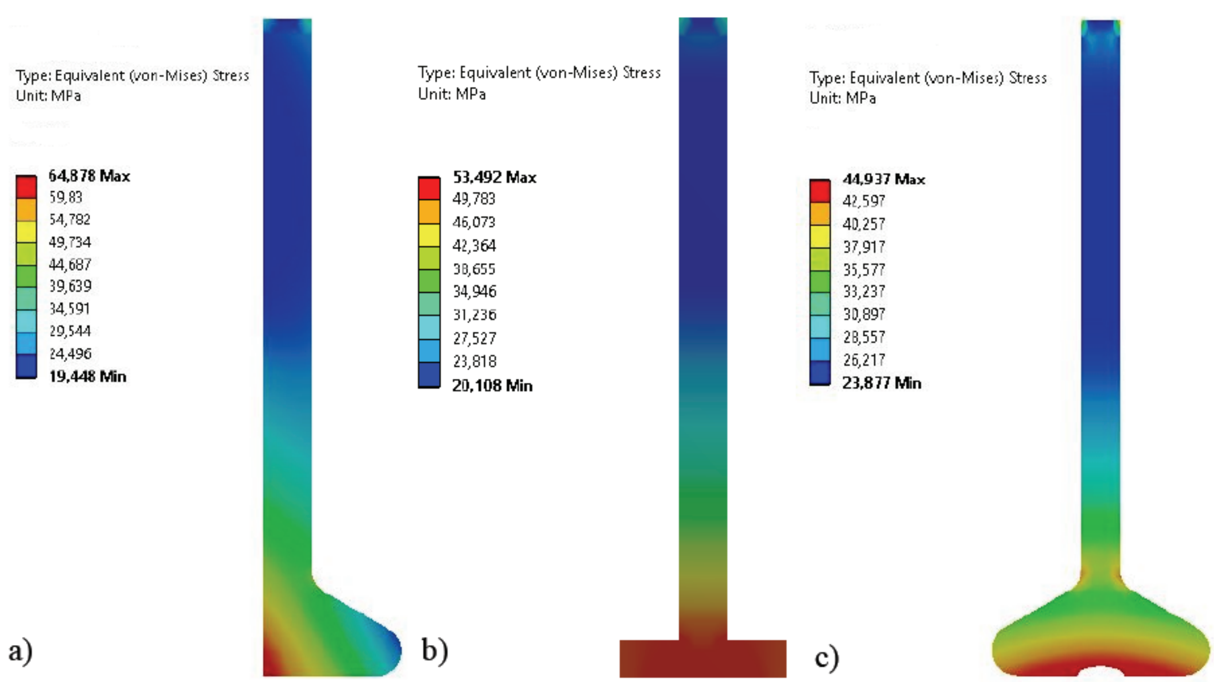

Figure 5. *Von-Mises stress distribution at the profile cross sections: (a) HP, (b) T, and (c) TP*

material. Figure 6 shows the distribution of the deflections in the cross sections. According to the contours, the maximum deflections in the y-axis are 0.237 mm, 0.202 mm, and 0.185 mm for the HP, T, and TP profiles, respectively.

The deflection in the y-direction is maximum for the HP profile. Furthermore, the HP section experiences some torsion during bending with a deflection of 0.19 mm on the x-axis. The x-axis deflections for the T and TP profiles are negligible based on the centroid's position.

On the other hand, the maximum Von-Mises stress values on the connecting plates are obtained as 47.32 MPa, 41.38 MPa, and 41.27 MPa for the HP-joint, T-joint, and TP-joint plates, respectively. The HP-joint plate has the maximum Von-Mises stress because of asymmetry in the section that causes torsion. T-joint and TP-joint plates are symmetrical and magnitudes of the Von-Mises stress on the plates are close to each other. Besides, the maximum deflections on the connecting plates are obtained as 0.401 mm for the HP plate, 0.321 mm for the T plate, 0.323 mm for the TP plate. Compared to analytical solutions based on the beam theory, results obtained from 3D models are quite different. This is because the beam theory does not include shear strain variations that should be calculated for moderately thick and short beams [35].

4.2.2. Case 2

In Case 2, the structure is fixed at both ends and a 40-kN/m uniformly distributed load is applied on the top surface of the plate. According to the bending stress results, the maximum bending stresses of profiles are less in comparison with those obtained in Case 1. The HP profile is exposed to a 70% higher bending stress than the T and TP profiles due to the geometrical properties mentioned in the previous section. Moreover, T and TP profiles show approximately the same bending resistances so that the maximum bending stress of the TP profile is only 6% less than that of the T profile. On the other hand, proportional to the decrease of the maximum moment compared to Case 1, shear stresses are very small. The HP profile has better shear resistance in comparison with other sections. The average shear stress in the TP section is higher than those of the HP and T. In addition, the symmetrical profiles have symmetrical shear stress distributions. Figure 7 shows the Von-Mises stresses for the profile cross sections in Case 2. The average Von-Mises stresses are about 8.5 MPa for all sections. Note that the exerted force is relatively small for two-side fixed bodies.

Figure 8 shows the deflections in the cross sections. According to the results, average deflections in the y-axis are 0.0155 mm, 0.0141 mm, and 0.0154 mm for the HP, T, and TP profiles, respectively. As a result, no significant difference is observed in the deflection of structures in the y-direction under stated boundary and loading conditions.

Besides, the maximum Von-Mises stresses on the connecting plates are 29.17 MPa, 28.44 MPa, and 28.64 MPa for the HP-joint, T-joint, and TP-joint plates, respectively. The maximum Von-Mises stress is obtained from the HP-joint plate, while the T-joint and TP-joint plates are quite similar. The maximum deflections on the connecting plates are obtained as 0.234 mm for the HP plate, 0.224 mm for the

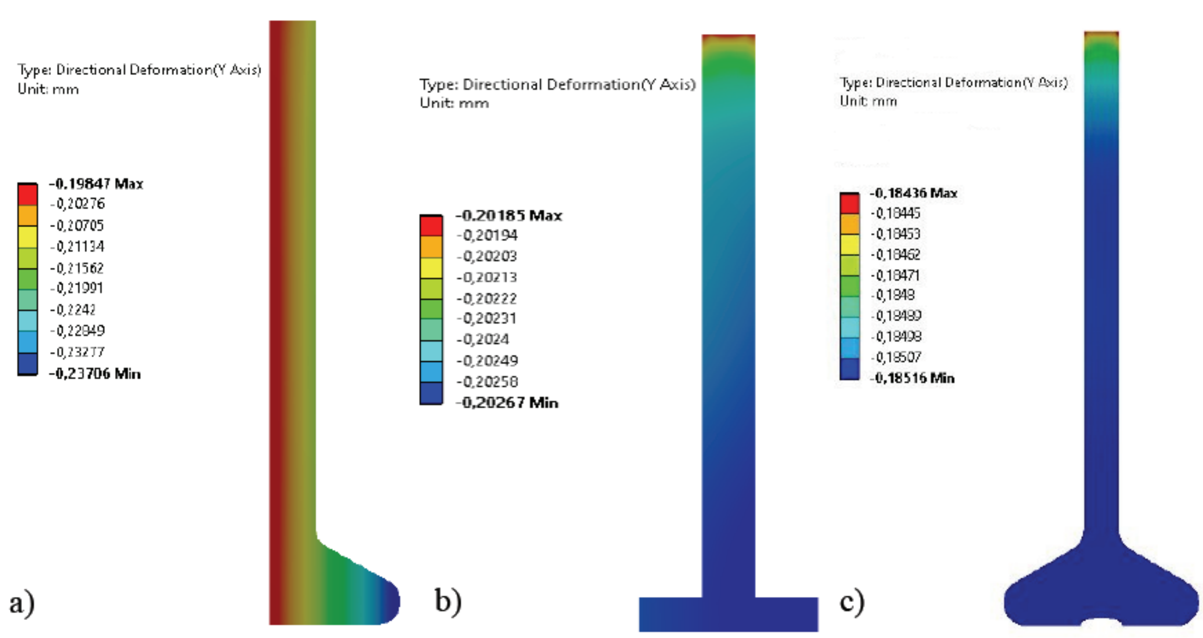

Figure 6. *Distribution of deflections in the y-axis for the cross sections: (a) HP, (b) T, and (c) TP*

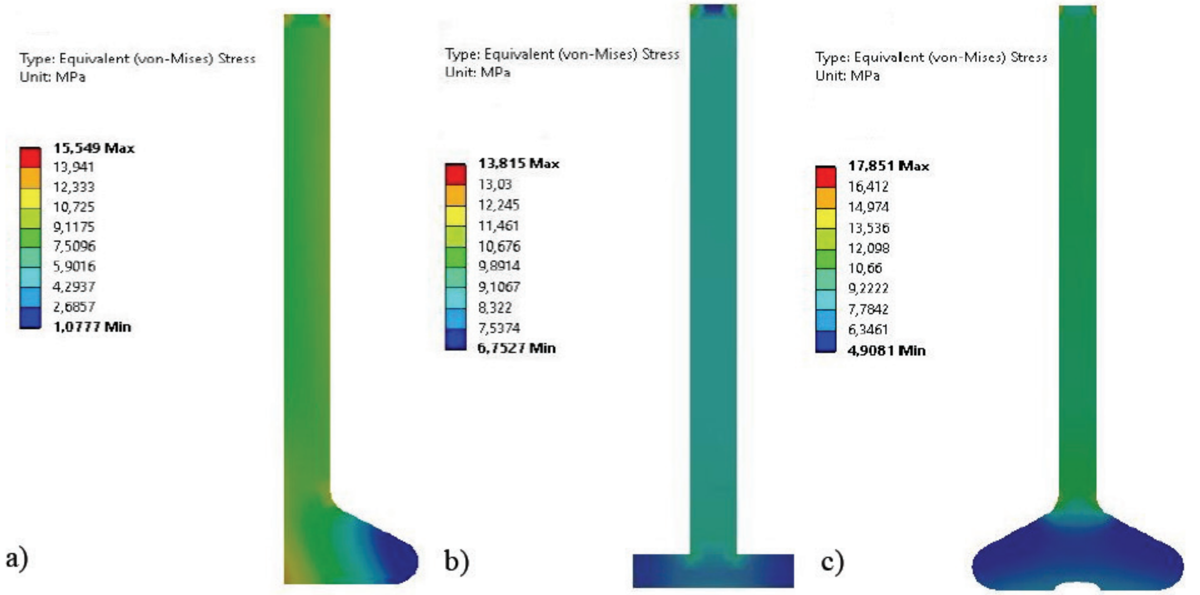

Figure 7. *Von-Mises stress distribution of the profile cross sections: (a) HP, (b) T, and (c) TP*

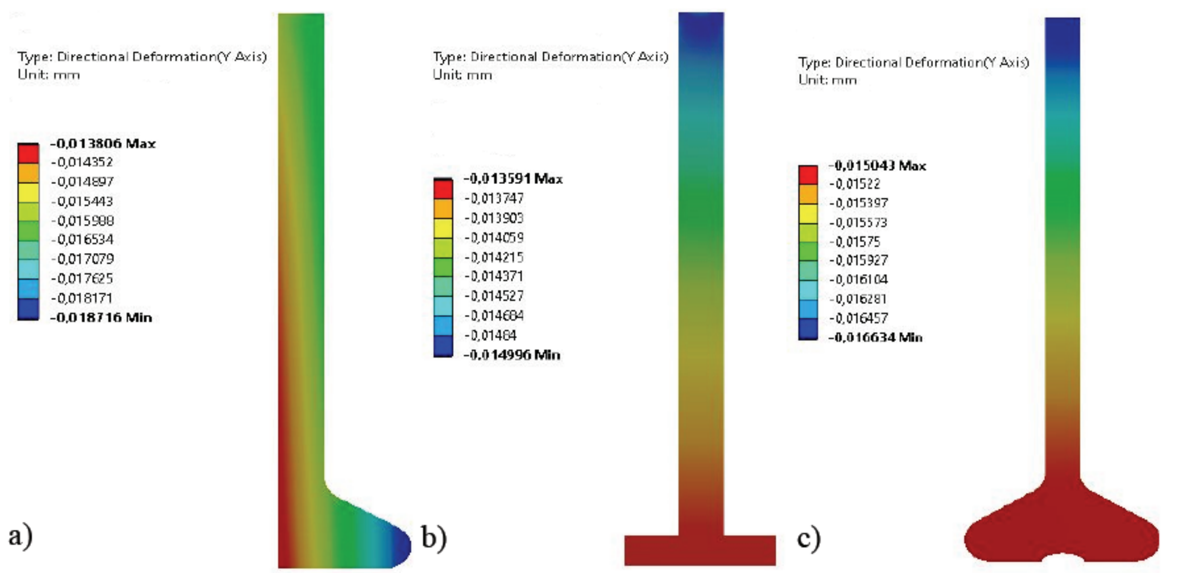

Figure 8. *Deflections in the y-axis for the profile cross sections: (a) HP, (b) T, and (c) TP*

T plate, and 0.229 mm for the TP plate. The HP-joint plate seems less favorable in comparison with other sections because of the reasons explained in Case 1.

5. Conclusion

Strength performances of the HP, T, and TP profile-joint plates are investigated under two common loading cases used in shipbuilding. The bending, shear, and equivalent stress along with the deflections of the profile-joint plates are analyzed numerically and analytically. Results indicate that the equivalent stress of the TP profile is about 30% and 16% less compared to those of HP and T profiles, respectively. Moreover, the deflection of the TP profile is calculated as 21% and 8% less compared with those of HP and T profiles, respectively. As a result, the following conclusions are drawn:

- Symmetrical profiles eliminate the additional torsion under bending cases. Therefore, stresses and deflections are remarkably lower compared to the results of the HP profile.
- The TP profile shows a higher equivalent stress resistance and has less deflection in cases compared to the HP and T profiles.

- There are very small differences between the beam element used for the numerical and analytical solutions. However, 3D effects including axial shear stresses and deformations highly influence the results.
- Results show that the TP profile can increase the hull performance and contribute to fuel-saving depending on the lighter hull.
- The study gives promising results that the TP profile has an important potential to decrease the building and labor costs based on less material consumption during ship construction.

In future work, the optimization of the TP profile will be performed for different scales under more complex loading cases to increase the axial moments of inertia. Furthermore, the optimal design will be verified using both experiments and numerical computations.

Authorship Contributions

Concept design: A. Taşdemir, S. Nohut, Data Collection or Processing: S. Nohut, M. Akman, Analysis or Interpretation: A. Taşdemir, S. Nohut, M. Akman, Literature Review: A. Taşdemir, M. Akman, Writing, Reviewing and Editing: A. Taşdemir, S. Nohut, M. Akman.

Funding: The author(s) received no financial support for the research, authorship, and/or publication of this article.

References

[1] UNCTAD, "Developments in international seaborne trade," *Review of Maritime Transport* 2014, pp. 1-25. https://doi.org/10.18356/e9e3b605-en

[2] Statista, "The world merchant fleet," 2019. [online]. Available: https://www.statista.com/statistics/264024/number-of-merchant-ships-worldwide-by-type/. [Retrieved: 8 October 2020].

[3] S. Parks, "The Impact of Mega Ships - Case-Specific Policy Analysis. International Transport Forum," 2015, pp. 5.

[4] OECD, "Shipbuilding Market Developments", 2018. [Online]. Available: https:// https://www.oecd.org/sti/ind/shipbuilding-market-developments-Q2-2018.pdf. [Accessed: Oct. 8, 2020].

[5] D. Broderick, R. Kattan and P. Wright, "The design challenges associated with coating ships," *11th International Symposium on Practical Design of Ships and Other Floating Structures, PRADS,* Houston, Texas, 2010, pp. 635-643.

[6] S.M. Hamberger, B.D. Blackwell, L.E. Sharp, and D. B. Shenton, "H-1 design and construction," *Fusion Technology*, vol. 17, pp. 123-130, Jan 1990.

[7] Y.V. Satish Kumar and M. Mukhopadhyay, "Finite element analysis of ship structures using a new stiffened plate element," *Applied Ocean Research*, vol. 22, pp. 361-374, Dec 2000.

[8] O. Lueger, "Lexikon der gesamten technik und ihrer hilfswissenschaften," Stuttgart: Leipzig, 1908, pp. 663-673.

[9] A. Tasdemir, and S. Nohut, "Practical experience with efficient generation of finite-element models of ships using POSEIDON," *11th International Conference on Computer and IT Applications in the Maritime Industries*, Liege, Belgium, 2012, pp. 19-26.

[10] A.K.P. Patel, S.K. Satsangi and R. Verma, "Analysis of ship structural plate panels during service by the method of finite elements," *Journal of The Institution of Engineers (India): Series C*, vol. 100, pp. 433-437, 2019.

[11] J.K. Paik, D.K. Kim, D.H. Park, H.B. Kim, A.E. Mansour, J.B. Caldwell, "Modified Paik-Mansour formula for ultimate strength calculations of ship hulls," *Ships and Offshore Structures*, vol. 8, pp. 245-260, 2013.

[12] A. Abubakar and R.S. Dow, "Simulation of ship grounding damage using the finite element method," *International Journal of Solids and Structures*, vol. 50, pp. 623-636, Mar 2013.

[13] A.R. Prabowo, T. Putranto and J.M. Sohn, "Simulation of the behaviour of a ship hull undergrounding: Effect of applied element size on structural crashworthiness," *Journal of Marine Science and Engineering*, vol. 7, pp. 1-15, Aug 2019.

[14] F. Ahmadi, A. Rahbar Ranji and H. Nowruzi, "Ultimate strength prediction of corroded plates with center-longitudinal crack using FEM and ANN," *Ocean Engineering*, vol. 206, pp. 107- 281, Jun 2020.

15] M. Storheim and J. Amdahl, "On the sensitivity to work hardening and strain-rate effects in nonlinear FEM analysis of ship collisions," *Ships and Offshore Structures*, vol. 12, pp. 100-115, 2017.

[16] Paik, Jeom Kee, Kim, B. J., and Seo, J. K., "Methods for ultimate limit state assessment of ships and ship-shaped offshore structures: Part I-Unstiffened plates," *Ocean Engineering*, vol. 35, pp. 261-270, Aug 2007.

[17] T. Xia, P. Yang, C. Li and K. Hu, "Numerical research on residual ultimate strength of ship hull plates under uniaxial cyclic loads," *Ocean Engineering*, vol. 172, pp. 385-395, Jan 2019.

[18] A. Tasdemir and S. Nohut, "Fatigue analysis of ship structures with hinged deck design by finite element method. A case study: Fatigue analysis of the primary supporting members of 4900 PCTC," *Marine Structures*, vol. 25, pp. 1-12, Oct 2011.

[19] I. Gledic, J. Parunov, P. Prebeg and M. Corak, "Low-cycle fatigue of ship hull damaged in collision," *Engineering Failure Analysis*, vol. 96, pp. 436-454. Nov 2018.

[20] W. Shen, R. Yan, S. Li, and L. Xu, "Spring-back analysis in the cold-forming process of ship hull plates," *International Journal of Advanced Manufacturing Technology*, vol. 96, pp. 2341-2354, May 2018.

[21] C. Rao and D. Wan, "Numerical study of the wave-induced slamming force on the elastic plate based on MPS-FEM coupled method," *Journal of Hydrodynamics*, vol. 30, pp. 70-78, Oct 2017.

[22] K. Niklas, and J. Kozak, "The effect of numerical 2d and 3d fem element modelling on strain and stress distributions at laser weld notches in steel sandwich type panels," *Polish Maritime Research*, vol. 25, pp. 121-127, 2018.

[23] W. Fricke, "Ship Structural Design I," Hamburg: Hamburg University of Technology, 2009.

[24] A.F. Blaisedell, "Our bodies and how we live", Boston:Ginn & Company, 1898.

[25] E. Arendt, J. Agel, C. Heikes and H. Griffiths, "Stress injuries to bone in college athletes: a retrospective review of experience at a single institution," *The American Journal of Sports Medical,* vol. 31, pp. 959-968, Nov 2003.

[26] E.M. Hennig, T.L. Milani and M.A. Lafortune, "Three-dimensional acceleration of the tibia during walking and running," *Journal of Applied Biomechanics*, vol. 9, pp. 306-314.1993.

[27] M.A. Lafortune, "Three-dimensional acceleration of the tibia during walking and running," *Journal of Biomech*anics, vol. 24, pp. 877-886, May 1991.

[28] C. Milgrom, A. et al. "In-vivo strain measurements to evaluate the strengthening potential of exercises on the tibial bone," *The Bone & Joint Journal,* vol. 82, pp. 591-594, May 2000.

[29] A.S. Tenforde, E. Kraus and M. Fredericson, "Bone stress injuries in runners," *Physical Medicine & Rehabilitation Clinics*, vol. 27, pp. 139-149, Feb 2016.

[30] O.A. Bauchau and J.I. Craig, "Euler-Bernoulli beam theory," in *Solid Mechanics and Its Applications*, Vol 163, Structural Analysis, O.A. Bauchau and J.I. Craig, Eds. Dordrecht: Springer, 2009.

[31] J.N. Reddy, *Energy Principles and Variational Methods in Applied Mechanics*. 3rd ed. Hoboken, New Jersey: John Wiley & Sons Inc., 2017.

[32] H. Zohoor, and F. Kakavand, "Timoshenko versus Euler-Bernoulli beam theories for high speed two-link manipulator," *Scientia Iranica*, vol. 20, pp. 172-178, Feb 2013.

[33] ANSYS Inc. 2017. SOLID186 Element Description [Online], Available: https://www.mm.bme.hu/~gyebro/files/ans_help_v182/ans_elem/Hlp_E_SOLID186.html. [Accessed: Oct. 7, 2020]

[34] G. Bekdaş and N.K. Öztorun, "Aspect ratio factor for finite element method analysis of axially symmetric cylindrical shell walls," *Engineering Structures and Technologies*, vol. 6, pp. 169-177, Mar 2015.

[35] M.E Onyia and E.O. Rowland-Lato, "Finite element analysis of timoshenko beam using energy separation principle," *International Journal of Engineering Research and Technology,* 2020, vol. 13, pp. 28-35.

ORIGINAL RESEARCH (AR) DOI: 10.4274/jems.2021.93685

Journal of ETA Maritime Science 2021;9(3):210-220

An Extended Event Tree Risk Analysis Under Fuzzy Logic Environment: The Case of Fire in Ship Engine Room

Ahmet Lutfi Tuncel, Emre Akyuz, Ozcan Arslan

İstanbul Technical University, Maritime Faculty, Department of Maritime Transportation and Management Engineering, İstanbul, Turkey

Abstract

Ship engine room fire is one of the major dangers that threaten the safety of the ships. An effective firefighting in the engine room is critical to prevent possible destructive consequences on-board ship. Fire detection and firefighting systems, which are designed for an effective fire prevention on-board ship, need to work flawlessly. In order to achieve this, the deficiencies of the designed systems must be determined and necessary control actions must be taken. In this study, failure probabilities of fire detection and firefighting systems on-board ship is calculated by event tree analysis and fuzzy logic environment. The possible consequences that may be encountered in case the systems fail under various scenarios are determined. Solutions have been proposed in order to minimize the risk that may arise by reducing the failure probability of each system. The outcome of this paper will be utilised by safety engineers, shipping companies and safety inspectors to prevent potential engine room fires.

Keywords

Risk analysis, Event tree, Fuzzy logic, Engine room fire

1. Introduction

Ship fires may cause great financial losses as well as loss of life, property and environmental pollution. These fires, which may have devastating outcomes, are among the most dangerous of maritime accidents [1-3]. There is also a common view that ship fires are among the most frequent accidents [2,4,5]. Although navigation safety has increased a considerable amount with the fire prevention systems installed on ships, large-scale ship fires continue to occur [6]. In this respect, an effective firefighting system is significant with regard to reducing the destruction caused by fires.

In efforts to control ship fires, the compartment in which the fire has started is of great importance, in addition to the type and the size of the fire. One of the compartments of ships in which fires frequently occur is the engine room. Upon an examination of fires that occurred on 165 ships between 1992 and 1997, it was concluded that approximately two-thirds of those fires had started in engine rooms [7]. In addition, engine rooms are the most important sections of ships regarding both the generation of power and electricity and the critical equipment they contain [8-10]. In this respect, engine room fires may also cause various other related accidents, such as collisions or groundings following a blackout [11].

Fire detection and fighting systems have been designed to control ship fires in a short time to reduce the destruction that ship fires cause. The construction properties and requirements of these systems are determined under the International Convention for the Safety of Life at Sea (SOLAS 74), Chapter II-2 [12]. In addition, the technical and engineering requirements of these systems are elaborated in the International Code for Fire Safety Systems (FSS Code) [13]. Firefighting systems used on ships may exhibit differences regarding the specific properties of the ships in accordance with the provisions of SOLAS 74.

It is of great importance to determine to what extent the fire detection and firefighting systems are ready against fires

Address for Correspondence: Ahmet Lutfi Tuncel, İstanbul Technical University, Maritime Faculty, Department of Maritime Transportation and Management Engineering, İstanbul, Turkey
E-mail: tuncel.ahmet@itu.edu.tr
ORCID ID: orcid.org/0000-0003-2306-6996

Received: 02.05.2021
Accepted: 07.09.2021

To cite this article: A.L, Tunçel, E. Akyuz, and O. Arslan, "An Extended Event Tree Risk Analysis Under Fuzzy Logic Environment: The Case of Fire in Ship Engine Room." *Journal of ETA Maritime Science*, vol. 9(3), pp. 210-220, 2021.

that may occur in the engine room of the ships. In this study, it is aimed to determine the probability of failure of the existing fire detection and fire extinguishing systems during a possible fire response in the engine rooms of the ships.

In this context, a model created using fuzzy logic and event tree analysis (ETA) methods was applied and the failure probabilities of these systems were calculated. In addition, possible consequences that may be encountered as a result of the systems failure were determined and thus a comprehensive quantitative risk analysis was performed. The paper is organised as follows. Section 1 gives brief definition about fire safety and firefighting system on-board ship. Section 2 summarises literature reviewing about fire safety on-board ships. Section 3 introduces methodologies. Section 4 performs empirical risk analysis for firefighting systems in engine rooms. Section 5 evaluates the outputs of the risk analysis. Section 6 concludes the research and advise further studies.

2. Literature Review

The literature contains many risk analysis studies on ship fires. For instance, Puisa et al. [11] examined the causes of accidents resulting in engine room fires in modern ships using the Causal Analysis Based on STAMP method, taking a real cruise ship fire as a case study. Uğurlu [14] analyzed the root causes and causal factors leading fires and explosions in tanker vessels carrying hazardous liquid cargo using a model that created with fault tree analysis (FTA), Monte Carlo simulation and the fuzzy extended analytical hierarchy process (AHP). Similarly, Guan et al. [15] revealed the root causes that lead to fire and explosion accidents in engine rooms of dual-fuel ships navigating in Chinese internal waters, using FTA. Karahalios [16] examined 77 accident reports and investigated the dangers of engine room fires using the AHP. In the study, it was also emphasised the significance of the Master's coping with the factor of stress in deciding to firefighting. In another study, Baalisampang et al. [3] investigated the causes of fire and explosion accidents occurred in the maritime sector between 1990 and 2015. The study also focused on the effect of alternative fuels on the elimination of accident causes [3].

It has been emphasised that human errors are the primary elements that cause marine accidents, in many studies in the literature [17-20]. In this respect, there are also studies specifically investigating the effect of human factors on the occurrence of ship fires. For example, Sarıalioğlu et al. [8] investigated the root causes leading fire and explosion accidents that occurred between 2000 and 2017 in the engine rooms of ships of 500 GRT using fuzzy FTA and Human Factors Analysis and Classification System (HFACS) methods. Schröder-Hinrichs et al. [21] examined 41 fire and explosion accident reports that occurred in the engine rooms of the ships and revealed the reasons of the accident with the model created as a result of minor modifications in the HFACS method. Soner et al. [22] analyzed the root causes of deficiencies linked to ship fires using a model that created with the fuzzy cognitive mapping and HFACS methods.

There are also studies investigating ship fires using various software and simulation techniques. Among these, Sarvari et al. [23] provided solutions for safe evacuation of passengers from fast ferries in the case of fire in ship engine room, using various simulations. In addition, Su and Wang [9] investigated fire formation and development processes in multi-layer structured engine rooms, using 3D modelling software.

There are also studies in the literature that address the effect of training in preventing ship fires. For instance, Tac et al. [24] measured the effectiveness of firefighting drills on an oil/product ship using fuzzy decision-making trial and evaluation laboratory method. Also, Tao et al. [25] emphasised the significance of simulation techniques in their studies investigating the most efficient and the least costly training to be provided to a ship's crew about firefighting.

Studies investigating the effects of present risk analysis approaches on preventing potential fires also stand out. Among these, McNay et al. [26] investigated the most efficient approaches in providing prevention of fire accidents in ship engine rooms by analysing accident research methods and current regulations such as formal safety assessment. Jin and Jang [27] stated that current fire risk assessment (FRA) analyses are not sufficient for the structural safety of offshore platforms against fire accidents and they provided a new risk analysis approach. Yang et al. [28] asserted that floating liquefied natural gas (LNG) offshore platforms contain numerous hazardous elements that may cause fires and they analysed how reliable fire safety measures were for these platforms using computational fluid dynamics code.

When the studies on ship fires in the literature are examined in detail, it is seen that most of them investigate the causes of fire accidents and offers solutions to prevent the occurrence of such accidents [3,8,11,14-16,21,22]. In this study, the probabilities of failure of fire detection and extinguishing systems used in the fight against an engine room fire were investigated. In this context, it is aimed to identify the system with the highest probability of failure. In addition, the results of various levels of risks that may be encountered as a result of the failure of the designed fire extinguishing systems have been investigated. In this respect, it is distinguished from other studies in the literature. The study is important in terms of determining the failure levels of the systems used during the fight against engine room fires and presenting what kind of measures should be taken in order to improve the systems with a high probability of failure. In addition, various levels of risks that may be encountered after a possible engine room fire have been digitized with a model created from fuzzy logic and ETA methods. In the study, an approach was obtained that will allow the risk levels to be evaluated both quantitatively and qualitatively, in this regard it is thought that it will contribute to the literature.

3. Materials and Methodology

In this study, a quantitative risk analysis was conducted on fire detection and firefighting systems used to control engine room fires with the application of the model created with fuzzy logic and ETA methods. The steps in the implementation of these methods are elaborated in the following sections.

3.1. Fuzzy Sets

Fuzzy set theory is an approach developed as a result of the insufficiency of conventional probability methodologies in explaining the ambiguities in decision-making processes [29]. This method enables the obtaining of linguistic expressions by referring to expert opinions [30]. The linguistic expressions obtained from expert opinions are subsequently converted into numerical values. Zadeh [29] explained that a fuzzy subset A in X can be demostrated by a membership function $\mu_A(x)$, which is associated with each element x in X (a crisp set which is a collection of elements or objects) via a real number between 0 and 1.

Additionally, membership functions can take different types of shapes, with triangular and trapezoidal being the most commonly used membership functions [31,32]. In this study, trapezoidal membership functions were used. Equation (1) gives the trapezoidal fuzzy set of numbers labelled (a, b, c, d) [33].

$$\mu_A(x) = \begin{cases} \frac{x-a}{b-a}, a \leq x \leq b \\ 1, \quad b \leq x \leq c \\ \frac{d-x}{d-c}, \quad c \leq x \leq d \\ 0, \quad or\ else \end{cases} \quad , \quad a < b < c < d \qquad (1)$$

3.2. ETA

ETA is an inductive risk analysis method that enables both qualitative and quantitative evaluations [34]. The analysis process of ETA starts with the occurrence of a specific initiating event (IE). This analytical technique also provides the possibility of a bottom-up approach and enables the investigation of various scenarios (i.e., event sequences) that may occur following the IE [35]. In other words, ETA shows the logical combination of different events that may be encountered after the IE [36]. ETA divides the findings into new paths depending on whether the designed barriers fail or not and allows us to predict the outcomes we may encounter after each process [37,38]. In addition, it provides quantitative evaluation by calculating the probability values of the each outcome that may be encountered [35]. In this respect, it enables us to test how functional the designated barriers are. ETA has a wide area of implementation in safety engineering in addition to nuclear and chemical safety [37,38]. There are also risk analysis studies using ETA in the maritime field [39,40]. For instance, Fu et al. [39] analyzed the potential risks that could be encountered in the event of a possible LNG leakage on LNG-fueled ships by utilizing ETA. In another study, Raiyan et al. [40] analyzed various types of maritime accidents in Bangladesh waters using the ETA.

The concept of barrier or safety barrier has varying definitions in the literature. While Duijm [41] defined this concept as the rules, equipment and structural tools that would prevent the occurrence of an accident, Sklet [42] interpreted it as all instruments, physical and non-physical, to prevent undesired events or incidents or to reduce their severity. In addition, Rausand [43] categorised safety barriers into two groups as primary and secondary barriers. In this respect, the barriers designed in accordance with ETA can be argued to be types of mitigation barriers to minimise the level of risk that may arise as a result of an accident. Safety barrier analyses, on the other hand, enable the determination of how efficient the designed safety systems are and the detection of deficiencies [44].

3.3. ETA in Fuzzy Environments: Integrated Methodology

In this section, the model created as a result of the integration of fuzzy logic and ETA methods are explained.

3.3.1. Constructing the Event Tree (ET) Diagram

First, the IE was determined. The IE was considered as fire accidents occurring after an explosion in ship engine rooms. Thereafter, appropriate mitigation barriers to overcome fire accidents in ship engine rooms with the least damage were selected and the ET diagram was drawn.

3.3.2. Calculation of Possibilities from Expert Judgements

Since there are not sufficient data available to conduct risk analysis on specific issues in the maritime sector, the use of expert opinions provides practical solutions [45]. Experts with different levels of knowledge, experience and training were asked about the probabilities of the failure of each mitigation barrier defined in this study. Regarding this topic, Yuhua and Datao [46] developed a weighting score for obtaining the most efficient evaluation from experts with different backgrounds. Akyuz et al. [47] defined such experts as heterogeneous expert groups. In addition, Hsu and Chen [48] introduced an approach known as the similarity aggregation method (SAM), which can convert linguistic evaluations obtained from a non-uniform group of experts into relevant fuzzy numbers. The implementation phases of the SAM are explained below.

Phase 1. Aggregating obtained possibilities

Let us assume that $E_{u,v}$ $(u, v = 1, 2, 3, .., m)$ expert opinions from m experts were referred to in this study. Every expert would make evaluations regarding the predetermined linguistic variables. The linguistic evaluations obtained are converted into relevant fuzzy numbers further on in the process. The details of this conversion are presented below [45]:

Step 1. Calculate the degree of agreement

In the first sub-stage, E_u and E_v represent each pair of experts. $S_{u\ v}(\tilde{R}_u, \tilde{R}_{u,})$ symbolise expert opinions within the interval $\in$ [0,1]. In this regard, both $\bar{A} = (a_1, a_2, a_3, a_4)$ and $\bar{B} = (b_1, b_2, b_3, b_4)$ are generic trapezoidal fuzzy numbers. Similarities between two fuzzy numbers can be calculated with "S", a similarity function [45], as explained in Equation (2).

$$S(\tilde{A}, \tilde{B}) = 1 - 1/4 \sum_{i=1}^{4} |a_i - b_i| \quad (2)$$

Here, $S(\tilde{A}, \tilde{B}) \in [0,1]$.

Step 2. Compute average agreement (AA) degree $AA(E_u)$ of the experts

In the second sub-stage, Equation (3) is used to specify the AA degree.

$$AA(E_u) = \frac{1}{M-1} \sum_{u \neq v}^{M} S(\tilde{R}_u, \tilde{R}_v) \quad (3)$$

Step 3. Determine relative agreement (RA) degree $RA(E_u)$ of the experts

In the third sub-stage, Equation (4) is employed to calculate the RA degree.

$$E_u(u = 1,2,3, \dots, M) \ as \ RA(E_u) = \frac{A(E_u)}{\sum_{u=1}^{M} A(E_u)} \quad (4)$$

Step 4. Predict consensus coefficient (CC) degree $CC(E_u)$ of the experts

In the fourth sub-stage, Equation (5) is utilised to predict the consensus coefficient degree.

$$E_u: (u = 1,2,3, \dots, M)$$
$$CC(E_u) = \beta . w(E_u) + (1 - \beta) . RA(E_u) \quad (5)$$

Here, $w(E_u)$ represents weighting score of a pair of expert.

Step 5. Aggregate the result of the experts' judgements

In the final sub-stage of the SAM, Equation (6) is used to aggregate the result of each expert's judgment (AG).

$$\tilde{R}_{AG} = CC(E_1) \times \tilde{R}_1 + CC(E_2) \times \tilde{R}_2 + \dots + CC(E_M) \times \tilde{R}_M \quad (6)$$

Phase 2. Defuzzify of the aggregated experts' judgement (fuzzy possibility)

In this process, the aggregated trapezoidal fuzzy numbers are converted into crisp values. Here, the aim is defuzzifying with a centre of area (COA) technique, as presented in Equation (7) [45,49].

$$X^* = \frac{\int u_i(x) x dx}{\int u_i(x)} \quad (7)$$

In this context, X^* denotes fuzzy possibility, $u_i(X)$ denotes the aggregated membership function and x denotes the output variable.

Phase 3. Turn possibilities into probabilities

In this process, possibilities obtained as a result of expert judgements are transformed into probability values. With this aim, Onisawa [50] introduced a formula in light of a new approach to convert fuzzy failure possibilities into fuzzy failure probabilities. Fuzzy probabilities (*FPr*) can be obtained from the fuzzy possibilities (*FPs*). In this context, Equations (8) and (9) are used for the calculations. Here, K, as shown in Equation (9), is a constant value that represents safety criteria depending on fault rates or routine fault rates [47,51].

$$FPr = \begin{cases} \frac{1}{10^k}, FPs \neq 0 \\ 0, FPs = 0 \end{cases} \quad (8)$$

$$K = [\left(\frac{1 - FPs}{FPs}\right)]^{1/3} \times 2.301 \quad (9)$$

3.4. Probability Calculation of Each Outcome

In this section of the study, calculations of the probabilities for each outcome to be encountered in the constructed ET diagram are performed. First, the success probability value was obtained using the calculated failure probability for each designed barrier. The relation between the probability of failure and probability of success is presented in Equation (10) [52].

$$P(B1) + P(B1') = 1 \quad (10)$$

Here, as an example, P(B1) is the B1 barrier's failure probability, while P(B1′) is the probability that barrier B1 will not fail, i.e. probability of success.

Each end point in the ET diagram indicates an outcome to be encountered. The probability of each outcome will be the conditional probability of failure or success for all barriers on the path starting from the IE [35,52]. For instance, the probability of the outcome to be obtained in a scenario in which the B1 barrier fails and the B2 barrier succeeds is presented in Equation (11).

$$P(O) = P(IE) \times P(B1) \times P(B2') \quad (11)$$

Here, *P(O)* denotes the probability of the outcome, *P(IE)* denotes the probability of the IE, *P(B1)* denotes the B1 barrier's failure probability and *P(B2′)* denotes the probability that the B2 barrier does not fail.

In this study, the most critical barrier is defined as the barrier with the highest probability of failure among all designed barriers.

4. Empirical Analysis of Ship Fire Detection and Firefighting Systems

In this study, a comprehensive risk analysis was conducted to determine the functionality of the designated barriers to fight fires that may occur in the engine rooms of ships of 500 GRT and above.

4.1. Examined Systems (Designated Barriers)

In this study, systems used in fighting ship engine room fires are examined within six categories.

4.1.1. Fire detection and alarm systems

Early detection of ship fires is of great importance for efficient firefighting and thus for minimising the risks a fire may pose to the crew, the environment and the ship. These systems are designed for the timely detection of potential fires that can be encountered on- board ships. They comprise an alarm panel, fire buttons, fire detectors and several electronic and mechanical parts. Of these parts, the fire detectors are classified into three groups regarding their operational principles. These are flame detectors, smoke detectors and heat detectors [53]. Flame detectors are installed in the compartments with high probabilities of having flaming fires. Smoke detectors enable the early detection of relatively slow-developing fires. Heat detectors operate by sensing the temperature of a heating layer of air [53]. The failure or outage of the fire detection system may prevent the automatic activation of local fixed fire extinguishing systems, which operate synchronously with the system, in addition to the failure in detecting the fire early.

4.1.2. Water mist systems

Water mist systems are local fixed fire extinguishing systems that enable the dispersal of water in mist form via nozzles and they can be used to fight potential fires in ship engine rooms. They can be used in places with temperatures higher than those seen in other compartments of the engine room, such as the auxiliary boiler room, auxiliary generators, purifier room and incinerator room. Technically, they can be activated in two ways: automatically and manually. For automatic activation, a fire should be detected by the fire detectors and the fire alarm system should be actively working. Failure of the water mist system may allow fires in critical compartments of the engine room to grow and spread to other compartments.

4.1.3. Portable fire extinguishers

Portable fire extinguishers, placed in different compartments of ship engine rooms to fight different types of fires, are designed with different types and capacities. Their types may include carbon dioxide (CO_2), water, foam and chemical dust. The failure of these fire extinguishers may allow easily controllable fires to grow.

4.1.4. Fire pumps

Considering the type and the size of the fire that occurs, sea water may be used as an extinguisher. In such a case, fire pumps are the water pumps that deliver high-pressure sea water to the compartment in which the water will be used via fire lines. The outage of the fire pump or failure in using it may delay the intervention and allow the fire to grow.

4.1.5. Emergency fire pumps

In the case of any malfunction in the fire pump, the whole fire line will be out of the loop. In this case, an emergency fire pump may be used alternatively for sea water intake. According to Chapter 12 of the FSS Code, this pump should be activated by a stationary power source that is operated separately [13]. In the case of failure in using this system, the fire may become more devastating.

4.1.6. Fixed firefighting systems: CO_2 flooding systems

CO_2 flooding systems are the most common fixed fire systems found in many types of ships. In a potential ship engine room fire, they are used to bring the fire under control by dispensing CO_2 into the compartment. They are used when a fire cannot be brought under control with portable or other fire extinguishing systems or in line with the directions of the decision-maker depending on the specific conditions of the fire. Technically, these systems comprise many elements such as CO_2 bottles, common manifolds, distribution valves, distribution pipe lines and nozzles. In cases in which the fixed firefighting system cannot be operated, the fire may spread throughout the ship and may even devastatingly become incontrollable, in which case the Master would make the decision to abandon the ship.

4.2. Quantitative Analysis of Ship Engine Room Firefighting Systems

In this study, SOLAS 74, the FSS Code, the SOLAS Fire Training Manual, FRA and several ship firefighting systems were examined in detail. In addition, a risk analysis of the systems used in fighting potential fires in the engine rooms of ships was performed while referring to marine expert opinions. The IE in this study was determined as a ship engine room fire. Also, six different barriers were determined that could minimise the negative outcomes that fires cause and make it possible to bring fires under control. These are fire detection and alarm system (B1), water mist system (B2), portable fire extinguishers (B3), fire pump (B4), emergency fire pump (B5) and fixed CO_2 fire extinguishing system (B6). The probabilities of failure for these designed barriers were calculated and the outcomes were determined in line with different scenarios formed according to the ET diagram. Since there are no statistical data available on the outages, i.e. failures, of the designed barriers, the probabilities of failure for each barrier were obtained by referring to expert opinions. In this study, an expert group comprising 4 chief engineers, 1 academician and 1 electrical engineer was assembled and evaluations were obtained from this group. The ET diagram was also systematically constructed by experts. The profile details of the experts who participated in the study are presented in Table 1.

Different weightings were calculated for the feedback obtained from these experts, since they were not homogeneous in their profiles. This weighting process was conducted using the scales proposed by Lavasani et al. [45] and Kuzu et al. [54]. Weighting scores of the non-homogeneous experts are presented in Table 2.

The expert opinions obtained in this study were converted to numbers using the fuzzy logic method [55]. The linguistic expressions and trapezoidal fuzzy numbers used in this study are presented in Table 3 [56].

Each maritime expert, all of whom were weighted considering their professional positions, education levels and sea and shore service times, participated in the study

Table 1. *Profile details of the maritime experts*

Maritime Experts	Position	Maritime Experience (Years)	Shore Service Time (Years)	Educational Level
1	Chief Engineer	20	4	BSc
2	Chief Engineer	13	9	BSc
3	Chief Engineer	12	5	BSc
4	Chief Engineer	9	2	MSc
5	Academician	4	10	PhD
6	Electrical Engineer	15	3	MSc

Table 2. *Weighting scores of non-homogenous experts*

Group	Classification	Score
Professional position (a_1)	Master/Chief engineer	5
	Pilot	4
	Academician	3
	Chief officer	2
	Junior officer/Electrical engineer	1
Sea service time (a_2)	≥16 years	5
	11-15	4
	6-10	3
	3-5	2
	≤2	1
Shore service time (a_3)	≥20 years	5
	15-19	4
	10-14	3
	6-9	2
	≤5	1
Education level (a_4)	PhD	5
	Master	4
	Bachelor	3
	Higher national diploma	2
	School level	1

Table 3. *Linguistic terms with trapezoidal fuzzy numbers*

Linguistic terms	Fuzzy numbers
Very low (VL)	(0.0, 0.0, 0.1, 0.2)
Low (L)	(0.1, 0.2, 0.2, 0.3)
Medium low (ML)	(0.2, 0.3, 0.4, 0.5)
Medium (M)	(0.4, 0.5, 0.5, 0.6)
Medium high (MH)	(0.5, 0.6, 0.7, 0.8)
High (H)	(0.7, 0.8, 0.8, 0.9)
Very high (VH)	(0.8, 0.9, 1.0, 1.0)

at different levels. The weights of each expert profile are presented in Table 4. Linguistic evaluations obtained from the experts for each designed barrier are presented in Table 5.

After obtaining the evaluations of the maritime experts for each designed barrier, the aggregation stage was completed using Equations (2-5). In this context, the similarity functions and similarity values calculated for B1 are presented in Table 6. In addition, the average agreement of the maritime experts (AA), RA of the maritime experts and consensus coefficient (CC) values calculated for B1 are presented in Table 7. Since all experts in this case are maritime experts, the β value is taken as 0.5 in the calculations [57]. Later, in order to obtain the aggregated expert judgement values for each failure of barriers built for fighting ship engine room fires, Equation (6) was used. Following these calculations, fuzzy numbers were converted to crisp values using Equation (7) and the defuzzification process was completed. The aggregated expert judgements and the defuzzified failure possibilities of the six barriers in this study are presented in Table 8.

The possibilities pertaining to the barriers obtained from expert evaluations were converted to probabilities to calculate the probability values for each outcome constructed in line with the ET diagram. This conversion was done using Equations (8-9). After that, the probability calculation stage for seven different outcomes determined in the ET diagram was subsequently commenced. Sarıalioğlu et al. [8] calculated the probability of fire accidents in engine rooms of ships of 500 GRT and above as 7.401E-02. In this study, the said value was considered the occurrence probability of the IE. In this respect, using Equations (10-11), the probability values for each outcome in the ET diagram were calculated. The calculated failure probabilities pertaining to each barriers and outcomes are presented in Table 9.

Table 4. *Weights of the maritime experts*

Maritime expert no	Weighting factor				Total weight	Weighting score
1	5	5	1	3	14	0.18
2	5	4	2	3	14	0.18
3	5	4	1	3	13	0.17
4	5	3	1	4	13	0.17
5	3	2	3	5	13	0.17
6	1	4	1	4	10	0.13

Table 5. *Linguistic evaluations of the maritime experts for priorities of each barrier*

Barriers (B)	M. Exp 1	M. Exp 2	M. Exp 3	M. Exp 4	M. Exp 5	M. Exp 6
B1	L	L	ML	VL	ML	M
B2	L	ML	ML	L	M	ML
B3	VL	VL	VL	L	VL	ML
B4	VL	VL	L	VL	ML	ML
B5	VL	VL	VL	VL	ML	L
B6	VL	VL	VL	VL	VL	L
L: Low, VL: Very low, ML: Medium low						

Table 6. *Similarity functions for B1*

No	Similarity function	Value
1	S(E1&E2)	1.000
2	S(E1&E3)	0.850
3	S(E1&E4)	0.875
4	S(E1&E5)	0.850
5	S(E1&E6)	0.700
6	S(E2&E3)	0.850
7	S(E2&E4)	0.875
8	S(E2&E5)	0.850
9	S(E2&E6)	0.700
10	S(E3&E4)	0.725
11	S(E3&E5)	1.000
12	S(E3&E6)	0.850
13	S(E4&E5)	0.725
14	S(E4&E6)	0.575
15	S(E5&E6)	0.850

Table 7. *AA, RA and CC values of maritime experts for B1*

M. Exp. No	AA	RA	CC
1	0.855	0.17	0.178
2	0.855	0.17	0.178
3	0.855	0.17	0.171
4	0.755	0.15	0.161
5	0.855	0.17	0.171
6	0.735	0.15	0.140
AA: Average agreement, RA: Relative agreement, CC: Consensus coefficient			

Table 8. *Aggregated expert judgements and defuzzified failure possibilities for each barrier*

Barriers	Aggregated expert judgements on failures				Defuzzified possibility
B1	0.160	0.244	0.294	0.394	0.274
B2	0.198	0.298	0.348	0.448	0.323
B3	0.044	0.074	0.157	0.257	0.136
B4	0.079	0.126	0.209	0.309	0.183
B5	0.046	0.076	0.161	0.261	0.139
B6	0.014	0.028	0.114	0.214	0.095

The final version of the ET diagram constructed in line with the data obtained from the analyses is shown in Figure 1.

5. Results and Discussion

Upon the conclusion of the risk analysis of the barriers designed in this study, it was found that the barrier with the highest probability of failure is the water mist system [P(B2): 1.14E-03]. In this respect, technical investigations should be performed on the factors that may cause the outage of water mist system, with the highest probability of failure, to better fight against potential ship engine room fires. It is known that fire detectors should operate synchronously and that fire detection and alarm systems should be active for the automatic activation of water mist system. In this respect, it should be considered that any failure or non-compliance related to these systems would prevent the automatic activation of the water mist systems. In addition, the manual operation procedures of the systems and regular repair and maintenance also require attention. Accordingly, the water mist system (B2), which was found to have the highest probability of failure, is also considered the most critical barrier.

__Table 9.__ Failure probabilities for each barriers and outcomes

Barriers	Probabilities obtained from possibilities	Outcomes	Calculated probabilities for each outcomes
B1	6.55E-04	O1	7.40E-02
B2	1.14E-03	O2	4.84E-05
B3	5.43E-05	O3	5.53E-08
B4	1.63E-04	O4	3.00E-12
B5	5.88E-05	O5	4.90E-16
B6	1.35E-05	O6	2.88E-20
		O7	3.88E-25

It is remarkable that the barrier with the second highest probability of failure was found to be the fire detection and alarm system [P(B1): 6.55E-04]. Early detection of fires on ships is of critical significance [1,58,59]. In this respect, it was expected that these systems designed for the first stage of firefighting processes would be less likely to fail. The electronic and mechanical components of these system, in addition to the main and emergency power supplies that feed them, should be checked regularly to reduce the probability of failure of the system.

When the other barriers are considered, the probability of failure ranges from highest to lowest for the fire pump [P(B4):1.63E-04], emergency fire pump [P(B5): 5.88E-05], portable fire extinguishers [P(B3): 5.43E-05] and fixed CO_2 fire extinguishing system [P(B6): 1.35E-05], respectively. When the probability of failure for all barriers is considered, it is relatively low. However, considering that engine rooms are of vital importance for ships [8], and that fire accidents have great potential to occur spontaneously, it is clearly of the utmost importance to conduct appropriate technical checks to further reduce the probability of failure of the barriers examined in this study.

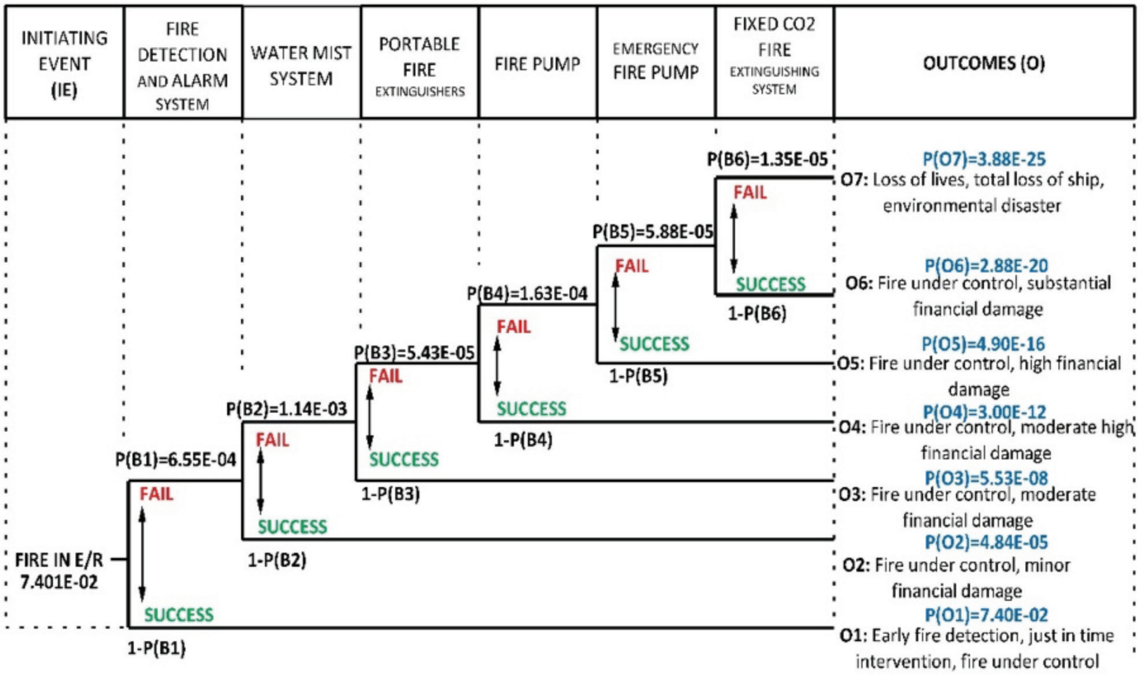

***Figure 1.** ET diagram for ship (E/R) fires with probabilities and relevant outcomes*

ET: Event tree

All conducted repairs and maintenance, tests and surveys should comply with the provisions of SOLAS Chapter II-2/14.2.2 [12], and the minimum criteria defined in International Maritime Organization MSC.1/Circ.1432 [60], and MSC.1/Circ.1516 [61]. In addition, the repair and maintenance directives determined by the manufacturer of each individual system and the requirements of flag administrations should be fulfilled.

From a different perspective, it appears that several risks can be encountered in the event that designed barriers fail. These risks are defined as minor, moderate, moderately high, high and substantial in terms of financial damage, total loss of the ship, environmental disaster and loss of lives [62,63]. As can be seen, failures in the systems used in fighting engine room fires may have outcomes including loss of human lives in addition to financial and environmental losses. In this context, as the probability of failure of the systems designed for firefighting increases, it will be difficult to control the fire. This will increase the magnitude of the risk encountered.

6. Conclusion

A technical risk analysis of the fire detection and fire-fighting systems that can be used against potential fires in the engine rooms of ships of 500 GRT and above was conducted in this study. It is concluded that risks of various severity may be encountered in the event of the failure or outage of the systems designed for fighting fires. In this respect, repair, maintenance and testing are of great importance to ensure the efficient operation of the systems designed for fighting engine room fires. In addition, with the calculation of the probabilities of failure for each barrier and the outcomes to be encountered in different scenarios using the model constructed with fuzzy logic and ETA, a quantitative risk analysis was conducted. This has enabled better awareness of the different levels of risks that may be encountered as a result of ship engine room fire accidents. The water mist system has been determined as the most critical barrier as it has the highest probability of failure among the designed barriers. In this context, root causes that lead to malfunctions in systems with a higher probability of failure should be investigated [64]. In addition, the findings obtained in the study serve as a source for other risk analysis studies that can be done regarding fire extinguishing systems in the future.

It is believed that studying the effect of human factors on the failures of fire-fighting systems in ship engine rooms in future studies will further contribute to the minimisation of malfunctions or misuses of these systems. In this respect, ETA model can be designed from human errors at various levels, thus the probability of human-induced malfunctions in these systems can be measured and solutions can be offered for the elimination of these errors.

Authorship Contributions

Concept design: A.L. Tuncel, E. Akyuz, O. Arslan, Data Collection or Processing: A.L. Tuncel, E. Akyuz, O. Arslan, Analysis or Interpretation: A.L. Tuncel, E. Akyuz, Literature Review: A.L. Tuncel, Writing, Reviewing and Editing: A.L. Tuncel, O. Arslan.

Funding: The author(s) received no financial support for the research, authorship, and/or publication of this article.

References

[1] H.C. Kuo and, H.K. Chang, "A real-time shipboard fire-detection system based on grey-fuzzy algorithms," *Fire Safety Journal,* vol. 38, pp. 341-363, Jun 2003.

[2] A. Salem, "Fire engineering tools used in consequence analysis," *Ships and Offshore Structures,* vol. 5, pp. 155-187, 2010.

[3] T. Baalisampang, R. Abbassi, V. Garaniya, F. Khan, and M. Dadashzadeh, "Review and analysis of fire and explosion accidents in maritime transportation," *Ocean Engineering,* vol. 158, pp. 350-366, June 2018.

[4] R.M. Darbra, and J. Casal, "Historical analysis of accidents in seaports," *Safety Science,* vol. 42, pp. 85-98, Feb 2004.

[5] Ö. Uğurlu, U. Yıldırım, and E. Yüksekyıldız, "Marine accident analysis with GIS," Journal of Shipping and Ocean Engineering, vol. 3, pp. 21-29, Feb 2013.

[6] L. Wang, J. Wang, M. Shi, S. Fu, and M. Zhu, "Critical risk factors in ship fire accidents," *Maritime Policy & Management*, pp. 1-19, Sep 2020.

[7] Det Norske Veritas, *Engine room fires can be avoided*. Veritasveien, Norway: Det Norske Veritas, 2020.

[8] S. Sarıalioğlu, Ö. Uğurlu, M. Aydın, B. Vardar, and J. Wang, "A hybrid model for human-factor analysis of engine-room fires on ships: HFACS-PV&FFTA," *Ocean Engineering*, vol. 217, pp. 107992, Dec 2020.

[9] S. Su, and L. Wang, "Three dimensional reconstruction of the fire in a ship engine room with multilayer structures," *Ocean Engineering,* vol. 70, pp. 201-207, Sep 2013.

[10] R. Bellas, M.A. Gómez, A. González-Gil, J. Porteiro, and J. L. Míguez, "Assessment of the fire dynamics simulator for modeling fire suppression in engine rooms of ships with low-pressure water mist," *Fire Technology,* vol. 56, pp. 1315-1352, Nov 2019.

[11] R. Puisa, S. Williams, and D. Vassalos, "Towards an explanation of why onboard fires happen: the case of an engine room fire on the cruise ship 'Le Boreal'," *Applied Ocean Research*, vol. 88, pp. 223-232, Jul 2019.

[12] International Maritime Organization, *SOLAS Consolidated Edition 2020*. London: International Maritime Organization Publishing, 2020.

[13] International Maritime Organization, *FSS Code: International code for fire safety systems*. London: International Maritime Organization Publishing, 2015.

[14] Ö. Uğurlu, "Analysis of fire and explosion accidents occurring in tankers transporting hazardous cargoes," *International Journal of Industrial Ergonimics,* vol. 55, pp. 1-11, Sep 2016.

[15] Y. Guan, J. Zhao, T. Shi, and P. Zhu, "Fault tree analysis of fire and explosion accidents for dual fuel (diesel/natural gas) ship engine rooms," *Journal of Marine Science and Application,* vol. 15, pp. 331-335, Jul 2016.

[16] H. Karahalios, "Effect of human behaviour in shipboard firefighting decisions: the case of fire in engine rooms," *Journal of Contingencies and Crisis Management*, vol. 25, pp. 256-268, Jan 2017.

[17] J.R. Harrald, et al. "Using system simulation to model the impact of human error in a maritime system," *Safety Science*, vol. 30, pp. 235-247, Dec 1998.

[18] A. Toffoli, J.M. Lefevre, E. Bitner-Gregersen, and J. Monbaliu, "Towards the identification of warning criteria: analysis of a ship accident database," *Applied Ocean Research*, vol. 27, pp. 281-291, Dec 2005.

[19] P. Antao and C.G. Soares, "Fault-tree models of accident scenarios of RoPax vessels," International Journal of Automation and Computing, vol. 2, pp. 107-116, 2006.

[20] O. Arslan, and I.D. Er, "A SWOT analysis for successful bridge team organization and safer marine operations.," *Process Safety Progress,* vol. 27, pp. 21-28, Jul 2007.

[21] J.U. Schröder-Hinrichs, M. Baldauf, K.T. Ghirxi, "Accident investigation reporting deficiencies related to organizational factors in machinery space fires and explosions," *Accident Analysis & Prevention,* vol. 43, pp. 1187-1196, May 2011.

[22] O. Soner, U. Asan, and M. Celik, "Use of HFACS-FCM in fire prevention modelling on board ships," *Safety Science,* vol. 77, pp. 25-41, Aug 2015.

[23] P.A. Sarvari, E. Çevikcan, M. Çelik, and A. Üstündağ, "A simulation aided methodology suggestion for managing emergency evacuation operation under engine room sourced fire conditions," *Journal of ETA Maritime Science*, vol. 5, pp. 362-385, Oct 2017.

[24] B.O. Tac, E. Akyuz, and M. Celik, "Analysis of performance influence factors on shipboard drills to improve ship emergency preparedness at sea," *International Journal of Shipping and Transport Logistics,* vol. 12, pp. 92-116, 2020.

[25] R. Tao, H.X. Ren, and X.Q. Peng, "Ship fire-fighting training system based on virtual reality technique," in *Proceedings of 17th Asia Simulation Conference, part 2,* M.S.M. Ali, H. Wahid, N.A.M. Subha, S. Sahlan, M.A.M. Yunus, A.R. Wahap, Eds. Singapore: Springer, 2020, pp. 249-260.

[26] J. McNay, R. Puisa, and D. Vassalos, "Analysis of effectiveness of fire safety in machinery spaces. *Fire Safety Journal,* vol. 108, pp. 102859, Sep 2019.

[27] Y. Jin, and B.S. Jang, "Probabilistic fire risk analysis and structural safety assessment of FPSO topside module," *Ocean Engineering,* vol. 104, pp. 725-737, Aug 2015.

[28] R. Yang, F. Khan, M. Yang, D. Kong, and C. Xu, "A numerical fire simulation approach for effectiveness analysis of fire safety measures in floating liquefied natural gas facilities," *Ocean Engineering,* vol. 157, pp. 219-233, Jun 2018.

[29] L.A. Zadeh, "Fuzzy sets," *Information and Control,* vol. 8, pp. 338-353, Jun 1965.

[30] F. Castiglia, and M. Giardina, "Analysis of operator human errors in hydrogen refuelling stations: comparison between human rate assessment techniques," *International Journal of Hydrogen Energy*, vol. 38, pp. 1166-1176, Jan 2013.

[31] A. Barua, L.S. Mudunuri, and O. Kosheleva, "Why trapezoidal and triangular membership functions work so well: towards a theoretical explanation," *Journal of Uncertain Systems,* vol. 8, Oct 2013.

[32] J. Wang, et al. "Use of advances in technology for maritime risk assessment," *Risk Analysis,* vol. 24, pp. 1041-1063, Sep 2004.

[33] P. Badida, Y. Balasubramaniam, and J. Jayaprakash, "Risk evaluation of oil and natural gas pipelines due to natural hazards using fuzzy fault tree analysis," *Journal of Natural Gas Science and Engineering,* vol. 66, pp. 284-292, Jun 2019.

[34] J.X. Wang, and M.L. Roush, *What every engineer should know about risk engineering and management.* New York: CRC Press, 2000.

[35] N. Ramzali, M.R.M. Lavasani, and J. Ghodousi, "Safety barriers analysis of offshore drilling system by employing fuzzy event tree analysis," *Safety Science*, vol. 78, pp. 49-59, Oct 2015.

[36] R. Ferdous, F. Khan, R. Sadiq, P. Amyotte, and B. Veitch, "Handling data uncertainties in event tree analysis," *Process Safety and Environmental Protection,* vol. 87, pp. 283-292, Sep 2009.

[37] T. Aven, *Reliability and risk analysis*. London and New York: Elsevier Applied Science, 1992.

[38] S. Mannan. *Lees' Loss prevention in the process industries: Hazard identification, assessment and control.* 4th ed. Vol. 1, Oxford: Elsevier, 2012.

[39] S. Fu, X. Yan, D. Zhang, C. Li, and E. Zio, "Framework for the quantitative assessment of the risk of leakage from LNG-fueled vessels by an event tree-CFD," *Journal of Loss Prevention in the Process Industries*, vol. 43, pp. 42-52, Sep 2016.

[40] A. Raiyan, S. Das, and M. R. Islam, "Event tree analysis of marine accidents in Bangladesh," *Procedia Engineering,* vol. 194, pp. 276-283, 2017.

[41] N. J. Duijm, "Safety-barrier diagrams as a safety management tool," *Reliability Engineering & System Safety*, vol. 94, pp. 332-341, Feb 2009.

[42] S. Sklet, "Safety barriers: definition, classification, and performance," *Journal of Loss Prevention in the Process Industries,* vol. 19, pp. 494-506, Sep 2006.

[43] M. Rausand, *Risk assessment: theory, methods and applications.* Hoboken, New Jersey: John Wiley & Sons, 2013.

[44] A.D. Livingston, G. Jackson, and K. Priestley, "Root causes analysis: Literature review," HSE Contract Research Report 325/2001, WS Atkins Consultants Ltd for the Health and Safety Executive, Norwich, United Kingdom, 2001.

[45] S.M. Lavasani, N. Ramzali, F. Sabzalipour, and E. Akyuz, "Utilisation of Fuzzy Fault Tree Analysis (FFTA) for quantified risk analysis of leakage in abandoned oil and natural-gas wells," *Ocean Engineering,* vol. 108, pp. 729-737, Nov 2015.

[46] D. Yuhua, and Y. Datao, "Estimation of failure probability of oil and gas transmission pipelines by fuzzy fault tree analysis," *Journal of Loss Prevention in the Process Industries,* vol. 18, pp. 83-88, Mar 2005.

[47] E. Akyuz, O. Arslan, and O. Turan, "Application of fuzzy logic to fault tree and event tree analysis of the risk for cargo liquefaction

on board ship," *Applied Ocean Research,* vol. 101, pp. 102238, Aug 2020.

[48] H.M. Hsu, and C.T. Chen, "Aggregation of fuzzy opinions under group decision making," *Fuzzy Sets and Systems,* vol. 79, pp. 279-285, May 1996.

[49] H.T. Nguyen and N.R. Prasad, Eds., *Fuzzy modeling and control: Selected works of M*. Sugeno. Boca Raton, Florida: CRC Press, 1999.

[50] T. Onisawa, "An approach to human reliability in man-machine systems using error possibility," *Fuzzy Sets and Systems,* vol. 27, pp. 87-103, Aug 1998.

[51] A.D. Swain, and H.E. Guttmann, "Handbook of human-reliability analysis with emphasis on nuclear power plant applications," Final Report (NUREG/CR-1278), United States, 1983.

[52] S. Mineo, G. Pappalardo, A. D'Urso, and D. Calcaterra, "Event tree analysis for rockfall risk assessment along a strategic mountainous transportation route," *Environmental Earth Science,* vol. 76, pp. 620, Sep 2017.

[53] S. Zhang, "Fire protection onboard: enhance fire safety by design," Master dissertion, (MSc Thesis). World Maritime University, Malmö, Sweden, 2000.

[54] A.C. Kuzu, E. Akyuz, and O. Arslan, "Application of fuzzy fault tree analysis (FFTA) to maritime industry: a risk analysing of ship mooring operation," *Ocean Engineering,* vol. 179, pp. 128-134, May 2019.

[55] B. Sahin, "Consistency control and expert consistency prioritization for FFTA by using extent analysis method of trapezoidal FAHP," *Applied Soft Computing,* vol. 56, pp. 46-54, Jul 2017.

[56] S.J. Chen, and C. L. Hwang, (1992). "Fuzzy Multiple Attribute Decision Making Methods," *in Fuzzy Multiple Attribute Decision Making: Methods and Applications* Berlin, Heidelberg: Springer-Verlag, 1992, pp. 289-486.

[57] Y.E. Senol, Y.V. Aydogdu, B. Sahin, and I. Kilic, "Fault tree analysis of chemical cargo contamination by using fuzzy approach," *Expert Systems with Applications,* vol. 42, pp. 5232-5244, Jul 2015.

[58] S.J. Wang, D.L. Jeng, and M.T. Tsai, "Early fire detection method in video for vessels," *Journal of Systems and Software,* vol. 82, pp. 656-667, Apr 2009.

[59] H. Sim, W.J. Ha, and Y.S. Park, "A basic study on standardization of fire-fighting drill scenarios on board," *Journal of International Maritime Safety Environmental Affairs and Shipping*, vol. 3, pp. 28-35, Dec 2019.

[60] International Maritime Organization, *Revised guidelines for the maintenance and inspection of fire protection systems and appliances (MSC.1/Circ.1432).* London: International Maritime Organization, 2012.

[61] International Maritime Organization, *Amendments to the revised guidelines for the maintenance and inspection of fire protection systems and appliances (MSC.1/Circ.1516).* London: International Maritime Organization, 2015.

[62] E. Akyuz, E. Celik, and M. Celik, "A practical application of human reliability assessment for operating procedures of the emergency fire pump at ship," *Ships and Offshore Structures,* vol. 13, pp. 208-216, 2018.

[63] E. Akyuz, and E. Celik, "The role of human factor in maritime environment risk assessment: a practical application on Ballast Water Treatment (BWT) system in ship," *Human and Ecological Risk Assessment: An International Journal,* vol. 24, pp. 653-666, 2018.

[64] M. Aydin, E. Akyuz, O. Turan, and O. Arslan, "Validation of risk analysis for ship collision in narrow waters by using fuzzy Bayesian networks approach," *Ocean Engineering*, vol. 231, pp. 108973, Jul 2021.

Reviewer List of Volume 9 Issue 3 (2021)

Aleksandra Łapko	Maritime University of Szczecin	Poland
Ali Doğrul	National Defense University	Turkey
Aykut Safa	Yıldız Technical University	Turkey
Burak Acar	Poseidon Marine Engineering and Construction Co	Turkey
Eda Boltürk	İstanbul Technical University	Turkey
Fatma Kutlu Gündogdu	National Defense University	Turkey
Halil Saraçoğlu	İstanbul Technical University	Turkey
İsmail Altın	Karadeniz Technical University	Turkey
Karsten Fach	Managing Director at Marine Service	Deutschland
Murat Ozdemir	Ordu University	Turkey
Olena Karpenko	University of Strathclyde	United Kingdom
Ömer Kemal Kınacı	İstanbul Technical University	Turkey
Yavuz Hakan Özdemir	Çanakkale Onsekiz Mart University	Turkey
Wafaa Ahmed Nour Eldin Elias	Minia University	Egypt

Volume 9 Issue 3 (2021) is indexed in